LIQUID-WATER-CONTENT AND HYDROMETEOR SIZE-DISTRIBUTION INFORMATION FOR THE SAMS MISSILE FLIGHTS OF THE 1971-72 SEASON AT WALLOPS ISLAND, VIRGINIA - AFCRL/SAMS REPORT NUMBER 3

Vernon G. Plank

Air Force Cambridge Research Laboratory
L. G. Hanscom Field, Massachusetts

2 July 1974

Unclassified
Security Classification

DOCUMENT CONTROL DATA - R&D AD/A-002 370

(Security classification of title, body of abstract and indexing annotation must be entered when the overall report is classified)

1. ORIGINATING ACTIVITY *(Corporate author)*
Air Force Cambridge Research Laboratories (LYC)
L. G. Hanscom Field
Bedford, Massachusetts 01730

2a. REPORT SECURITY CLASSIFICATION
Unclassified

2b. GROUP

3. REPORT TITLE
LIQUID-WATER-CONTENT AND HYDROMETEOR SIZE-DISTRIBUTION INFORMATION FOR THE SAMS MISSILE FLIGHTS OF THE 1971-72 SEASON AT WALLOPS ISLAND, VIRGINIA – AFCRL/SAMS REPORT NO. 3

4. DESCRIPTIVE NOTES *(Type of report and inclusive dates)*
Scientific. Interim.

5. AUTHOR(S) *(First name, middle initial, last name)*
Vernon G. Plank

6. REPORT DATE
2 July 1974

7a. TOTAL NO. OF PAGES
140

7b. NO. OF REFS
4

8a. CONTRACT OR GRANT NO.

b. PROJECT, TASK, WORK UNIT NOS. 627A

c. DOD ELEMENT 63311F

d. DOD SUBELEMENT

9a. ORIGINATOR'S REPORT NUMBER(S)
AFCRL-TR-74-0296

9b. OTHER REPORT NO(S) *(Any other numbers that may be assigned this report)*
Special Reports, No. 178

10. DISTRIBUTION STATEMENT
Approved for public release; distribution unlimited.

11. SUPPLEMENTARY NOTES
TECH, OTHER

12. SPONSORING MILITARY ACTIVITY
Air Force Cambridge Research Laboratories (LYC)
L. G. Hanscom Field
Bedford, Massachusetts 01730

13. ABSTRACT

Radar, aircraft, and surface measurement information is presented concerning the liquid-water-content values and size distribution properties of the hydrometeors that existed along the trajectory paths of the five SAMS missiles that were fired into Wallops storms during the 1971-72 season.

The storm situations are described by reference to weather maps, satellite photographs, and time-altitude cross sections. The radar-echo structure of the storms is illustrated by radar photographs. The hydrometeor conditions at the launch times of the missiles, in the launch direction, are assessed from surface rainfall information, from detailed radar data, and from aircraft measurements made during storm flights that immediately followed the missile firings. The procedures are explained whereby the values of liquid-water-content and the size-distribution parameters were determined for the missile trajectories. All data results of immediate, direct pertinence to SAMS are summarized in convenient, tabular form.

DD FORM 1 NOV 68 1473

Unclassified
Security Classification

14. KEY WORDS	LINK A		LINK B		LINK C	
	ROLE	WT	ROLE	WT	ROLE	WT
Rain erosion						
Precipitation physics						
Radar meteorology						
SAMS-ABRES						
Extra tropical storms						
Hydrometeors						
Hydrometeor/measurement						
Hydrometeor size distribution						
Hydrometeor liquid-water-content						
Wallops Island, Virginia						

Preface

The AFCRL program of measurements supporting the SAMS rain erosion project at Wallops Island, Virginia during the 1971-72 season was conducted as a joint team effort by various members of the Weather Radar and Convective Cloud Physics Branches of the Meteorology Laboratory, AFCRL. Contractual support was provided by the Applied Physics Laboratory of Johns Hopkins University and by Meteorology Research Inc., Altadena, California. The program was directed by Dr. Robert M. Cunningham, of the Convective Cloud Physics Branch, and supervised by Dr. Kenneth R. Hardy, of the Weather Radar Branch.

The AFCRL and contract contributors to the measurement program are identified in the following list, and their efforts toward the accomplishment of the SAMS objectives are acknowledged. In addition, special thanks are extended to Mr. Alfred A. Spatola for his help in assembling, reviewing, and criticizing the manuscript.

Name	Organization	Role
Dr. Morton L. Barad	LY*	Director, Meteorology Laboratory
Mr. Chankey N. Touart	LY	AFCRL Program Manager for Weather Erosion Programs June 1973 to present
Dr. Robert M. Cunningham	LYC**	Director of AFCRL Measurement Program at Wallops Island, Virginia
Dr. Kenneth R. Hardy	LYW†	Supervisor of AFCRL Radar Measurements Program at Wallops Island, Virginia

Name	Organization	Role
Mr. Kenneth M. Glover	LYW	
Mr. Graham M. Armstrong	LYW	
Mr. Edward F. Duquette	LYW	
Mr. Alexander W. Bishop	LYW	
Mr. Vernon G. Plank	LYC	
Lt. Col. James F. Church	LYC	
Mr. Alfred A. Spatola	LYC	
Ms. Barbara Main	LYC	
Mr. Donald W. McLeod	LYC	
Mr. Morton Glass	LYC	
Mr. George Ritscher	LYC	
Mr. Russell M. Peirce Jr.	LYC	
Mr. Konstantins Pocs	LYC	
CMSgt Thomas W. K. Hobbs	LYC	
Mrs. Elizabeth Kintigh	LYC	
TSgt James E. Bush	LYC	
Ms. JoAnne E. Waters	LYC	
MSgt Thomas W. Moraski	LYC	
SSgt Dennis E. Karoleski	LYC	
Sgt Curtis H. Waechtler	LYC	
Mr. Jack Howard	APL††	Radar Station Mgr. at Wallops Island, Virginia
Mr. Norris Beasley	APL	
Mr. Norm Gebo	APL	
Mr. Charles Ponder	APL	
Mr. Herbert Seeman	APL	
Mr. Norman Parker	APL	
Mr. Harold Lord	APL	
Mr. Richard Gagnon	APL	
Mr. Larry Greer	APL	
Dr. Isadore Katz	APL	
Dr. Thomas Konrad	APL	
Mr. James Meyer	APL	
Mrs. Ella Dobson	APL	
Mr. Donald Takeuchi	MRI†††	
Mr. Alfonso Ollivares	MRI	

Name	Organization	Role
Mr. Ralph Martin	MRI	
Mr. Larry Boardman	MRI	

*LY - Meteorology Laboratory, Air Force Cambridge Research Laboratories.

**LYC - Convective Cloud Physics Branch, Meteorology Laboratory.

†LYW - Weather Radar Branch, Meteorology Laboratory.

††APL - Applied Physics Laboratory, Johns Hopkins University, Silver Springs, Maryland.

†††MRI - Meteorology Research Inc., Altadena, California.

The SAMS (Sandia Air Force Materials Study) Program began in 1969 as a jointly funded effort between SAMSO/Air Force and Sandia Laboratories. By 1973 the program was being completely funded by SAMSO. The objective of the SAMS Program is to experimentally test the effects of precipitation and cloud particle (hydrometeor) impacts upon various full scale missile materials by flying high speed vehicles through actual storm and cloud environments. The test vehicle is launched at a relatively low elevation angle (typically 30°) and performs the impact erosion experiment during the ascending portion of its trajectory. The instrumented payload with its test nosetip and heatshield is subsequently recovered from the ocean by means of a parachute and flotation system.

The NASA Wallops Flight Center on the eastern shore of Virginia was selected for the site of these tests because it exhibits a relatively high frequency of occurrence of widespread stratiform storms, has the necessary support facilities, and is readily accessible. Storm environments are measured by instrumented aircraft and ground instruments including special weather radars. Further details of the test set up are contained in the SAMS Program Test Plan, by J.K. Cole, SC-DR-70-850, Sandia Laboratories, Albuquerque, New Mexico, December 1970, while test results are contained in various classified reports from Sandia Laboratories.

Contents

Contents

Illustrations

Tables

Tables

Tables

Liquid-Water-Content and Hydrometeor Size-Distribution Information for the SAMS Missile Flights of the 1971-72 Season at Wallops Island, Virginia - AFCRL/SAMS Report No. 3

1. INTRODUCTION

The liquid-water-content values and other associated hydrometeorological information for the trajectories of the SAMS missiles launched in the 1971-72 season are presented in this report, that were determined from radar, surface, and aircraft data obtained at Wallops Island, Virginia on the days of firing.

The dates, times, and circumstances of the missile launch operations are noted and the general weather conditions at the times of firing are indicated. The profiles of liquid-water-content and the integral of liquid-water-content pertaining to the trajectory paths of the missiles through the Wallops storms are presented that were determined from radar measurements. The values and variability of the precipitation rate and liquid-water-content at the surface level during the launch period are illustrated. The liquid-water-content values and size-distribution information acquired from aircraft measurements are summarized.

The report is organized such that the analytical results of immediate, direct pertinence to the erosion problem are presented in the main text. All background material and supplementary information are included in appendices. This format of presentation will be standard for all AFCRL/SAMS reports concerning data results.*

(Received for publication 1 July 1974)

*In accord with the agreement of the SAMS-ARRES Conference at AFCRL on 7-8 March 1974.

There are seven appendices, as identified in the Table of Contents. The weather, cloud, and precipitation situations on the days of the missile flights are discussed in Appendix A. The radar structure of the storms, in the launch directions, is illustrated in Appendix B. Values of the radar and hydrometeor parameters along the missile trajectories are described and tabulated in Appendix C. Surface measurements of precipitation rate and liquid-water-content are presented in Appendix D. The AFCRL, C-130 flights during the 1971-72 season are recounted in Appendix E, and the reasons explained why no missions were flown in the particular storms of the missile launchings. The aircraft storm data acquired by the Meteorology Research Inc. (MRI), Aztec aircraft are discussed in Appendix F. Size distribution information is provided in Appendix G, concerning the number concentration and liquid-water-content contribution of the various size-classes and types of hydrometeors along the missile trajectories.

The figures and tables of these appendices are presented in numerical order by "common subject", rather than by "storm date". This is advantageous, in fact almost necessary, for the logical discussion of the subject matter, but it poses difficulties for the reader who wishes to inspect and intercompare all of the measurement results pertaining to a single missile flight, or a single storm. The large number of the text figures and tables add to the difficulty. The author has attempted to alleviate these problems somewhat by having the "thumb edge pages" of the separate appendices indexed by "bleed printing". The beginning page number of each appendix, and the page number of each figure and table, are also listed in the front of the report, in the Table of Contents, the List of Figures, and the List of Tables.

It should be noted that the Wallops Island radars and the radar measurement techniques and calibration procedures were described in AFCRL/SAMS Report No. 1. The methods used to obtain liquid-water-content values from the radar data for the missile trajectories were discussed in AFCRL/SAMS Report No. 2. The uncertainties of measurement were also assessed in the latter report. These reports will subsequently be referenced as RNo. 1 and RNo. 2.

2. FLIGHT CIRCUMSTANCES AND WEATHER CONDITIONS

Five missiles were launched during the 1971-72 season. The first (Q25297, Unit No. R341403) was fired on 3 February 1972, at 1517 EST, into a storm associated with the passage of an open wave across the Wallops area. The second and third missiles (Q2-5298 and Q2-5299, Unit Nos. R341412 and R341404) were launched on 17 February 1972, at 1456 and 1515 EST, respectively, through the precipitation and clouds of an open-wave system that had passed south of the

Wallops vicinity about 8 hr previously. The fourth missile (Q2-5891, Unit No. R341413) was fired on 17 March 1972, at 1619 EST, into a storm caused by an occluded wave and cold front that had passed north of Wallops about 6 hr prior. The fifth and last missile of the season (Q2-5892, Unit No. R341405) was launched through shower-type clouds associated with a cold front and trailing squall line.

The missiles were of the two-stage, Terrier-Recruit type. They were fired from "Launch Pad Zero" in the 146° azimuth direction. The purposes of the flights, concerning erosion objectives, also the details of the missile instrumentation, the flight parameters, and the erosion results have been reported by Cole, Church, Marshall, and Rollsten, of the Sandia Laboratories, Albuquerque, N.M.

The storm conditions at the launch times, and before and after launch, are illustrated in Appendix A. Surface weather maps for the Eastern United States are shown for the times closest to the launch times and for times 3 hr prior and subsequent. Photographs from the ATS-3 and ESSA-9 satellites are presented which reveal the visual appearance of the storms. Time-altitude cross sections are also presented that depict the hydrodynamic composition of the storms.

The radar structure of the storms in the 146° launch direction of the missiles, at the launch times, is illustrated in Appendix B. RHI, "gray scale" photographs are shown which reveal the cross-sectional appearance of the integration signals (the $\underline{I}$ signals, see R No. 1) received from the storms.

3. PROFILES OF LIQUID-WATER-CONTENT AND INTEGRAL OF LIQUID-WATER-CONTENT FOR THE MISSILE TRAJECTORIES, AS DETERMINED FROM RADAR DATA

The solid-line profiles of Figures 1 through 5 show the radar-determined values of liquid-water-content (M) versus altitude for the five missile flights of the 1971-72 season. The values pertain to the missile trajectory, but they are plotted versus the altitude of the trajectory points above the ground (or sea) level. The range distances of the trajectory points from the RARF site of the radar measurements are listed in Tables C1 through C5. (The range distances from the launch pad can be obtained from the listed values by subtracting 1.8 N.M., or 3.3 km.)

The dashed-line profiles of Figures 1 through 5 show the values of the integral of liquid-water-content ($\int M\, dR_s$) which have been integrated, cumulatively, from the launch pad upward, along the course of the missile trajectories to the storm top altitudes. The maximum "total storm passage" value of the integral is indicated at the top of each profile by the drafted numbers. The units of the integral are gm m^{-2}. Hence, the values, in effect, pertain to a "tube" of unit (1 m^2) cross section that is circularly symmetric about the trajectory line of the missile

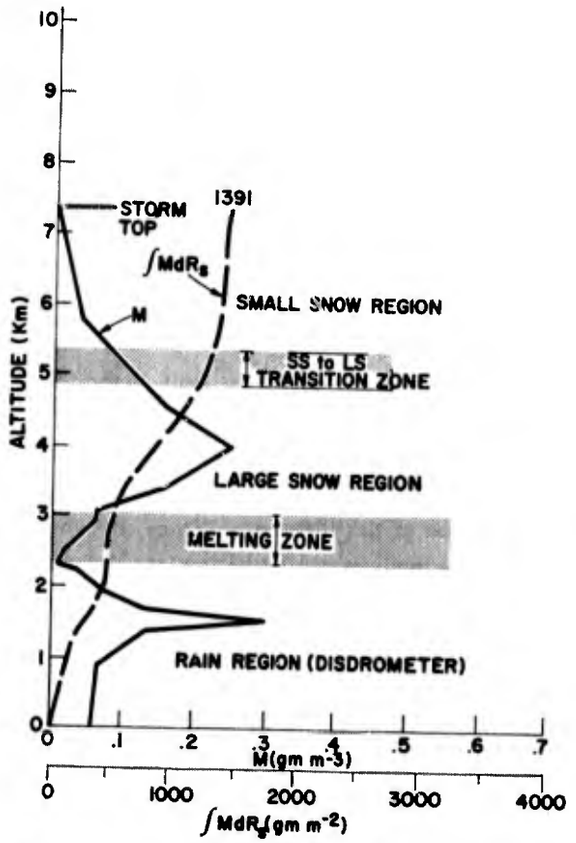

Figure 1. Profiles of Liquid-Water-Content and Integral of Liquid-Water for the Missile Trajectory of Flight Q2-5297 (Unit No. R341403) of 3 February 1972, Launched at 2017:00 GMT

and follows the trajectory. The amounts of liquid water actually intercepted by the missiles, per path distance, can be readily determined from the integral values of the profiles through knowledge of the missile cross section. The assumptions and equations used to compute the values of the integral were discussed in R No. 2.

The hydrometeor regions and transition zones of the storms are also indicated in Figures 1 through 5. These regions and zones were established from aircraft observations and/or radiosonde temperatures. The letter symbols used in the figures are identified in Table 1. This table additionally lists the empirical equations involving P vs Z, M vs Z, and M vs P (see R No. 2), that were employed in the liquid-water-content computations for the different hydrometeor categories and types defined for the 1971-72 season. The definitions are consistent with those of Table 2, R No. 2.

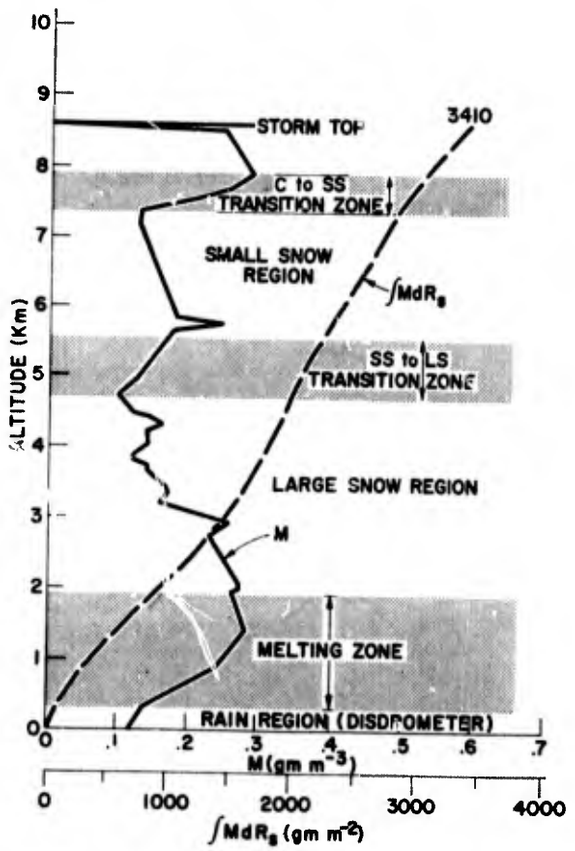

Figure 2. Profiles of Liquid-Water-Content and Integral of Liquid-Water for the Missile Trajectory of Flight Q2-5298 (Unit No. R341412) of 17 February 1972, Launched at 1456:00 GMT

Profiles of the radar integration signal, $\underline{\overline{I}}$, of the radar reflectivity factors for water and ice hydrometeors, Z_W and Z_I, and of the precipitation rate, P, are presented in Figures C1 through C15 of Appendix C. These parameters are the ones of direct radar measurement ($\overline{I}$) or ones essential to the computations of liquid-water-content, as explained in R No. 2. The profiles provide background and auxiliary information about the hydrometeor conditions along the missile trajectories.

The numerical values of these parameters, also the liquid-water-content values, are listed in Tables C1 through C5 for each data point altitude along the trajectories.

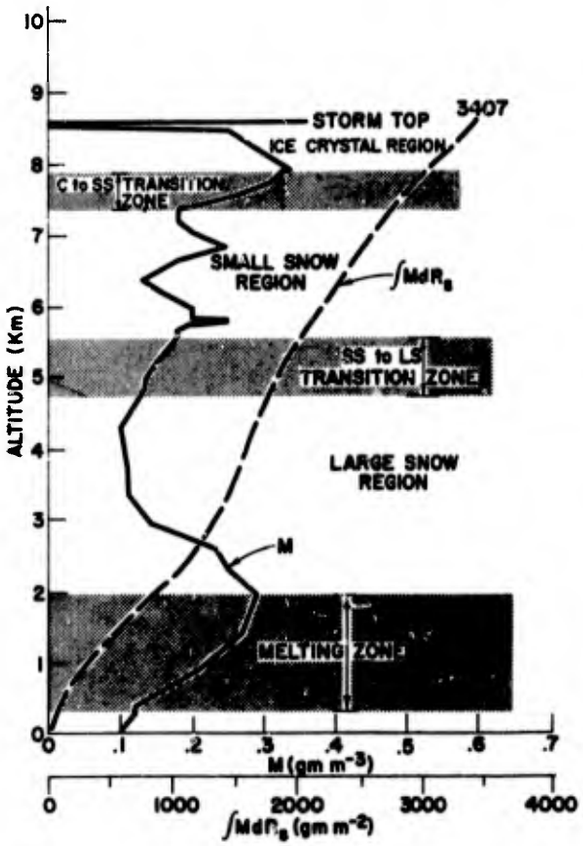

Figure 3. Profiles of Liquid-Water-Content and Integral of Liquid-Water for the Missile Trajectory of Flight Q2-5299 (Unit No. R341404) of 17 February 1972, Launched at 1512:00 GMT

4. CLOUD LIQUID-WATER-CONTENT VALUES FOR THE MISSILE TRAJECTORIES

In addition to the liquid-water-content values measured by the radar, which pertain to hydrometeors of precipitation size (drop diameters, or equivalent melted diameters, larger than about 80 microns), there is substantial liquid-water-content present in the Wallops storms in the cloud size-range of the hydrometeor spectrum (drop diameters smaller than about 80 microns). Aircraft measurements are required to determine the liquid-water-content values for these cloud-size droplets and particles.

Aircraft measurement and analytical information about cloud liquid-water-contents was rather sparse in the 1971-72 season. The AFCRL, C-130A aircraft

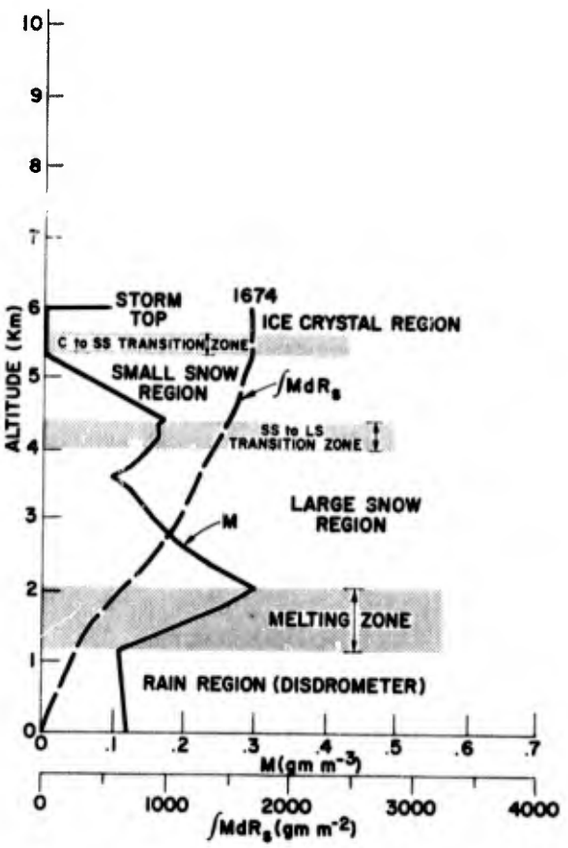

Figure 4. Profiles of Liquid-Water-Content and Integral of Liquid-Water for the Missile Trajectory of Flight Q2-5891 (Unit No. R341413) of 17 March 1972, Launched at 2119:00 GMT

was unable to make measurements in the storms into which the missiles were fired (see Appendix E). The MRI, Aztec aircraft flew in each of the storms, but its ceiling altitude prohibited measurements above 23,000 ft. Certain portions of the instrumental records of the Aztec were analyzed, and particular sample values of cloud size-distribution and liquid-water-content were determined. These samples are discussed and presented in Appendix F. Our best estimates of the cloud liquid-water-content values that pertain to the path trajectories of the missiles at the times of the missile firings are summarized in Tables C1 through C5 of Appendix C, also in Tables G2 through G6 of Appendix G. (The altitude points of the Appendix C tables are those of the radar measurement, whereas the altitude points of the Appendix G tables are for every 250 meters of altitude, from surface level to storm top.)

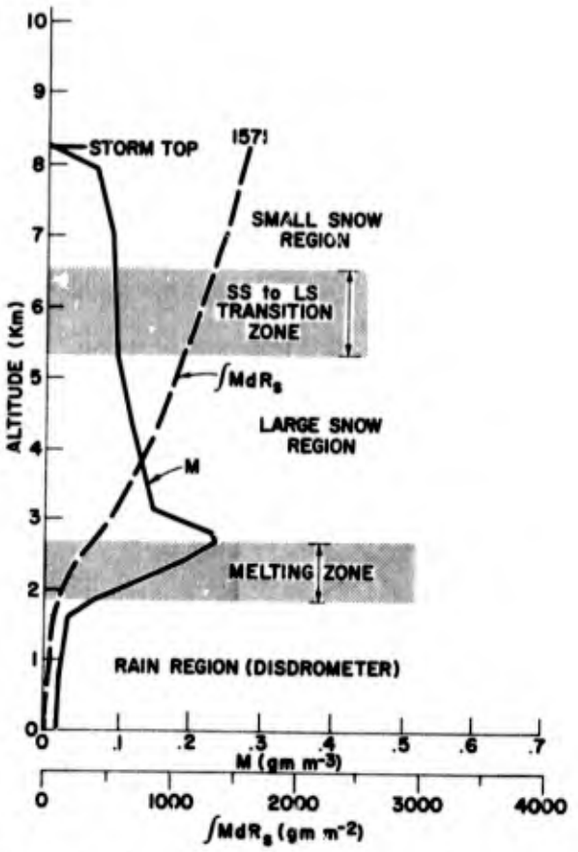

Figure 5. Profiles of Liquid-Water-Content and Integral of Liquid-Water for the Missile Trajectory of Flight Q2-5892 (Unit No. R341405) of 22 March 1972, Launched at 1548:00 GMT

5. COMMENTS

Because of the paucity of aircraft measurement data in the 1971-72 season, spectral information concerning the size-distribution of the number-concentration and liquid-water-content (contribution) of the hydrometeors along the missile trajectories was estimated from theoretical distribution functions of double-truncated type, as described in Appendix G. Three "distribution models" were used, one for the precipitation size-range of the hydrometeors, one for the cloud size-range, and one for the melting zone (where two different types of hydrometeors co-exist—fully-melted-liquid drops and water-coated-ice particles).

The results of these estimations, which are presented in Tables G2 through G6, are believed to be reasonably descriptive of the probable conditions along the missile trajectories.

Table 1. Hydrometeor Regions, Types and Equations Used in the 1971-72 Season. See R No. 2 for Description of How Equations Were Interpolated Across the Melting Zone and the Other Transition Zones. Note That No Ice Crystal Region Was Present at the Storm-Top Exit-Points of the Missiles on 3 February and 22 March 1972

Date of Storm	Hydrometeor Region or Zone	Symbol	Altitude Limits km	Equation Relating P and Z E_P i.e., $P = K_P Z^{E_P}$	Equation Relating M and P i.e., $M = kP^{\epsilon}$	Equation Relating M and Z E_M i.e., $M = K_M Z^{E_M}$
3 February 1972 Missile No. Q2-5297	Rain Region	R	Sfc. to 2.32	$P = .0181\ Z^{.698}$	$M = .0562\ P^{.91}$	$M = .00146\ Z^{.635}$
	Melting Zone	MZ	2.32 to 2.90			
	Large Snow Region	LS	2.90 to 4.85	$P = .0311\ Z^{.454}$	$M = .254\ P^{.847}$	$M = .01345\ Z^{.385}$
	SS to LS Transition Zone	SS-LS	4.85 to 5.33			
	Small Snow Region	SS	5.33 to 7.32	$P = .0365\ Z^{.625}$	$M = .250\ P^{.860}$	$M = .0145\ Z^{.538}$
17 February 1972 Missile No. Q2-5298	Rain Region	R	Sfc. to .335	$P = .0316\ Z^{.615}$	$M = .0664\ P^{.800}$	$M = .00419\ Z^{.490}$
	Melting Zone	MZ	.335 to 1.92			
	Large Snow Region	LS	1.92 to 4.72	$P = .0311\ Z^{.454}$	$M = .254\ P^{.847}$	$M = .01345\ Z^{.385}$
	SS to LS Transition Zone	SS-LS	4.72 to 5.55			
	Small Snow Region	SS	5.55 to 7.35	$P = .0365\ Z^{.625}$	$M = .250\ P^{.860}$	$M = .0145\ Z^{.538}$
	C to SS Transition Zone	C-SS	7.35 to 7.86			
	Crystal Region	C	7.86 to 8.53	$P = .100\ Z^{.719}$	$M = .206\ P^{.735}$	$M = .038\ Z^{.529}$
17 February 1972 Missile No. Q2-5299	Rain Region	R	Sfc. to .335	Equations for all hydrometeor regions are identical to those for Missile No. Q2-5298 above.		
	Melting Zone	MZ	.335 to 1.92			
	Large Snow Region	LS	1.92 to 4.72			
	SS to LS Transition Zone	SS-LS	4.72 to 5.55			
	Small Snow Region	SS	5.55 to 7.35			
	C to SS Transition Zone	C-SS	7.35 to 7.86			
	Crystal Region	C	7.86 to 8.53			
17 March 1972 Missile No. Q2-5891	Rain Region	R	Sfc. to 1.14	$P = .0293\ Z^{.675}$	$M = .0745\ P^{.846}$	$M = .00376\ Z^{.571}$
	Melting Zone	MZ	1.14 to 2.03			
	Large Snow Region	LS	2.03 to 4.15	$P = .0311\ Z^{.454}$	$M = .254\ P^{.847}$	$M = .01345\ Z^{.385}$
	SS to LS Transition Zone	SS-LS	4.15 to 4.39			
	Small Snow Region	SS	4.39 to 5.33	$P = .0365\ Z^{.625}$	$M = .250\ P^{.860}$	$M = .0145\ Z^{.538}$
	C to SS Transition Zone	C-SS	5.33 to 5.64			
	Crystal Region	C	5.64 to 5.94	$P = .100\ Z^{.719}$	$M = .206\ P^{.735}$	$M = .038\ Z^{.529}$
22 March 1972 Missile No. Q2-5892	Rain Region	R	Sfc. to 1.86	$P = .0154\ Z^{.734}$	$M = .0595\ P^{.909}$	$M = .00134\ Z^{.667}$
	Melting Zone	MZ	1.86 to 2.68			
	Large Snow Region	LS	2.68 to 5.33	$P = .0311\ Z^{.454}$	$M = .254\ P^{.847}$	$M = .01345\ Z^{.385}$
	SS to LS Transition Zone	SS-LS	5.33 to 6.55			
	Small Snow Region	SS	6.55 to 8.23	$P = .0365\ Z^{.625}$	$M = .250\ P^{.860}$	$M = .0145\ Z^{.538}$

Appendix A

Synoptic Weather Maps, Satellite Photographs, and Storm Cross Sections

Surface weather maps for the Eastern United States are presented in Figures A1 through A4 for each of the Wallops storms of the 1971-72 season through which missiles were fired. There are three maps in each figure, for the times

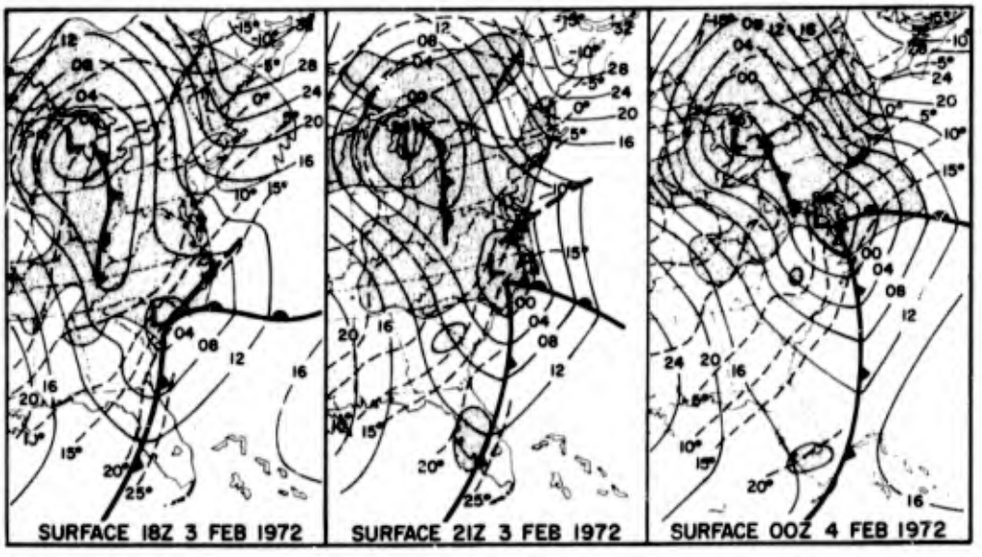

Figure A1. Surface Weather Maps for the Eastern United States for 1800, 2100, and 2400 GMT, 3 February 1972

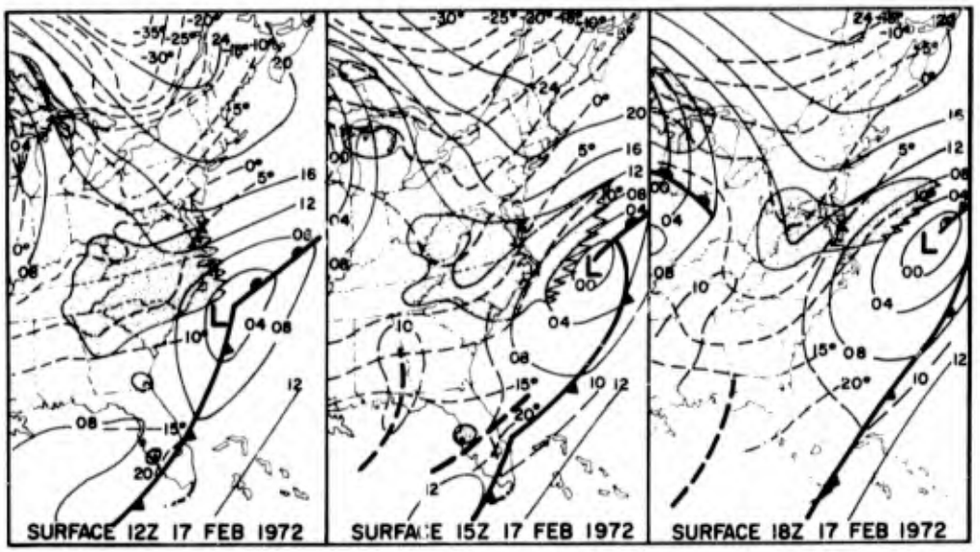

Figure A2. Surface Weather Maps for the Eastern United States for 1200, 1500, and 1800 GMT, 17 February 1972

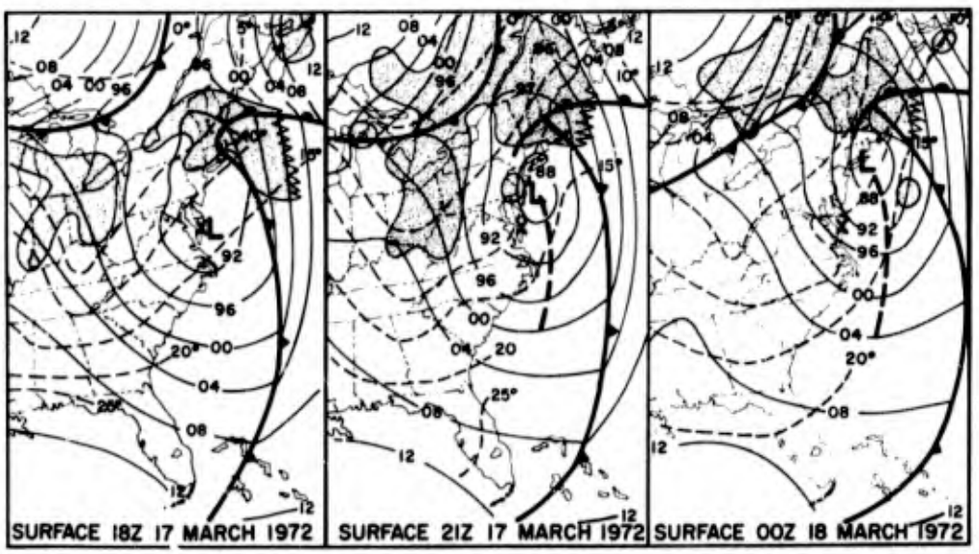

Figure A3. Surface Weather Maps for the Eastern United States for 1800, 2100, and 2400 GMT, 17 March 1972

closest to the launch times and for times 3 hr previous and 3 hr subsequent. The isobars, fronts, and precipitation areas are shown on these maps.

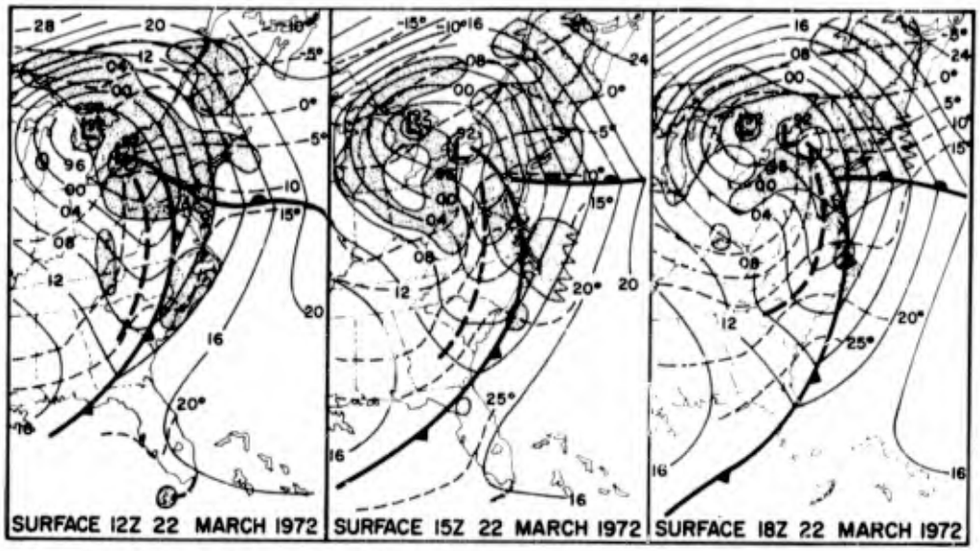

Figure A4. Surface Weather Maps for the Eastern United States for 1200, 1500, and 1800 GMT, 22 March 1972

Satellite photographs are illustrated in Figures A5 through A10 that reveal the appearance of the cloud shields associated with the storms. The dates and times are indicated, and the location of Wallops Island is shown on each photograph by a drafted "X". The photographs of Figures A5, A7, A9, and A10 were obtained from the synchronous satellite, ATS-3; those of Figures A6 and A8 were acquired from the polar-orbiting satellite, ESSA-9. The photographs for the storms of 3 February and 17 March 1972 were taken some 2 to 4 hr prior to the launch times; those for 17 February and 22 March were recorded fairly close to the launch times, within an hour or so.

Time-altitude cross sections are displayed in Figures A11 through A14 which depict the general cloud and precipitation structure of the storms that passed across the Wallops Island location. The cross sections pertain to 24-hr periods beginning at 00 Z on the days of the missile firings, and ending at 00 Z on the days after the firings. It should be noted that time increases from right to left across the abscissa scales of the figures and that the particular times of missile launching are indicated by drafted arrows. The isotherms, winds, and surface weather reports are also shown on the figures, the latter two being coded in accord with standard meteorological convention (see Federal Meteorological Handbooks of Surface and Winds Aloft Observations, Circulars N and O, U.S. Department of Commerce, Washington, D.C.).

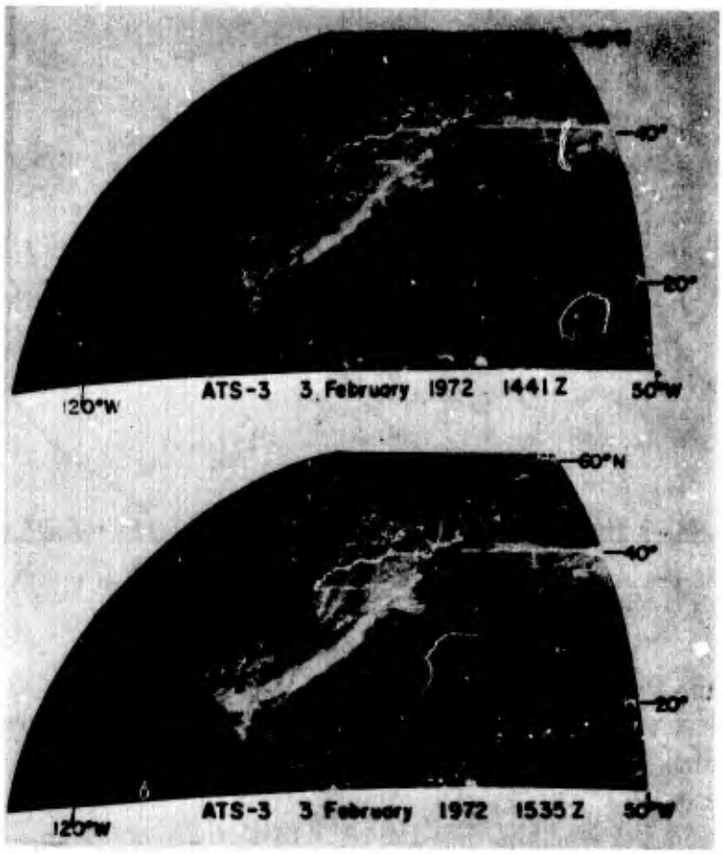

Figure A5. Photographs Obtained From the Synchronous Satellite, ATS-3, Showing the Cloud System Associated With the Storm of 3 February 1972

All of the aircraft flights on the missile launch days of the 1971-72 season were accomplished by the Aztec aircraft of Meteorology Research, Inc. (MRI), see Appendix F. The voice comments of the pilot of this aircraft concerning the storm conditions at the different flight levels were rather sparce, because he, being the only person aboard who was in a location suitable for observations, was mostly preoccupied with the problems of flight and navigation.

The principal characteristics of the four individual storms of the season are described below. The descriptions are based on the figures and tables referenced above, plus other synoptic, radar and aircraft information not specifically presented herein.

Figure A6. Photograph Obtained From the Polar-Orbiting Satellite, ESSA-9, Showing the Cloud System Associated With the Storm of 3 February 1972

The first storm of the season through which a missile was fired occurred on 3 February 1972. This storm was associated with an open-wave system that was traveling in a northeasterly direction and that passed about 200 mi south of Wallops. The cloud shield of the storm some 3 hr before the launch time (see Figure A6), had a visually "solid" appearance on the satellite photograph which extended out to at least a 200 mi radius from Wallops in all directions. The storm top at launch time (see Figure A11), was located at an altitude of about 24,000 ft. The top structure, we would judge, was relatively smooth and homogeneous (see Figure B1). The storm interior was also relatively homogeneous, in the sense that there were no obvious, pronounced layers of clouds or "growth discontinuities" in the falling, developing populations of precipitation particles. No layers of turbulence were reported by the aircraft pilot.

The precipitation area of the storm at the surface level at the synoptic scale (see Figure A1), was located principally to the north of Wallops during the time of storm passage. Thus, just the southern portion of the area crossed Wallops.

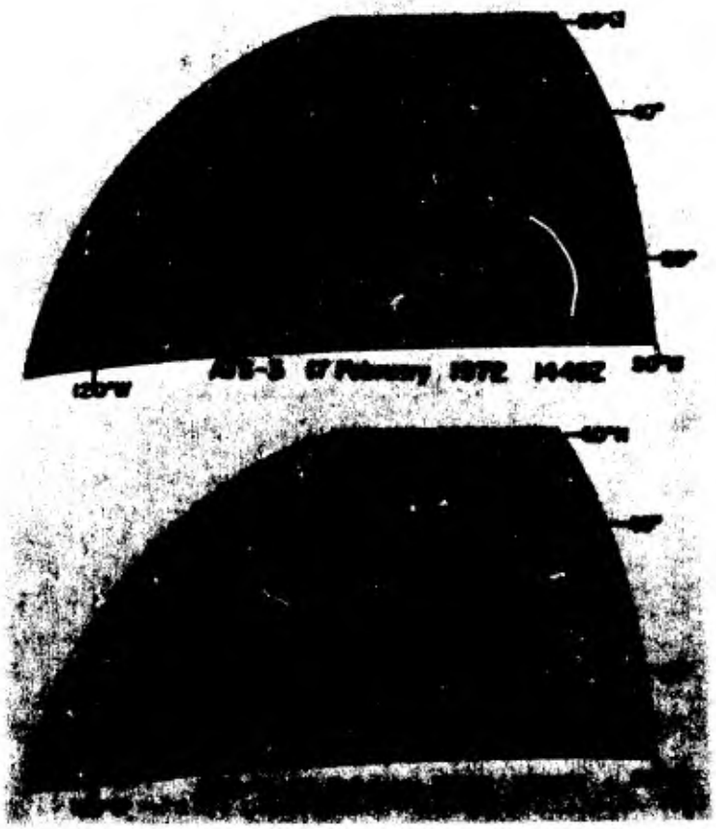

Figure A7. Photographs Obtained From the Synchronous Satellite, ATS-3, Showing the Cloud System Associated With the Storm of 17 February 1972

The surface rainfall at Wallops first began at about 17:30 Z, some 3 hr before the time of the missile launch (at 20:17 Z). The precipitation rates during the 1-hr period preceding launch ranged from about 0.7 to 5 mm hr^{-1}. At launch time, the rate was 1.2 mm hr^{-1} and the liquid-water-content of the precipitation was 0.06 gm m^{-3}. The rain gauges of the surface network revealed that the precipitation was quite uniform, spatially and temporally, at the firing time of the missile. (Reference is made to Figures 1, C11, D2, and D3, which provide the bases for these comments.)

The second operational storm of the season occurred on 17 February 1972. Two missiles were launched into this storm with a firing time separation of 16 min. The storm was associated with an open-wave system that had passed south of the Wallops Island vicinity (some 300 mi south) about 8 hr prior to the launch times.

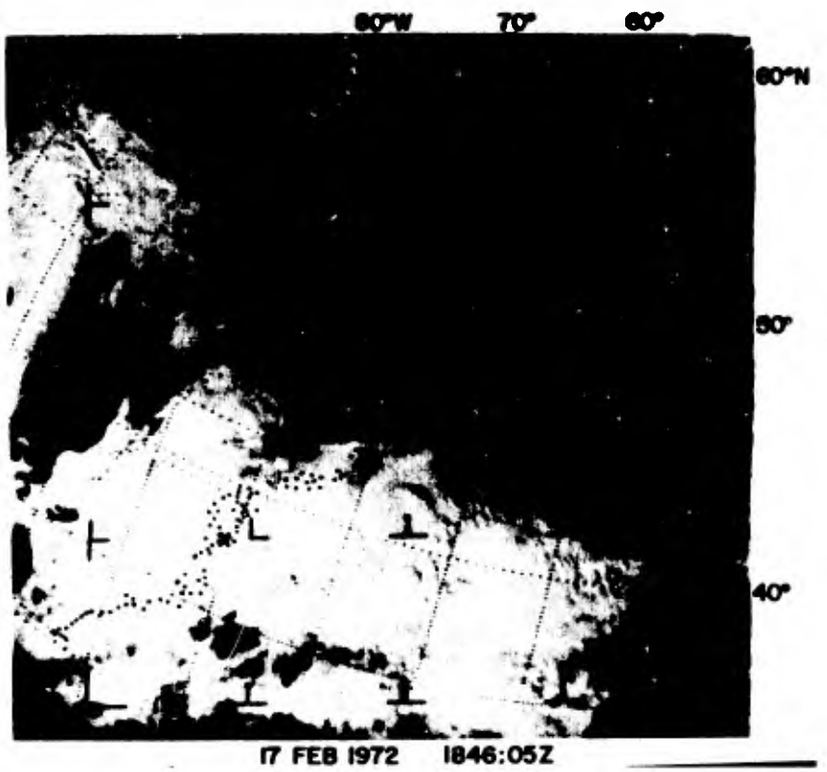

Figure A8. Photograph Obtained From the Polar-Orbiting Satellite, ESSA-9, Showing the Cloud System Associated With the Storm of 17 February 1972

At the launch times, the clouds of the storm existed primarily along the southern Atlantic coast and to the west, north, and east of Wallops (see Figure A7). The precipitation area at the surface level was located west of the low center and Wallops lay at the northern extremities of the area (see Figure A2).

The storm top at launch time extended to an altitude of about 28,000 ft and the top structure, as best judged, was probably smooth and relatively uniform. The interior of the storm was seemingly homogeneous, at least from the evidence of the radar structure (see Figure B2) and the aircraft pilot reports for altitudes below 23,000 ft. No turbulence was reported by the pilot.

The surface rainfall at Wallops began at approximately 13:00 Z, about 2 hr prior to the launch times. The precipitation rates over the rain-gauge network during the 1-hr period preceding and encompassing the launch times were relatively uniform. The variations were mostly in the range from 1.2 to 4 mm hr^{-1}. The precipitation rate at the launch pad at the time of the first missile firing

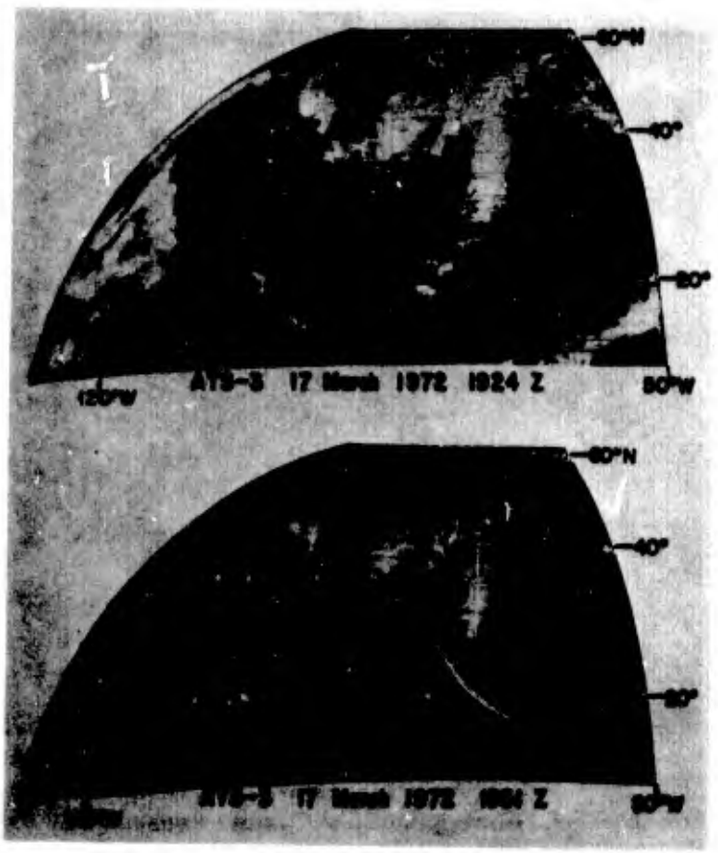

Figure A9. Photographs Obtained From the Synchronous Satellite, ATS-3, Showing the Cloud System Associated With the Storm of 17 March 1972

(at 14:56 Z) was 2.1 mm hr^{-1}; the liquid-water-content of the precipitation was 0.12 gm m^{-3}. The precipitation rate at the time of the second firing (at 15:12 Z) was 1.8 mm hr^{-1}; the liquid-water-content was 0.10 gm m^{-3}. (See Figures 2, 3, C12, C13, D4, and D5.)

The third storm of the season on 17 March 1972 was associated with an occluded wave and cold front that had passed Wallops about 6 hr prior to the launch time. The low center of the storm system was located about 100 mi NE of Wallops at the time of firing, and a trough line extended to the south from this low center (see Figure A3). The satellite pictures of Figure A9 reveal that the cloud coverage of the storm was located primarily along the course of the cold front off the Atlantic coast and to the west, north, and east of the low center at the surface level. There was a relatively short band of clouds which followed the

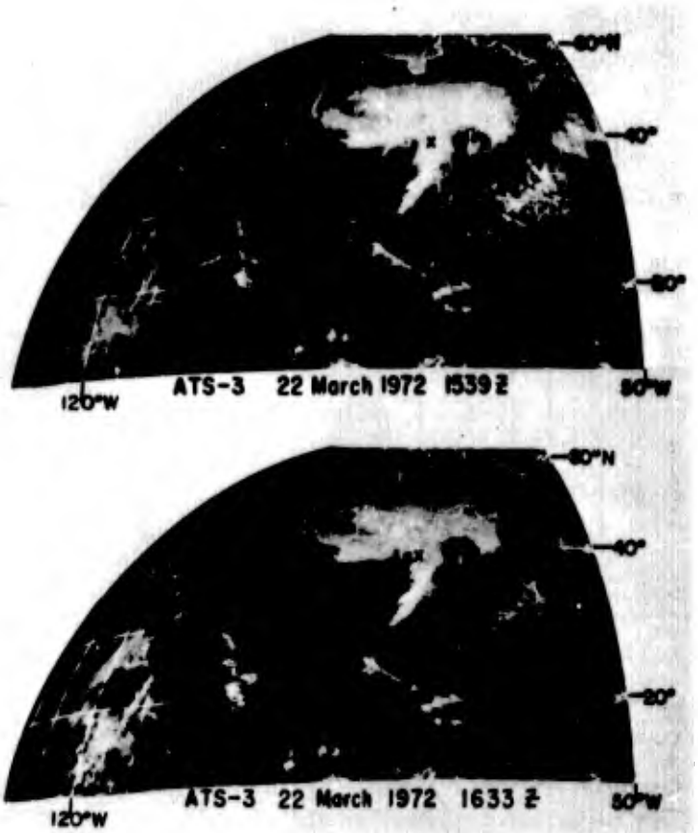

Figure A10. Photographs Obtained From the Synchronous Satellite, ATS-3, Showing the Cloud System Associated With the Storm of 22 March 1972

course of the "bent back" occlusion to the north, which crossed the low center and which were located behind the trough line shown on the weather map, at least along its northernmost portion. The SAMS missile on 17 March 1972 was launched into the clouds and precipitation of this band.

At launch time the clouds of the band extended to 20,000 ft and the top structure was convective and undulatory, as shown by the radar (see Figure B3), and reported by the aircraft pilot. The clouds and precipitation, internally within the band, also evidenced appreciable spatial and temporal variability. The radar showed the presence of numerous "cells" of echo return, and the aircraft measurements revealed considerable parameter variation along the traverse paths, and with altitude and time.

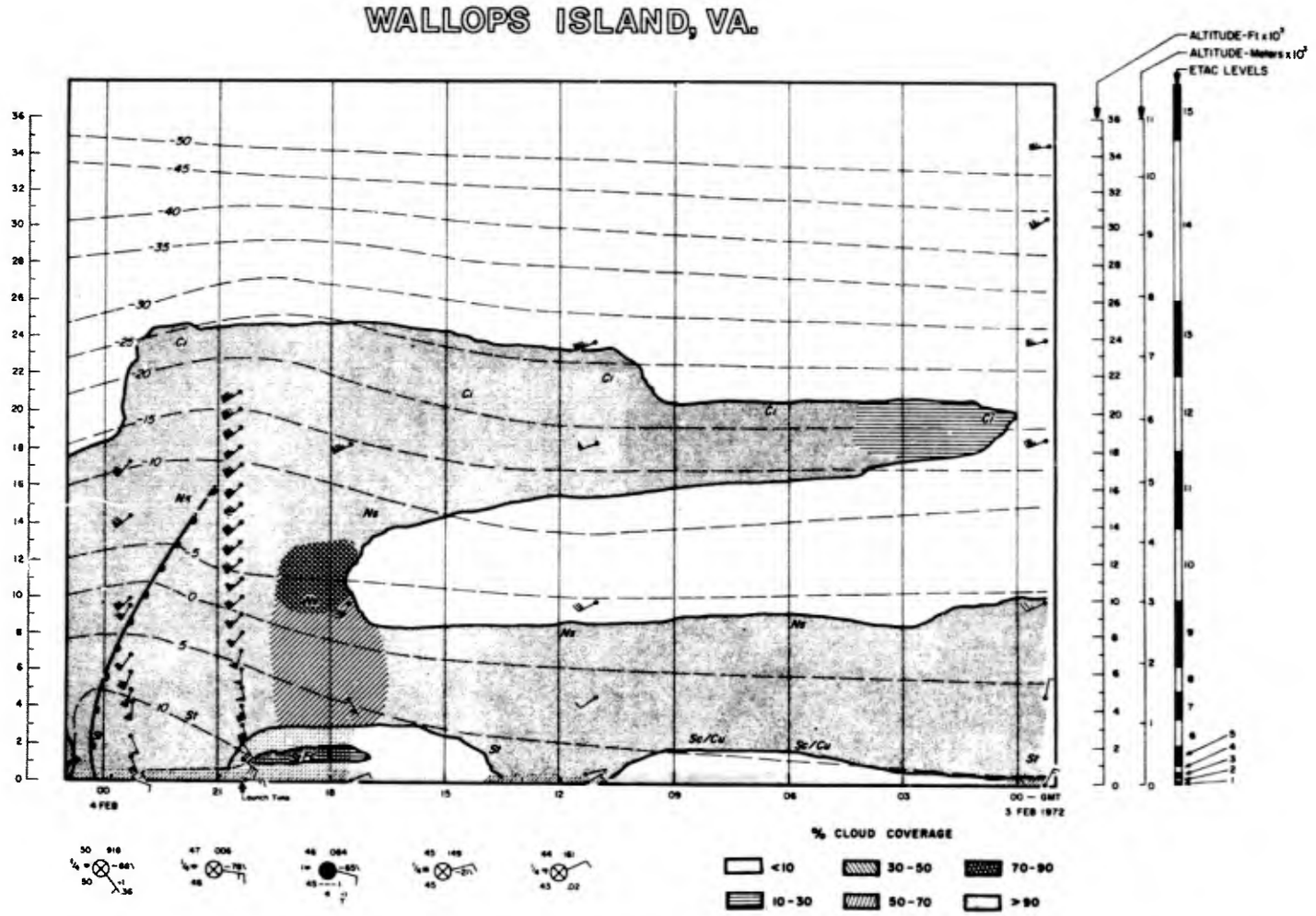

Figure A11. Time-Altitude Cross Section for the Wallops Storm of 3 February 1972, for the Time Period 00 GMT to 2400 GMT

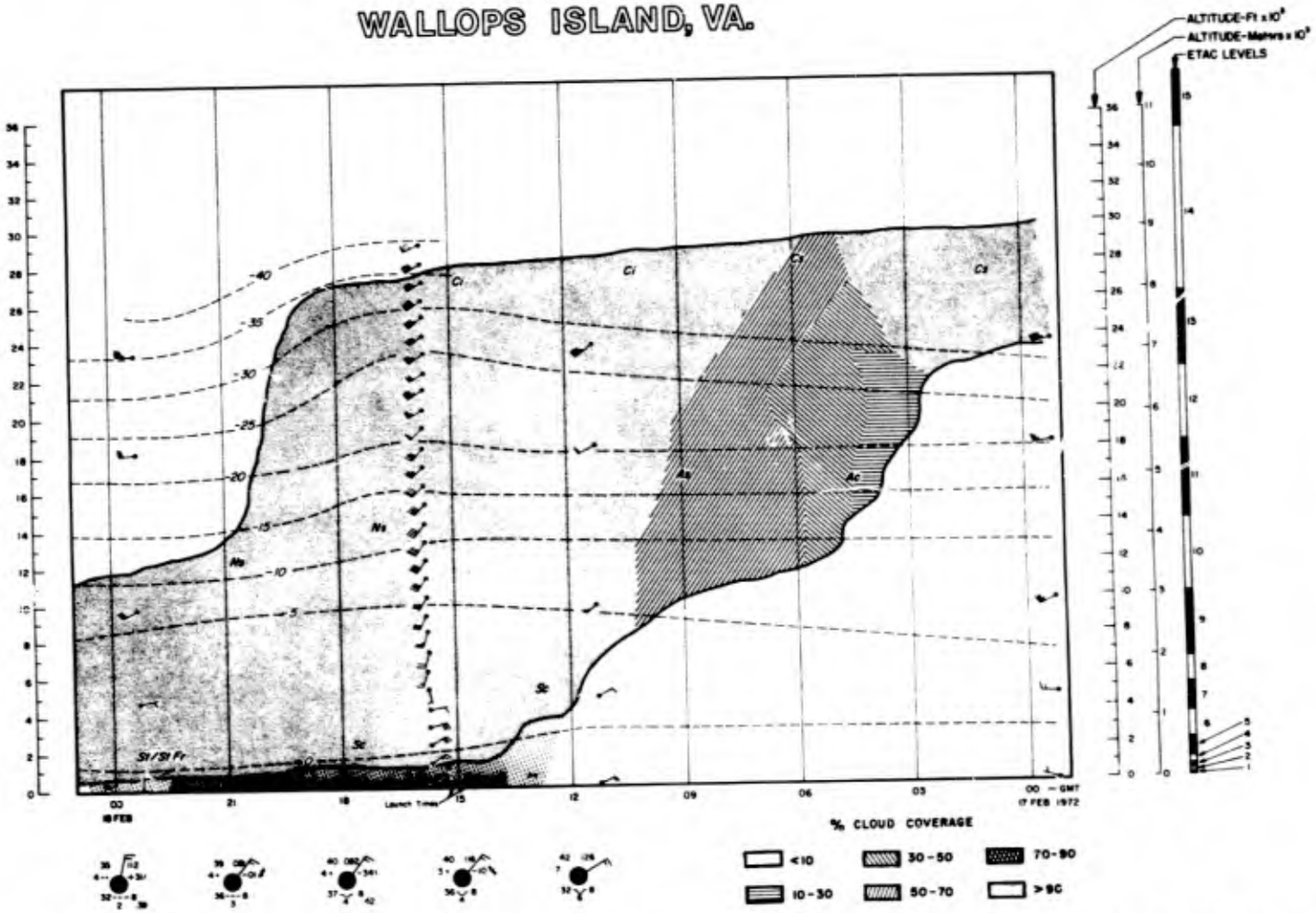

Figure A12. Time-Altitude Cross Section for the Wallops Storm of 17 February 1972, for the Time Period 00 GMT to 2400 GMT

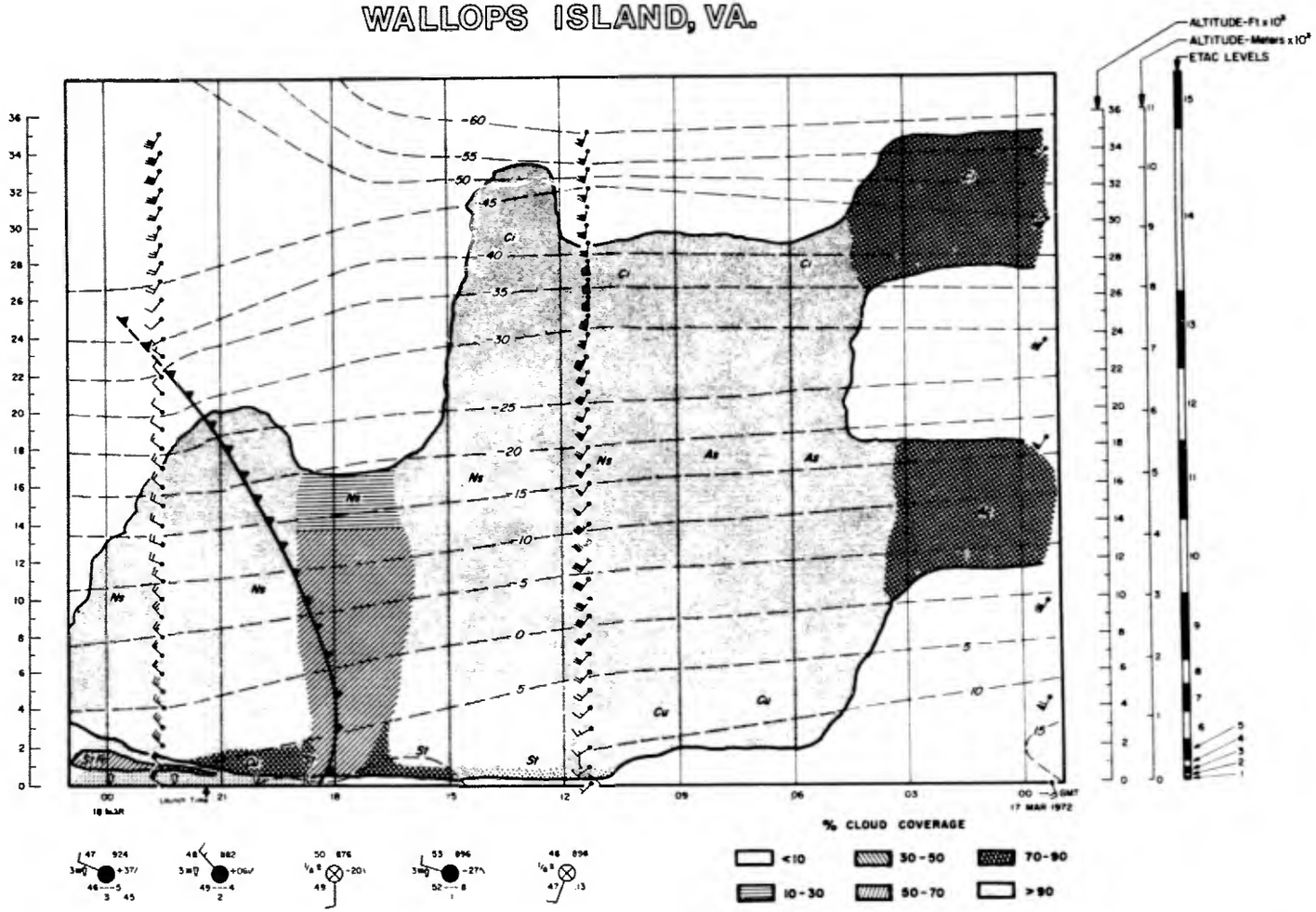

Figure A13. Time-Altitude Cross Section for the Wallops Storm of 17 March 1972, for the Time Period 00 GMT to 2400 GMT

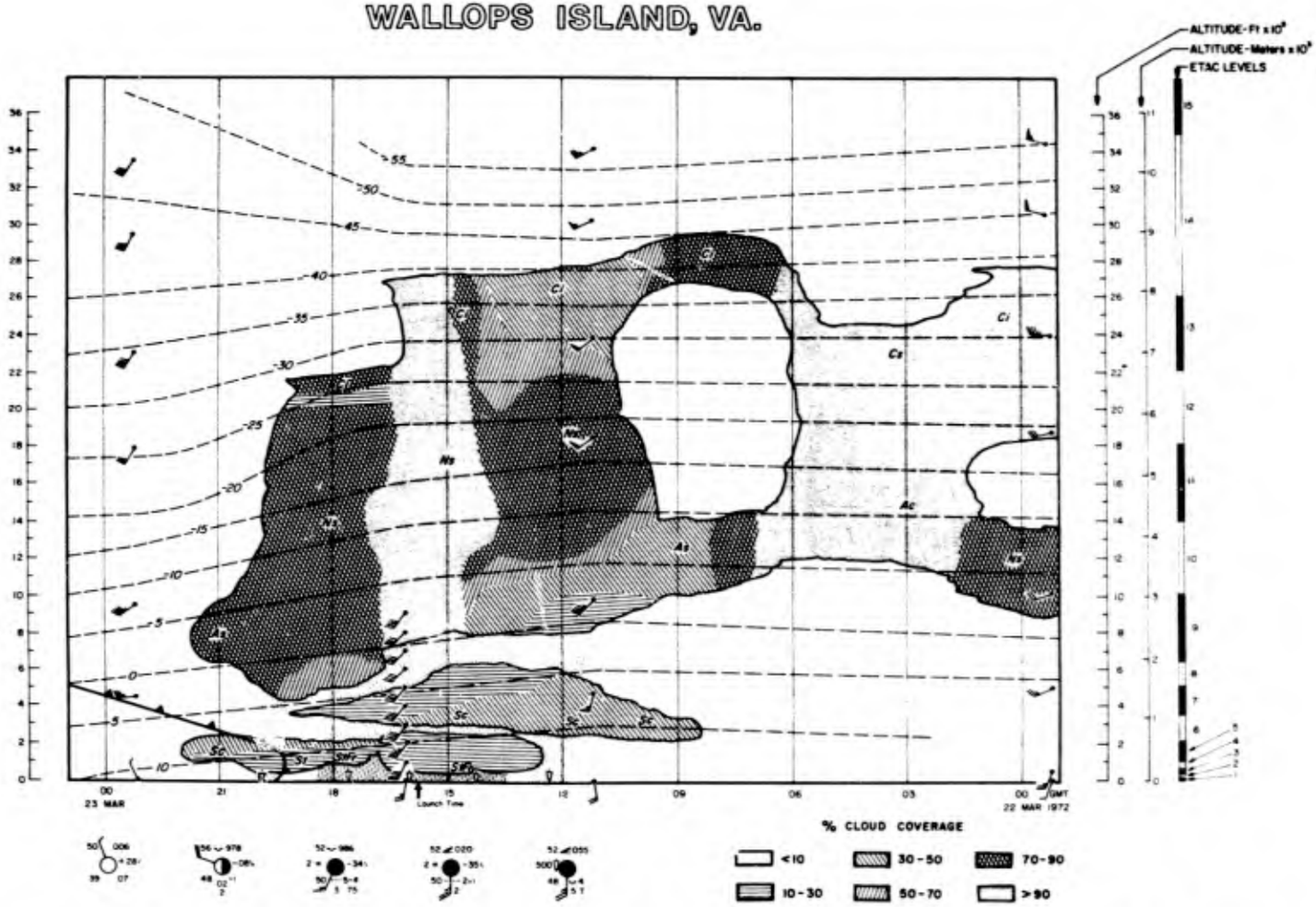

Figure A14. Time-Altitude Cross Section for the Wallops Storm of 22 March 1972, for the Time Period 00 GMT to 2400 GMT

The surface precipitation began at about 18:30 Z at Wallops on this day. The precipitation rates of the rain gauge network during the 1-hr period before and including launch were more variable than in the two previous storms. They ranged from about 0.04 to 20 mm hr^{-1}. The rates at the different sites of the network increased and decreased more or less in concert, indicating that the precipitation cells within the band were substantially larger than the spacing of the rain gauges. The precipitation rate at the launch pad at the time of firing (at 21:19 Z) was 1.8 mm hr^{-1}; the liquid-water-content of the precipitation was 0.12 gm m^{-3}. (See Figures 4, C14, D6, and D7.)

The last storm of the launch season occurred on 22 March 1972. A cold front extending southward from a low center over Lake Ontario passed Wallops about 19:30 Z on this day, and the missile was launched into the convective clouds associated with the front. The cloud band, which can be seen in the satellite photographs of Figure A10, was located ahead of the front and had a width of about 150 mi in the direction normal to the front.

The particular clouds of this band which existed over Wallops at the launch time extended to 27,000 ft altitude. The radar and aircraft measurements revealed substantial spatial and temporal variability of convective type within the frontal band (see Figure B4). The missile was launched into one of the convective cells.

The surface precipitation at Wallops began at about 13:30 Z, although there was some shower activity earlier at 12:00 Z. The precipitation rates as can be seen from Figures D8 and D9 were highly variable during the 1-hr period before and including launch. The rates ranged from 0 to 3 mm hr^{-1}. In fact, at the time of firing, at 15:48 Z, the rain rate at the launch pad was undergoing a marked increase, from values of about 0.1 to 0.3 mm hr^{-1}, 30 sec or so before firing, to values of about 12 mm hr^{-1}, 5 min after firing. The rain rate at launch time was estimated to be 0.3 mm hr^{-1}; the liquid-water-content of the precipitation was estimated to be 0.02 gm m^{-3}. (See Figures 5, C15, D8, and D9.)

Appendix B

Radar Structure of the Storms at the Missile Launch Times

The radar equations and measurement techniques employed in the SAMS rain erosion program at Wallops Island, Virginia have been summarized in RNo. 1. The radars and video-integration procedures used during the 1971-72 season were indicated in Section 4.2 of this report. The calibration methods were explained in Sections 3.3 and 3.4. Calibration data for the 1971-72 season were presented in Tables 4, 6, and 9.

The RHI photographs that were obtained with the FPS-18 radar at the launch times of the missiles that were fired into the storms of the 1971-72 season are shown in Figures B1 through B4 of this appendix. The approximate course of the missile trajectories across the photographs is shown. The threshold settings of the video integrator and the "gray scale shading information" pertaining to the photographs are noted in Table B1.

The RHI photographs that were acquired with this radar during the periods immediately preceding launch, and subsequent to launch, are presented in Figures B5 through B8. The photographs were selected, insofar as possible, to have the same threshold settings and "gray scale shading" as the launch time photographs for the same days.

Figures B1 and B5 show that the storm of 3 February 1972 was relatively homogeneous during the launch period. The echo tops of the storm extended to

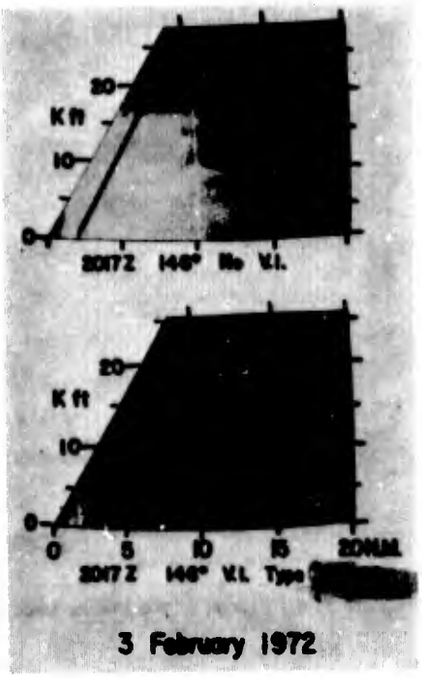

Figure B1. RHI Photographs Obtained With the FPS-18 Radar on 3 February 1972 at the Launch Time and in the Launch Direction of the Missile

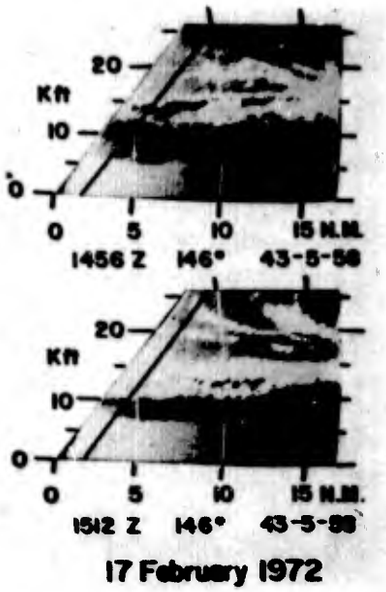

Figure B2. RHI Photographs Obtained With the FPS-18 Radar on 17 February 1972 at the Launch Times and in the Launch Directions of the Two Missiles Fired on This Day

about 20,000 ft (ATPVITS)* and a pronounced bright band was located at about 8000 to 10,000 ft altitude. It should be noted, however, that there is less "definition detail" in the photographs for this storm than in those for the other storms because a 10-db "threshcld spacing" of the gray-scale levels was used for the photographs of this day, as opposed to a 5-db spacing that was used for most of the photographs of the other days (see Table B1). It should also be noted that the white horizontal line shown in the upper part of the photographs, which is the altitude contour for the 20,000 ft level, only demarks this altitude to an accuracy of about ±200 ft, or so. (This comment likewise pertains to the RHI photographs of the other storm days. Range-altitude calibrations were performed on the radar in November 1972. The trajectory computations that are discussed and illustrated in the main text and in Appendices C and G were corrected for altitude differences between the photographs and the calibrations; the photo diagrams shown in Figures B1 through B8 herein were not.)

*ATPVITS, which is used several times in this appendix, stands for "at the particular video-integrator threshold settings". The reference is to the gray-scale types indicated on the photo diagrams which are specified in Table B1.

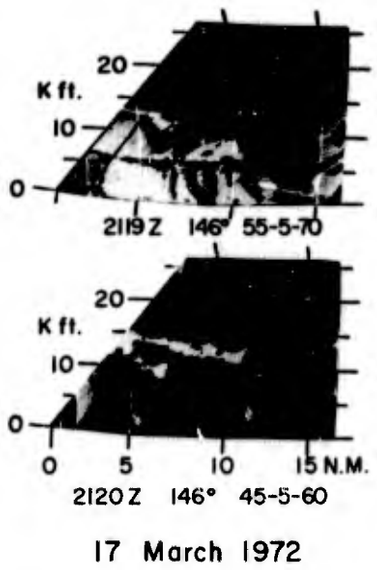

Figure B3. RHI Photographs Obtained With the FPS-18 Radar on 17 March 1972 at the Launch Time and in the Launch Direction of the Missile

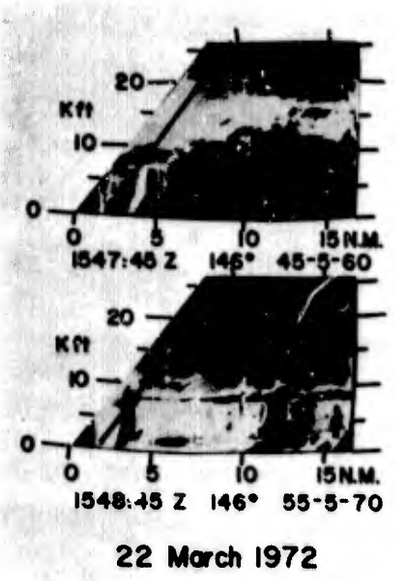

Figure B4. RHI Photographs Obtained With the FPS-18 Radar on 22 March 1972 at the Launch Time and in the Launch Direction of the Missile

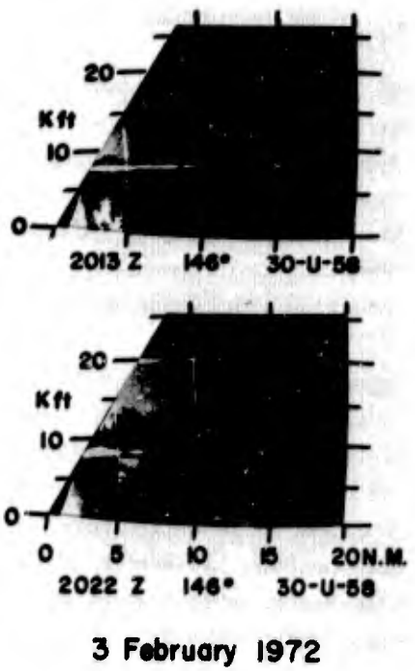

Figure B5. RHI Photographs Obtained With the FPS Radar on 3 February 1972 Which Were Taken in the Launch Direction 4 Min Before Launch and 5 Min After Launch

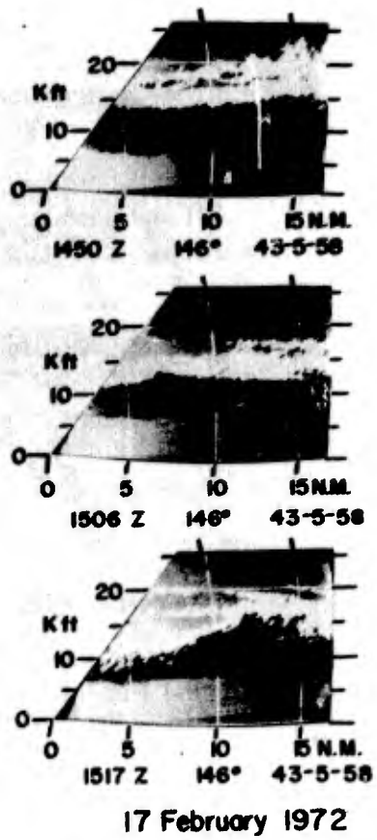

Figure B6. RHI Photographs Obtained With the FPS-18 Radar on 17 February 1972, Which Were Taken in the Launch Direction at 1450, 1506, and 1517 GMT, During the Period Before, Between, and After the Launch Times of the Two Missiles That Were Fired Into the Storm

The RHI photographs of Figures B2 and B6 reveal that the storm of 17 February 1972 was also relatively homogeneous in its spatial-temporal characteristics during the launch period. The radar echo tops of the storm extended to about 26,000 ft (ATPVITS). No distinctively obvious bright band can be seen in the photographs, although it may be reported that other photographs for this storm, taken at different threshold setting of the video integrator, revealed the presence of two bright bands, one located above the other, at altitudes of about 3000 and 5000 ft.

The RHI photos for the storm of 17 March 1972 show that this storm was more cellular and convective in structure than the previous storms. The echo tops of the storm were undulatory, ranging from about 15,000 to 18,000 ft (ATPVITS of the lower photograph of Figure B3) at the launch time of the missile. The interior of the storm during the launch period is seen to have considerably more "vertical, cellular, streamerform" structure, and less "laminar, horizontal" structure than the prior storms. A well-defined bright-band-region existed which was of variable thickness. The base levels ranged from about 3000 to 5000 ft; the top levels varied from about 5500 to 7000 ft.

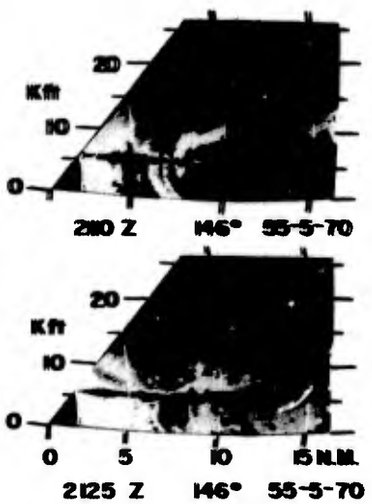

17 March 1972

Figure B7. RHI Photographs Obtained With the FPS-18 Radar on 17 March 1972 Which Were Taken in the Launch Direction 9 Min Before Launch and 6 Min After Launch

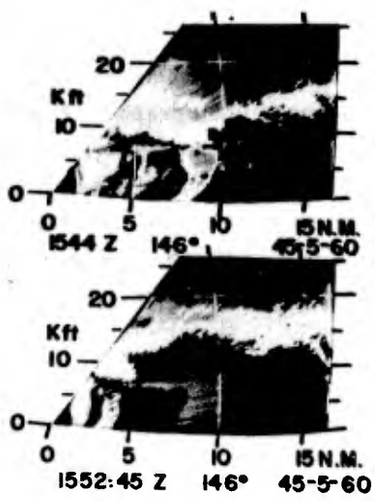

22 March 1972

Figure B8. RHI Photographs Obtained With the FPS-18 Radar on 22 March 1972 Which Were Taken in the Launch Direction 4 Min Before Launch and 4 Min 45 Sec After Launch

Table B1. Shading Code and Gray-Scale Types Employed With the Video Integrated RHI Photographs for the Missile Launch Times of the 1971-72 Season. The dB Values Listed are dB Above -90 dBm

Gray Shade on RHI Photograph	Shading Code Number	Threshold Signal Levels Employed for Gray Scale			
		Type 30-U-58 dB	Type 43-5-58 dB	Type 45-5-60 dB	Type 55-5-70 dB
Black	0	≤ 30	≤ 43	≤ 45	≤ 55
Dark Gray	1	38	48	50	60
Light Gray	2	58	53	55	65
White	3	68	58	60	70
Black	0	78	63	65	75
Dark Gray	1	85	68	70	80
Light Gray	2	≥ 85	≥ 68	≥ 70	≥ 80

The storm of 22 March 1972 also evidenced considerable convective structure, particularly in the lower levels below about 15,000 ft, as revealed by Figures B4 and B8. The radar echo tops extended to about 27,000 to 29,000 ft (ATPVITS of the upper photograph of Figure B4) at the launch time of the missile. There was considerable spatial-temporal variability of the radar signals from the lower, interior portions of the storm during the launch period. A bright band was present which is seen to be distorted and disrupted by the vertical echo structure associated with the convective cells. This band was located at altitudes ranging generally from about 7000 to 9000 ft.

Appendix C

Computation of Hydrometeor Parameters From the Radar Data

The trajectory values of the radar integration signal, $\underline{\overline{I}}$, in the 1971-72 season, were obtained from the launch-time RHI photographs presented in the previous appendix. The course of the missile trajectory across the corresponding RHI photograph was known (see Tables C1 through C5) and the $\underline{\overline{I}}$ signal values could be accurately determined for each point where the trajectory intersected with a boundary of the gray-scale regions shown on the photographs. The $\underline{\overline{I}}$ values between these points, that is, the values along the trajectories within the photographic gray regions themselves, were estimated or inferred by interpolation.

Profile values of $\underline{\overline{I}}$, thus established, are shown in Figures C1 through C5 for each of the missile launches of the 1971-72 season. The solid, middle portion of the profiles show the $\underline{\overline{I}}$ values that were determined from the RHI photographs within those altitude regions of the storms extending from above the radar ground-clutter layer near the surface level to the storm altitude aloft, where the $\underline{\overline{I}}$ values became minimum detectable. The dashed portion of the profiles, at the bottom, show the interpolated $\underline{\overline{I}}$ values that span the ground-clutter layer and that are consistent with the measured precipitation rate at the launch time of the missile (see R No. 2). The dotted portion of the profiles, at the top, show the $\underline{\overline{I}}$ values that were presumed to apply to the uppermost part of the missile trajectories, where the radar signals were below minimum detectable. (A linear decrease of $\underline{\overline{I}}$ with altitude was assumed from these minimum detectable points to the storm top altitudes, where $\underline{\overline{I}} = 0$; also see R No. 2.)

Table C1. Altitude, Horizontal Range, and Missile Velocity Information for Missile Flight Q2-5297 of 3 February 1972. Altitude points along the trajectory are listed for approximately every 1000 ft of altitude up to 26,000 ft. The corresponding horizontal ranges, from JAFNA, are tabulated, both in feet and in nautical miles. The missile launch time was 20:17:00 Z. The information of this table was extracted from the NASA smoothed positional data for the flight

Elapsed Time	Altitude	Horizontal Range From JAFNA		Missile Velocity
sec	ft	ft	N.M.	ft/sec
1.50	335	11,567	1.901	888
1.90	500	11,799	1.939	1,246
2.50	1,712	12,654	2.080	1,850
3.30	1,991	14,218	2.337	2,779
3.90	2,945	15,843	2.604	3,524
4.50	4,096	17,830	2.931	4,074
4.90	4,943	19,270	3.168	4,351
5.30	5,881	20,888	3.434	5,117
5.70	6,985	22,858	3.756	6,227
6.00	7,954	24,610	4.046	7,146
6.30	9,051	26,598	4.373	7,970
6.50	9,839	28,026	4.607	8,306
6.80	11,060	30,221	4.968	8,372
7.00	11,872	31,668	5.206	8,220
7.30	13,058	33,773	5.552	7,913
7.60	14,195	35,799	5.885	7,601
7.80	14,924	37,106	6.100	7,396
8.10	15,978	39,004	6.412	7,105
8.40	16,987	40,831	6.712	6,842
8.70	17,956	42,591	7.002	6,577
9.10	19,188	44,836	7.371	6,255
9.40	20,070	46,450	7.636	6,035
9.70	20,920	48,008	7.892	5,824
10.10	22,004	50,004	8.221	5,558
10.50	23,035	51,911	8.534	5,310
10.90	24,018	53,737	8.834	5.081
11.30	24,956	55,488	9.122	4,877
11.80	26,071	57,582	9.466	4,632

Table C2. Altitude, Horizontal Range, and Missile Velocity Information for Missile Flight Q2-5298 of 17 February 1972. Altitude points along the trajectory are listed for approximately every 1000 ft of altitude up to 26,000 ft. The corresponding horizontal ranges, from JAFNA, are tabulated, both in feet and in nautical miles. The missile launch time was 14:56:00 Z. The information of this table was extracted from the NASA smoothed positional data for the flight

Elapsed Time	Altitude	Horizontal Range From JAFNA		Missile Velocity
sec	ft	ft	N.M.	ft/sec
3.10	1,547	13,565	2.230	2,255
3.50	2,024	14,421	2.371	2,656
4.20	3,042	16,271	2.675	3,374
4.80	4,090	18,192	2.991	3,907
5.30	5,058	19,964	3.282	4,178
5.70	5,906	21,519	3.538	4,812
6.10	6,896	23,403	3.847	5,885
6.50	8,085	25,705	4.226	7,095
6.80	9,118	27,714	4.556	7,950
7.00	9,863	29,164	4.795	8,319
7.30	11,021	31,403	5.163	8,399
7.60	12,171	33,602	5.524	8,143
7.80	12,916	35,024	5.758	7,932
8.10	13,994	37,084	6.097	7,598
8.40	15,020	39,061	6.422	7,282
8.70	16,000	40,960	6.734	6,987
8.90	16,629	42,184	6.935	6,795
9.40	18,122	45,101	7.415	6,347
9.80	19,243	47,301	7.776	6,025
10.40	20,764	50,421	8.289	5,592
11.00	22,225	53,302	8.763	5,204
11.30	22,914	54,670	8.988	5,028
11.90	24,216	57,274	9.416	4,704
12.20	24,832	58,515	9.620	4,554
12.80	26,000	60,886	10.010	4,278

Table C3. Altitude, Horizontal Range, and Missile Velocity Information for Missile Flight Q2-5299 of 17 February 1972. Altitude points along the trajectory are listed for approximately every 1000 ft of altitude up to 26,000 ft. The corresponding horizontal ranges, from JAFNA, are tabulated, both in feet and in nautical miles. The missile launch time was 15:12:00 Z. The information of this table was extracted from the NASA smoothed positional data for the flight

Elapsed Time	Altitude	Horizontal Range From JAFNA		Missile Velocity
sec	ft	ft	N.M.	ft/sec
2.70	1,076	12,897	2.120	1,943
3.10	1,476	13,601	2.236	2,279
3.50	1,953	14,445	2.375	2,704
.80	2,976	16,277	2.676	3,474
4.80	4,028	18,179	2.989	3,886
5.30	4,997	19,917	3.274	4,130
5.80	6,090	21,892	3.599	4,931
6.20	7,149	23,861	3.923	6,001
6.60	8,426	26,255	4.316	7,165
6.80	9,147	27,609	4.539	7,699
7.00	9,911	29,041	4.774	8,084
7.40	11,489	31,970	5.256	8,245
7.60	12,269	33,401	5.491	8,206
7.80	13,030	34,796	5.720	8,061
8.20	14,485	37,478	6.161	7,880
8.40	15,179	38,769	6.374	7,682
8.60	15,852	40,028	6.581	7,480
9.00	17,141	42,456	6.980	7,288
9.40	18,358	44,760	7.359	7,114
9.60	18,941	45,869	7.545	6,944
10.00	20,063	48,012	7.893	6,760
10.40	21,129	50,057	8.229	6,397
10.70	21,894	51,531	8.472	6,244
11.00	22,634	52,956	8.706	5,955
11.30	23,348	54,334	8.933	5,662
11.60	24,039	55,670	9.152	5,424
11.90	24,707	56,966	9.365	5,135
12.20	25,351	58,223	9.572	4,961
12.50	25,974	59,443	9.772	4,803
12.80	26,576	60,629	9.967	4,577

Table C4. Altitude, Horizontal Range, and Missile Velocity Information for Missile Flight Q2-5891 of 17 March 1972. Altitude points along the trajectory are listed for approximately every 1000 ft of altitude up to 26,000 ft. The corresponding horizontal ranges, from JAFNA, are tabulated, both in feet and in nautical miles. The missile launch time was 21:19:00 Z. The information of this table was extracted from the NASA smoothed positional data for the flight

Elapsed Time	Altitude	Horizontal Range From JAFNA		Missile Velocity
sec	ft	ft	N.M.	ft/sec
3.00	1,196	12,909	2.12	1,909
3.30	1,503	13,442	2.21	2,198
3.70	1,979	14,270	2.35	2,591
4.40	3,005	16,067	2.64	3,325
5.00	4,073	17,959	2.95	3,885
5.50	5,066	19,702	3.24	4,154
5.90	5,937	21,212	3.49	4,678
6.30	6,955	23,008	3.78	5,734
6.60	7,860	24,630	4.05	6,675
6.90	8,901	26,502	4.36	7,610
7.20	10,063	28,597	4.70	8,292
7.40	10,881	30,062	4.94	8,454
7.70	12,119	32,259	5.31	8,322
7.90	12,930	33,689	5.54	8,133
8.20	14,110	35,767	5.88	7,823
8.40	14,868	37,109	6.10	7,616
8.70	15,964	39,058	6.42	7,315
9.00	17,011	40,932	6.73	7,029
9.30	18,015	42,735	7.03	6,755
9.60	18,977	44,470	7.31	6,501
9.90	19,902	46,143	7.59	6,267
10.30	21,081	48,282	7.94	5,967
10.60	21,925	49,819	8.19	5,754
11.00	23,003	51,790	8.52	5,504
11.40	24,031	53,678	8.83	5,266
11.80	25,012	55,487	9.13	5,049
12.20	25,950	57,226	9.41	4,852

Table C5. Altitude, Horizontal Range, and Missile Velocity Information for Missile Flight Q2-5892 of 22 March 1972. Altitude points along the trajectory are listed for approximately every 1000 ft of altitude up to 26,000 ft. The corresponding horizontal ranges, from JAFNA, are tabulated, both in feet and in nautical miles. The missile launch time was 15:48:00 Z. The information of this table was extracted from the NASA smoothed positional data for the flight

Elapsed Time	Altitude	Horizontal Range From JAFNA		Missile Velocity
sec	ft	ft	N.M.	ft/sec
2.60	1,172	12,918	2.124	1,834
2.90	1,491	13,464	2.213	2,225
3.30	1,989	14,325	2.355	2,640
4.00	3,067	16,199	2.663	3,360
4.50	3,982	17,805	2.927	3,855
5.00	4,980	19,547	3.214	4,144
5.50	6,085	21,485	3.532	5,046
5.90	7,139	23,389	3.845	6,180
6.30	8,402	25,695	4.224	7,402
6.50	9,115	27,000	4.439	7,931
6.70	9,873	28,387	4.667	8,264
6.90	10,660	29,821	4.903	8,253
7.10	11,457	31,262	5.139	8,063
7.30	12,246	32,683	5.373	7,851
7.50	13,020	34,075	5.601	7,440
7.70	13,775	35,433	5.825	7,243
7.90	14,507	36,758	6.043	7,061
8.10	15,218	38,049	6.255	6,703
8.30	15,909	39,309	6.462	6,356
8.50	16,581	40,041	6.583	6,205
8.70	17,235	41,743	6.863	5,913
9.10	18,488	44,050	7.242	5,643
9.30	19,089	45,159	7.424	5,454
9.70	20,246	47,302	7.776	5,270
10.10	21,345	49,343	8.112	5,101
10.50	22,390	51,292	8.432	4,948
11.00	23,630	53,617	8.815	4,793
11.30	24,340	54,951	9.034	4,644
11.60	25,024	56,242	9.246	4,509
12.10	26,115	58,312	9.586	4,373

The storm top altitudes in the 1971-72 season had to be estimated from radiosonde data, since the service ceiling of the Aztec aircraft was only about 23,000 ft, which was insufficient to surmount the storms. The storm "tops", from the radiosonde data, were assumed to be located at the altitudes where the relative humidity evidenced marked decreases with height.

Two abscissa scales have been drafted on the diagrams of Figures C1 through C5. The second, lower scale shows the decibel values of the radar volume reflectivity, defined in R No. 1. These scales of $\underline{\overline{\eta}}$ are related to the scales of $\underline{\overline{I}}$ as described by Eq. (47) of R No. 1. The scale relationships differ from one launch day to another, depending on the calibration constant of the radar.

Profiles of the radar reflectivity factors, Z_W and Z_I, for water and ice hydrometeors, are presented in Figures C6 through C10. The profile values were

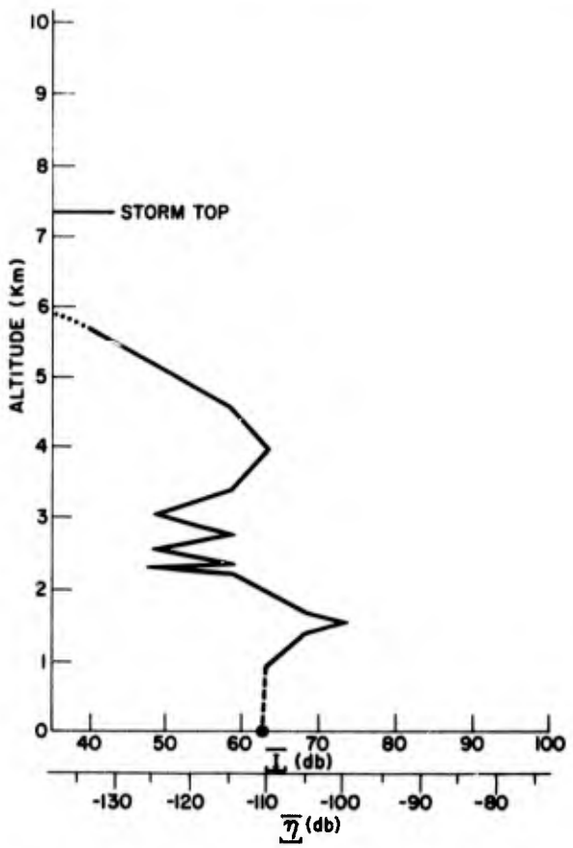

Figure C1. Profiles of the Radar Integration Signal and the Radar Volume Reflectivity for the Missile Trajectory of Flight No. Q2-5297 (Unit No. R341403) of 3 February 1972, Launched at 2017:00 GMT

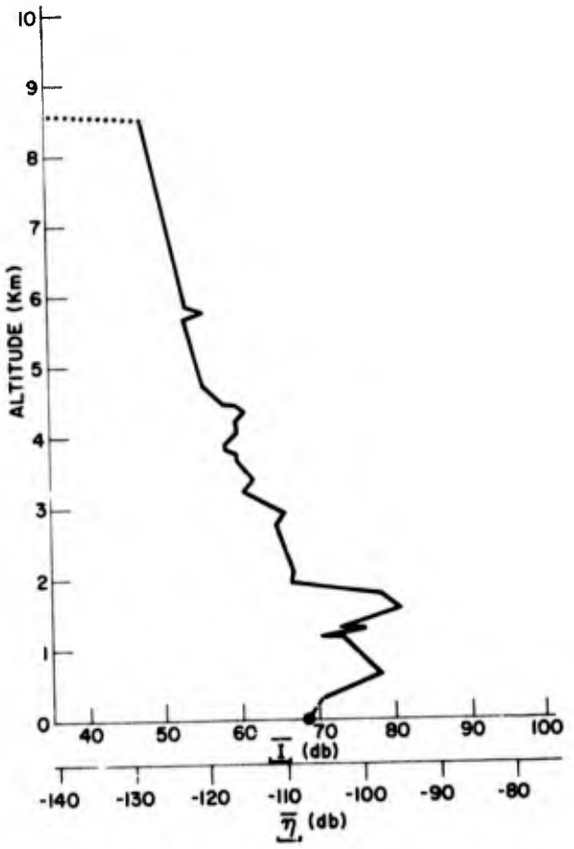

Figure C2. Profiles of the Radar Integration Signal and the Radar Volume Reflectivity for the Missile Trajectory of Flight No. Q2-5298 (Unit No. R341412) of 17 February 1972, Launched at 1456:00 GMT

computed from those of $\underline{I}$ using Eqs. (72) and (73) of R No. 1. The melting zones of the storms are indicated in the figures, and both the Z_W and Z_I profiles are shown extended across the zones. The reflectivity factor is indeterminant within the melting zone, as explained in R No. 1, and the two profiles provide indices concerning this indeterminancy. *

The hydrometeor regions and transition zones of the Wallops storms of the 1971-72 season are identified in Figures C11 through C15. The regions and zones below the 23,000 ft (7 km) service ceiling of the Aztec aircraft were determined

*The values of the reflectivity factor within the melting zone cannot be smaller than the Z_W values shown but they can exceed, in substantial, indeterminant amount, the values of Z_I.

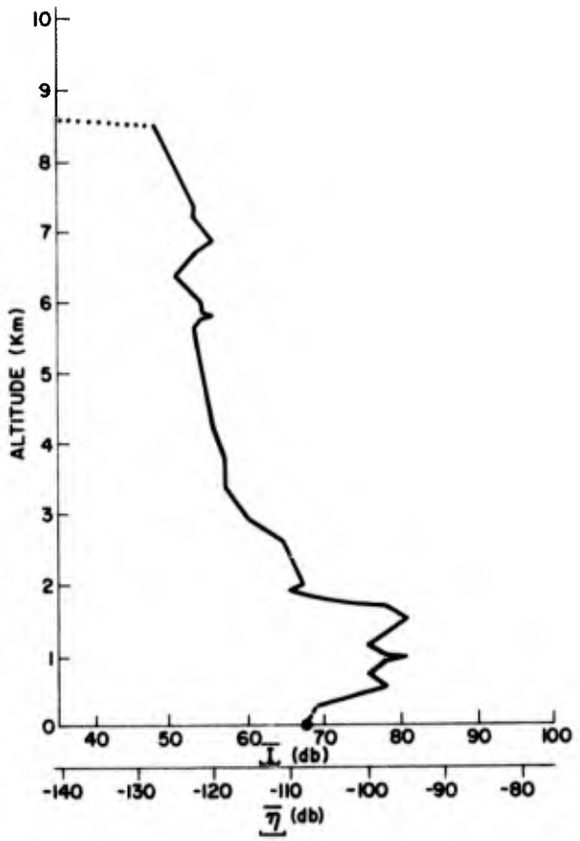

Figure C3. Profiles of the Radar Integration Signal and the Radar Volume Reflectivity for the Missile Trajectory of Flight No. Q2-5299 (Unit No. R341404) of 17 February 1972, Launched at 1512:00 GMT

from measurements and observations made from this aircraft. The regions and zones above this level were inferred from radiosonde data. The separation or transition zone between large-snow and small-snow was generally assumed to exist at temperatures of about -12°C to -20°C. The transition zone between small-snow and ice-crystals was assumed to exist at temperatures of about -26°C to -30°C.

Based on these measurements or assumptions about the altitude boundaries of the hydrometeor regions and transition zones within the storms, the trajectory profiles of precipitation rate, P, were computed from the Z_W and Z_I values (of Figures C6 through C10) utilizing the pertinent regression equations of Table 2, R No. 2, and the computational and interpolative techniques described in Section 4.5

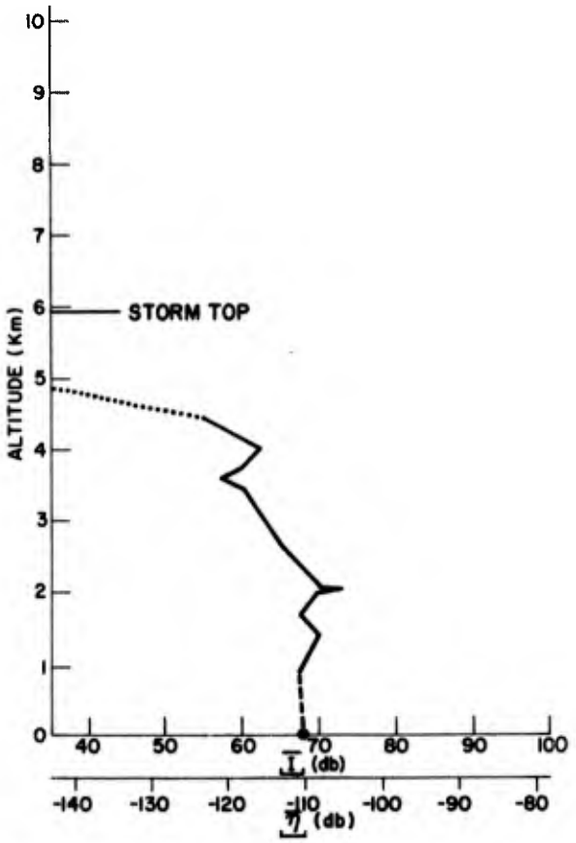

Figure C4. Profiles of the Radar Integration Signal and the Radar Volume Reflectivity for the Missile Trajectory of Flight No. Q2-5891 (Unit No. R341413) of 17 March 1972, Launched at 2119:00 GMT

of the same report. The resultant profiles of P are shown in Figures C11 through C15.

The trajectory values of the liquid-water-content, M, and of the integral of liquid-water-content, $M\,dR_s$, which are presented in Figures 1 through 5 of the main text, were computed from these profiles of P by procedures that are also described in Section 4.5 of R No. 2.

The numerical data, from where the Figures C1 through C15 and Figures 1 through 5 profiles were plotted, are listed in Tables C1 through C5. The altitudes of the data points are indicated and the radiosonde temperatures at these altitudes are shown. The $\overline{I}$, $\overline{\eta}$, Z_W (or Z_I), P, M, and $\int M\,dR_s$ values are given for each altitude. These are listed under the table section labeled "radar measured

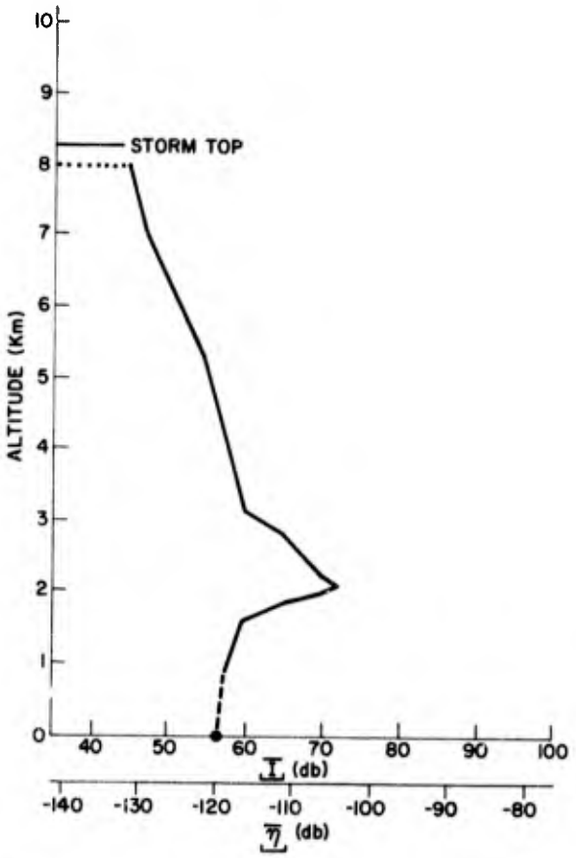

Figure C5. Profiles of the Radar Integration Signal and the Radar Volume Reflectivity for the Missile Trajectory of Flight No. Q2-5892 (Unit No. R341405) of 22 March 1972, Launched at 1548:00 GMT

parameters". The tables additionally list the cloud liquid-water-content values, w, (measured with the Johnson-Williams instrument of the Aztec aircraft) which, in our judgment, best typify or bound the trajectory cloud conditions at the missile launch times. The last column of the tables gives the values or value limits of the total liquid-water-content, composed of both precipitation-size drops or particles plus cloud-size drops in liquid form, either warm or supercooled.

There is an unresolved problem of nomenclature in Tables C6 through C10 that should be mentioned. The radar in the rain, large-snow, and small-snow regions primarily detects drops or snow particles of precipitable size, and the liquid-water-content values for these regions are listed under the table columns labeled "M". The radar in the ice-crystal region, however, detects particles

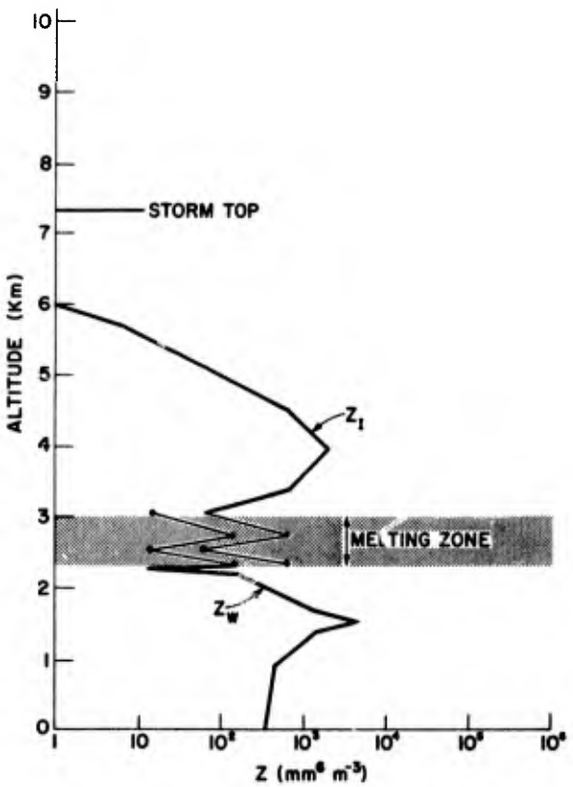

Figure C6. Profiles of the Radar Reflectivity Factors for Water and Ice Hydrometeors, for the Missile Trajectory of Flight No. Q2-5297 (Unit No. R341403) of 3 February 1972, Launched at 2017:00 GMT

which, at least in terms of their equivalent melted diameters, are partly in the cloud-size range. For this reason, the liquid-water-content values for ice crystals are listed in a separate column of the tables, labeled "ice cloud".

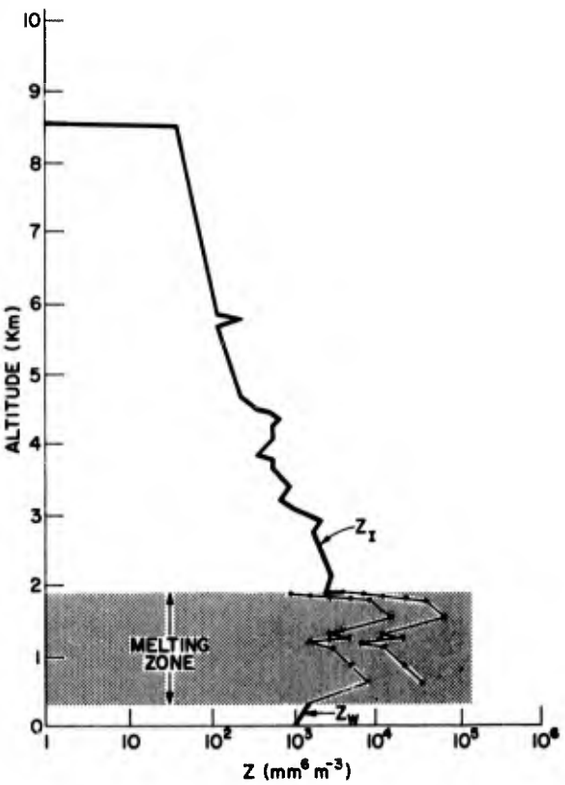

Figure C7. Profiles of the Radar Reflectivity Factors for Water and Ice Hydrometeors, for the Missile Trajectory of Flight No. Q2-5298 (Unit No. R341412) of 17 February 1972, Launched at 1456:00 GMT

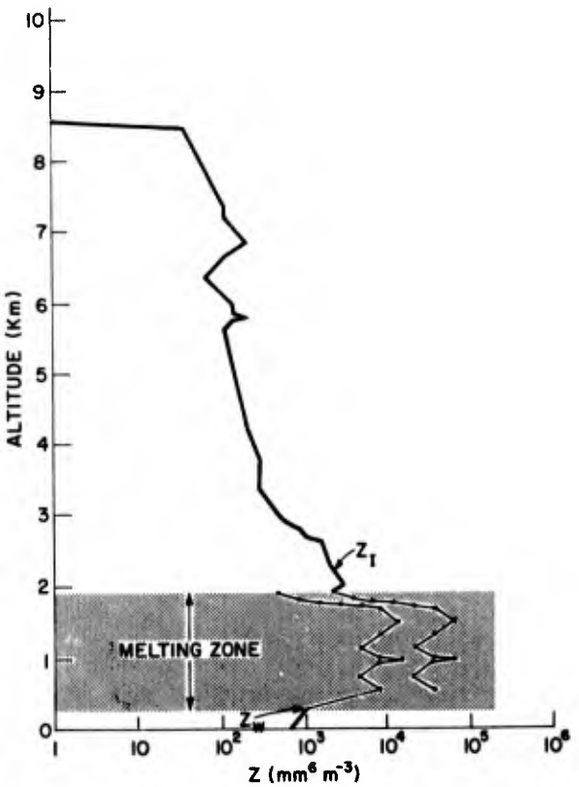

Figure C8. Profiles of the Radar Reflectivity Factors for Water and Ice Hydrometeors, for the Missile Trajectory of Flight No. Q2-5299 (Unit No. R341404) of 17 February 1972, Launched at 1512:00 GMT

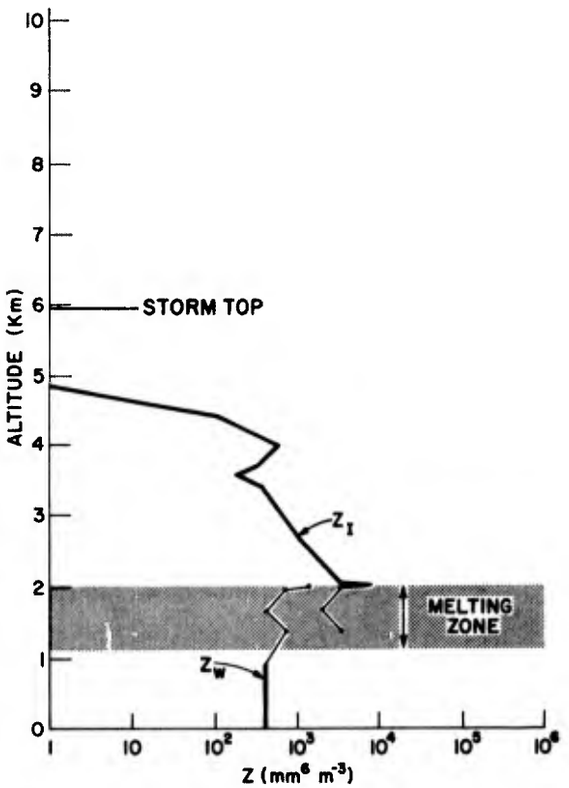

Figure C9. Profiles of the Radar Reflectivity Factors for Water and Ice Hydrometeors, for the Missile Trajectory of Flight No. Q2-5891 (Unit No. R341413) of 17 March 1972, Launched at 2119:00 GMT

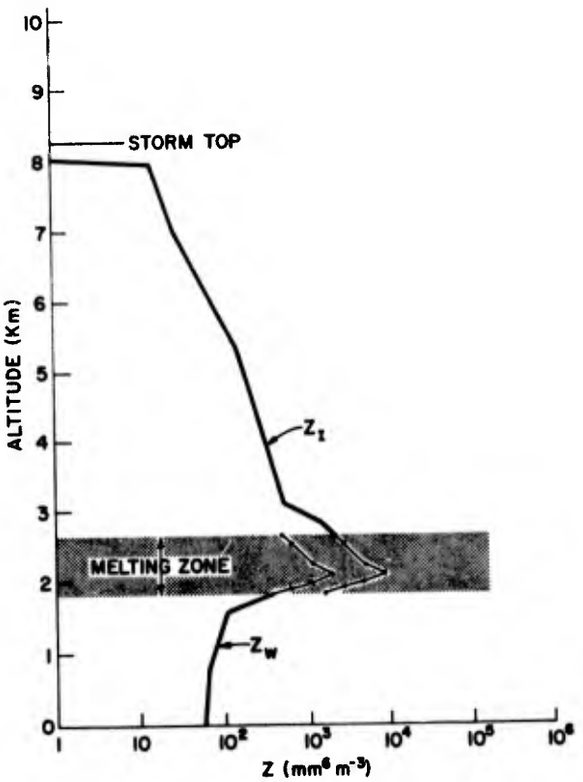

Figure C10. Profiles of the Radar Reflectivity Factors for Water and Ice Hydrometeors, for the Missile Trajectory of Flight No. Q2-5842 (Unit No. R341405) of 22 March 1972, Launched at 1548:00 GMT

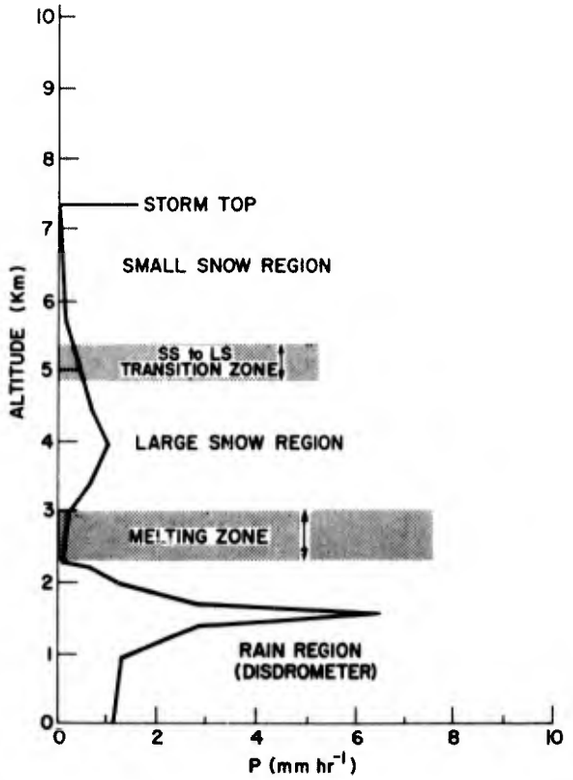

Figure C11. The Hydrometeor Regions and Zones Within the Storm of 3 February 1972 and the Profile of Precipitation Rate for the Missile Trajectory of Flight No. Q2-5297 (Unit No. R341403), Launched at 2017:00 GMT

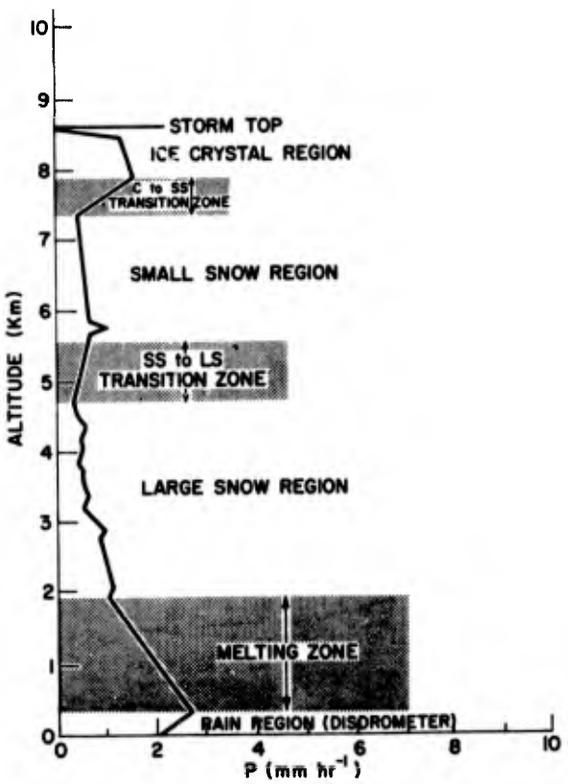

Figure C12. The Hydrometeor Regions and Zones Within the Storm of 17 February 1972 and the Profile of Precipitation Rate for the Missile Trajectory of Flght No. Q2-5298 (Unit No. R341412), Launched at 1456:00 GMT

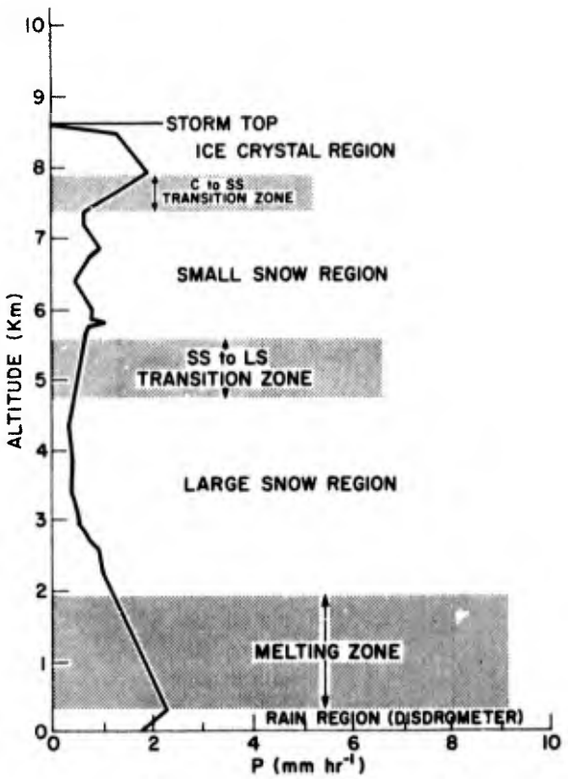

Figure C13. The Hydrometeor Regions and Zones Within the Storm of 17 February 1972 and the Profile of Precipitation Rate for the Missile Trajectory of Flight No. Q2-5299 (Unit No. R341404), Launched at 1512:00 GMT

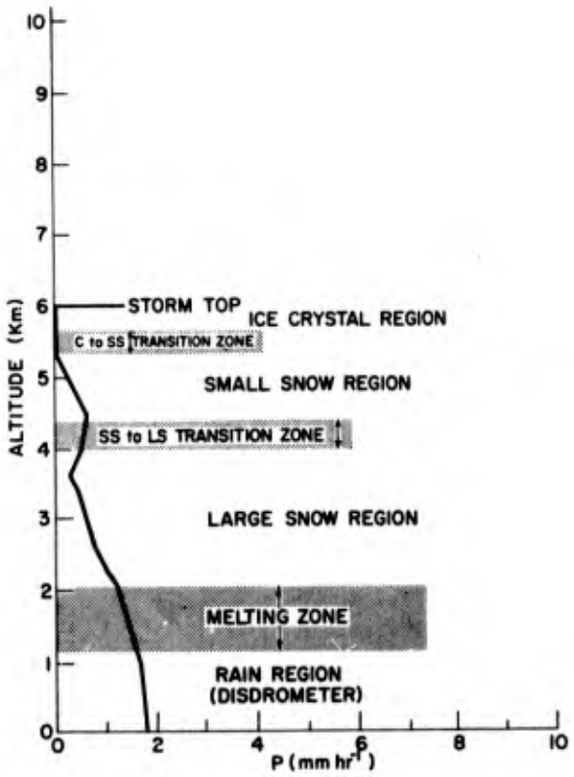

Figure C14. The Hydrometeor Regions and Zones Within the Storm of 17 March 1972 and the Profile of Precipitation Rate for the Missile Trajectory of Flight No. Q2-5891 (Unit No. R341413), Launched at 2119:00 GMT

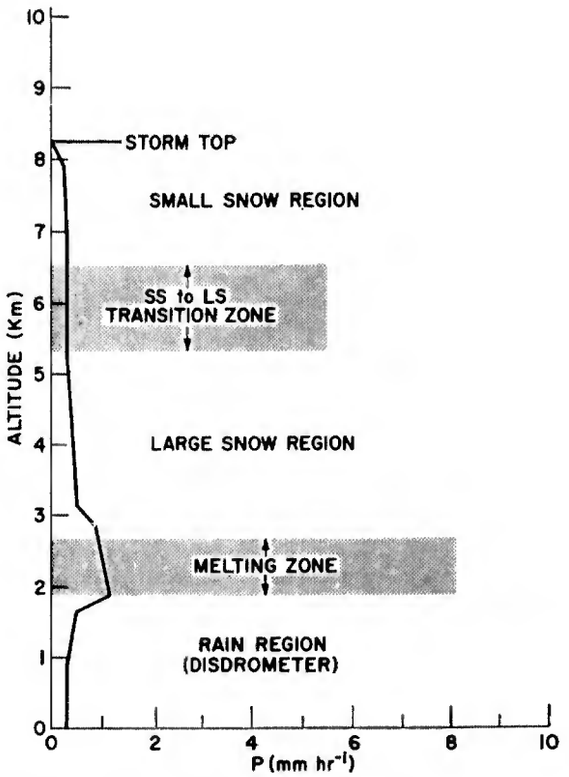

Figure C15. The Hydrometeor Regions and Zones Within the Storm of 22 March 1972 and the Profile of Precipitation Rate for the Missile Trajectory of Flight No. Q2-5892 (Unit No. R341405), Launched at 1548:00 GMT

Table C6. Tabulation of the Numerical Values of the Radar and Hydrometeor Parameters for Missile Flight No. Q2-5297 (Unit No. R341403) of 3 February 1972, Launched at 2017:00 GMT

Missile Altitude		Horizontal Range from JAFNA	Radiosonde Temperature	Hydrometeor Region or Zone	Precipitation Type	Radar-Measured Parameters						Acft. Msd Params		Total
						Integrator Signal Values	Volume Reflectivity	Reflectivity Factor	Precipitation Rate	Liquid-Water-Content M	Integral of M Along Missile Path	Liquid-Water Content		
										of Precipitation / of Ice Cloud		Water Cloud	Ice Cloud	
Km	K ft	N.M.	°C			I_S dB	η cm^{-1}	Z $mm^6 m^{-3}$	P $mm\,hr^{-1}$	gm m^{-3}	$\int_0^z M\,dR_S$ gm m^{-2}	w gm m^{-3}	i gm m^{-3}	
0	0	1.80	7.7	Rain Region	R_D	62	7.79×10^{-12}	359	1.10	.061	0	0		.061
0.9144	3.0	2.59	7.0			63	9.84×10^{-12}	454	1.29	.071	124	-		>.071
1.37	4.5	3.05	4.4			68	31.1×10^{-12}	1435	2.89	.148	226	-		>.148
1.52	5.0	3.17	3.6			73	98.4×10^{-12}	4536	6.46	.307	296	<.1		<.407
1.68	5.5	3.30	3.2			68	31.1×10^{-12}	1435	2.89	.148	367	<.1		<.248
1.95	6.4	3.62	2.9			63	9.84×10^{-12}	454	1.29	.071	428	<.1		<.171
2.23	7.3	3.85	2.3			58	3.11×10^{-12}	143	.58	.034	457	<.1		<.134
2.29	7.5	3.92	2.0			48	$.311 \times 10^{-12}$	14.3	.12	.008	460	<.1		<.108
2.32	7.6	3.95	1.9	Melting Zone		53	$.98 \times 10^{-12}$		.12	.008	461	<.1		<.108
2.51	8.23	4.13	1.1			49.8	$.48 \times 10^{-12}$		.14	.022	466	<.1		<.122
2.70	8.86	4.35	0.3			55.8	1.90×10^{-12}		.16	.039	478	<.1		<.139
2.90	9.50	4.52	-0.4			53.2	1.04×10^{-12}		.19	.061	498	<.1		<.161
3.06	10.05	4.67	-1.1	Large Snow	LS_C	48	$.311 \times 10^{-12}$	63.8	.21	.066	520	<.1		<.166
3.38	11.1	5.00	-2.1			58	3.11×10^{-12}	638	.58	.161	594	<.1		<.261
3.96	13.0	5.52	-4.8			63	9.84×10^{-12}	2017	.98	.251	837	<.1		<.351
4.54	14.9	6.10	-7.5			58	3.11×10^{-12}	638	.58	.161	1080	<.1		<.261
4.85	15.9	6.37	-9.4	Small Snow to Large Snow Transition Zone	SS_S and LS_C	52.9	$.96 \times 10^{-12}$		.46	.133	1172	-		-.133
5.0	16.43	6.52	-8.9			50.2	$.51 \times 10^{-12}$		.40	.116	1213	-		-.116
5.17	16.96	6.73	-9.6			47.4	$.27 \times 10^{-12}$		.34	.098	1248	-		-.098
5.33	17.5	6.87	-10.6			44.7	$.14 \times 10^{-12}$		.27	.082	1278	-		-.082
5.73	18.8	7.30	-12.9	Small Snow	SS_S	38	$.031 \times 10^{-12}$	6.4	.12	.039	1327	-		-.039
7.32	24.0	8.80	-22.9			0	0	0	0	0	1391	0		0

Table C7. Tabulation of the Numerical Values of the Radar and Hydrometeor Parameters for Missile Flight No. Q2-5298 (Unit No. R341412) of 17 February 1972, Launched at 1456:00 GMT

Missile Altitude		Horizontal Range from JAFNA	Radio-sonde Temper-ature	Hydro-meteor Region or Zone	Precipi-tation Type	Radar-Measured Parameters					Acft. Msd Params			Total
						Integrator Signal Values	Volume Reflectivity	Reflectivity Factor	Precipitation Rate	Liquid-Water-Content M	Integral of M Along Missile Path	Liquid-Water Content		
										of Precipitation / of Ice Cloud		Water Cloud	Ice Cloud	
Km	K ft	N.M.	°C			I_S dB	η cm^{-1}	Z mm^6m^{-3}	P $mmhr^{-1}$	$gm\ m^{-3}$	$\int_0^{R_S} M\,dR_S$ $gm\,m^{-2}$	$gm\,m^{-3}$	$gm\,m^{-3}$	
0	0	1.80	4.1	Rain Region	R_D	68.9	21.51×10^{-12}	992	2.2	.125	0	0		.125
.3048	1	2.12	0.8			70.35	30.34×10^{-12}	1389	2.72	.148	85	0		.148
.335	1.1	2.16	0.7	Melting Zone		71.1	36.18×10^{-12}		2.69	.146	94	0	CB 1.4	.146
.86	2.83	2.63	-1.5			75.6	100.7×10^{-12}		2.15	.241	309	-		>.241
1.39	4.56	3.13	-0.7			76.4	121.5×10^{-12}		1.61	.285	586	-		>.285
1.92	6.3	3.66	-0.9			67.0	14.03×10^{-12}		1.07	.270	884	-		>.270
1.95	6.4	3.69	-0.95	Large Snow Region	LS_C	66.0	11.14×10^{-12}	2284	1.04	.263	901	-		>.263
1.98	6.5	3.72	-1.0			66.5	12.5×10^{-12}	2563	1.10	.275	917	-		>.275
2.07	6.8	3.82	-1.2			66.5	12.5×10^{-12}	2563	1.10	.275	969	0		.275
2.41	7.9	4.16	-2.6			65.5	9.93×10^{-12}	2036	1.10	.252	1149	.2		.452
2.74	9.0	4.53	-3.8			64.5	7.89×10^{-12}	1617	.89	.230	1313	.15		.380
2.90	9.5	4.67	-4.6			65.5	9.93×10^{-12}	2036	1.10	.252	1388	~.15		~.402
3.05	10.0	4.77	-5.9			63.0	5.59×10^{-12}	1145	.76	.202	1459	.10		.302
3.2	10.5	4.99	-6.2			60.5	3.14×10^{-12}	644	.59	.162	1515	.1E		.262E
3.35	11.0	5.15	-7.0			61.5	3.95×10^{-12}	811	.65	.177	1568	<.1		<.277
3.5	11.5	5.29	-7.7			60.5	3.14×10^{-12}	644	.59	.162	1620	<.1		<.262
3.66	12.0	5.46	-8.4			59.5	2.50×10^{-12}	511	.53	.148	1668	<.1		<.248
3.73	12.25	5.54	-8.8			59.5	2.50×10^{-12}	511	.53	.148	1691	-		>.148
3.81	12.5	5.63	-9.2			58.0	1.77×10^{-12}	362	.45	.130	1713	-		>.130
3.84	12.6	5.65	-9.4			58.0	1.77×10^{-12}	362	.45	.130	1721	-		>.130
4.02	13.2	5.84	-10.5			59.5	2.50×10^{-12}	511	.53	.148	1773	.15		.298
4.21	13.8	6.04	-11.6			59.5	2.50×10^{-12}	511	.53	.148	1828	-		>.148
4.31	14.15	6.16	-12.2			60.5	3.14×10^{-12}	644	.59	.162	1861	-		>.162
4.42	14.5	6.27	-12.7			59.5	2.50×10^{-12}	511	.53	.148	1895	-		>.148
4.45	14.6	6.29	-12.8			58.0	1.77×10^{-12}	362	.45	.130	1904	<.1		<.230
4.66	15.3	6.52	-14.0			55.5	0.99×10^{-12}	204	.35	.104	1954	-		>.104
4.72	15.5	6.58	-14.4	S.S. to L.S.	SS_S	55.3	0.96×10^{-12}		.37	.109	1968	-		>.109
5.0	16.4	6.85	-16.1			54.6	0.81×10^{-12}		.47	.133	2036	-		>.133
5.27	17.3	7.17	-17.9	Trans. Zone	LS_C	53.9	0.69×10^{-12}		.57	.156	2116	-		>.156
5.55	18.2	7.47	-19.6			53.2	0.59×10^{-12}		.67	.178	2210	-		>.178
5.64	18.5	7.57	-20.0			53.0	0.56×10^{-12}	114	.71	.185	2244	-		>.185
5.73	18.8	7.67	-20.5			55.5	0.99×10^{-12}	204	1.01	.253	2284	-		>.253
5.82	19.1	7.77	-20.9			53.0	0.56×10^{-12}	114	.71	.185	2325	-		>.185
7.15	23.45	9.18	-25.1	Small Snow	SS_S	50.5	0.31×10^{-12}	64	.49	.136	2760	0E		.136
7.32	24.0	9.37	-26.4			50.2	0.29×10^{-12}	60	.47	.131	2806	0E		.131
7.35	24.1	9.4	-26.7	Ice to Small Snow	C_1	50.1	0.29×10^{-12}		.53	.144	2815	0E		.144
7.52	24.66	9.59	-28.1			49.8	0.27×10^{-12}		.88	.210	2877	0E		.210
7.69	25.23	9.78	-29.5	Trans. Zone	SS_S	49.5	0.25×10^{-12}		1.23	.256	2960	0E		.256
7.86	25.8	9.99	-30.9			49.1	0.23×10^{-12}		1.56	.288	3056	0E		.288
7.88	25.85	9.75	-30.5	Ice	C_1	49.1	0.23×10^{-12}	47	1.58	.289	3065	0E		.289
8.47	27.8	10.67	-35.9			48.0	0.18×10^{-12}	36	1.32	.253	3394	0E		.253
8.53	28.0	10.73	-36.6			0	0	0	0	0	3410	0		0

Table C8. Tabulation of the Numerical Values of the Radar and Hydrometeor Parameters for Missile Flight No. Q2-5299 (Unit No. R341404) of 17 February 1972, Launched at 1512:00 GMT

Missile Altitude		Horizontal Range from JAFNA	Radio-sonde Temper-ature	Hydro-meteor Region or Zone	Precipi-tation Type	Radar-Measured Parameters						Acft. Msd Params		Total
						Inte-grator Signal Values	Volume Reflectivity	Reflectivity Factor	Precipi-tation Rate	Liquid-Water-Content M of Precipi-tation	Liquid-Water-Content M of Ice Cloud	Integral of M Along Missile Path	Liquid-Water Content: Water Cloud	Liquid-Water Content: Ice Cloud	
						I_S	η	Z	P			$\int_o^* M\,dR_S$			
Km	K ft	N.M.	°C			dB	cm^{-1}	mm^6m^{-3}	$mmhr^{-1}$		$gm\,m^{-3}$	$gm\,m^{-2}$	$gm\,m^{-3}$	$gm\,m^{-3}$	
0	0	1.80	4.1	Rain Region	R_D	67.4	15.5×10^{-12}	716	1.8	.106		0	0		.106
.26	.85	2.06	1.3			69.11	22.8×10^{-12}	1051	2.28	.128		62	0		.128
.34	1.1	2.16	0.7	Melting Zone		71.7	41.6×10^{-12}		2.23	.126		868	0	CB 1.4	.126
.86	2.83	2.63	-1.5			77.3	151.9×10^{-12}		1.89	.216		266	-		>.216
1.39	4.56	3.13	-0.7			79.4	242.9×10^{-12}		1.54	.274		531	-		>.274
1.92	6.3	3.66	-0.9			65.8	10.64×10^{-12}		1.20	.296		838	-		>.296
1.98	6.5	3.72	-1.0	Large Snow Region	LS_C	67.0	14.03×10^{-12}	2876	1.16	.287		874	-		>.287
2.29	7.5	4.02	-2.0			65.5	9.93×10^{-12}	2036	0.99	.252		1042	0		.252
2.59	8.5	4.37	-3.2			64.5	7.89×10^{-12}	1617	0.89	.230		1191	.2		.430
2.68	8.8	4.46	-3.6			63.0	5.59×10^{-12}	1145	0.76	.202		1232	~.15		~.352
2.77	9.1	4.56	-4.0			62.0	4.44×10^{-12}	909	0.69	.185		1268	.15		.335
2.87	9.4	4.64	-4.4			60.5	3.14×10^{-12}	644	0.59	.162		1300	~.1		~.262
2.96	9.7	4.74	-4.9			59.5	2.50×10^{-12}	511	0.53	.148		1329	.10		.248
3.35	11.0	5.15	-7.0			57.0	1.40×10^{-12}	288	0.41	.119		1436	<.1		<.219
3.75	12.3	5.52	-8.9			57.0	1.40×10^{-12}	288	0.41	.119		1532	<.1		<.219
4.28	14.05	6.05	-12.1			55.5	0.99×10^{-12}	204	0.35	.104		1653	.15		.254
4.72	15.5	6.50	-14.4	S.S. to L.S. Trans Zone	SS_S and LS_C	54.7	0.82×10^{-12}		0.47	.133		1760	-		>.133
5.0	16.4	6.76	-16.1			54.2	0.73×10^{-12}		0.54	.149		1839	-		>.149
5.27	17.3	7.05	-17.9			53.7	0.65×10^{-12}		0.61	.165		1927	-		>.165
5.55	18.2	7.32	-19.6			53.1	0.58×10^{-12}		0.69	.181		2024	-		>.181
5.62	18.45	7.37	-20.0	Small Snow Region	SS_S	53.0	0.56×10^{-12}	115	0.71	.185		2052	-		>.185
5.73	18.8	7.50	-20.5			54.0	0.70×10^{-12}	144	0.82	.210		2095	-		>.210
5.76	18.9	7.53	-20.6			55.5	0.99×10^{-12}	204	1.01	.253		2109	-		>.253
5.79	19.0	7.55	-20.8			54.0	0.70×10^{-12}	144	0.82	.210		2124	-		>.210
5.93	19.45	7.68	-21.4			54.0	0.70×10^{-12}	144	0.82	.210		2183	-		>.210
6.07	19.9	7.83	-22.1			53.0	0.56×10^{-12}	115	0.71	.185		2238	-		>.185
6.34	20.8	8.14	-23.4			50.5	0.31×10^{-12}	64	0.49	.136		2328	0		.136
6.61	21.7	8.43	-23.6			53.0	0.56×10^{-12}	115	0.71	.185		2418	-		>.185
6.81	22.35	8.64	-23.8			55.5	0.99×10^{-12}	204	1.01	.253		2506	-		>.253
7.01	23.0	8.82	-24.3			54.0	0.70×10^{-12}	144	0.82	.210		2600	-		>.210
7.16	23.5	9.0	-25.2			53.0	0.56×10^{-12}	115	0.71	.185		2661	0E		.185
7.32	24.0	9.17	-26.1			53.0	0.56×10^{-12}	115	0.71	.185		2719	0E		.185
7.35	24.1	9.22	-26.4	Trans. Zone Ice Crystal to S.S. Trans. Zone	C_I and SS_S	52.9	0.54×10^{-12}		0.78	.189		2731	0E		.189
7.52	24.66	9.37	-27.7			52.1	0.45×10^{-12}		1.17	.268		2813	0E		.268
7.69	25.23	9.55	-28.8			51.3	0.38×10^{-12}		1.57	.313		2916	0E		.313
7.86	25.8	9.73	-30.4			50.6	0.32×10^{-12}		1.96	.338		3030	0E		.338
7.88	25.85	9.75	-30.5	Ice Crystal Region	C_I	50.5	0.31×10^{-12}	64	2.0		.343	3041	0E		.343
8.47	27.7	10.37	-35.6			48.0	0.18×10^{-12}	36	1.32		.253	3383	0E		.253
8.53	28.0	10.45	-36.6			0	0	0	0		0	3407	0		0

Table C9. Tabulation of the Numerical Values of the Radar and Hydrometeor Parameters for Missile Flight No. Q2-5891 (Unit No. R341413) of 17 March 1972, Launched at 2119:00 GMT

Missile Altitude		Horizontal Range from JAFNA	Radio-sonde Temper-ature	Hydro-meteor Region or Zone	Precipi-tation Type	Radar-Measured Parameters						Acft. Msd Params		Total
						Inte-grator Signal Values	Volume Reflectivity	Reflectivity Factor	Precipi-tation Rate	Liquid-Water-Content M	Integral of M Along Missile Path	Liquid-Water-Content		
						I_S	η	Z	P	of Precipi-tation / of Ice Cloud	$\int_0^Z M\,dR_S$	Water Cloud	Ice Cloud	
Km	K ft	N.M.	°C			dB	cm^{-1}	$mm^6 m^{-3}$	$mm\,hr^{-1}$	$gm\,m^{-3}$		$gm\,m^{-3}$	$gm\,m^{-3}$	
0	0	1.80	7.8	Rain Region	R_D	67.9	9.68×10^{-12}	446	1.8	.123	0	0 CB		.123
.91	3.0	2.60	1.8			67.5	8.85×10^{-12}	408	1.7	.116	223	-		>.116
1.14	3.75	2.80	0.3	Melting Zone		68.8	11.8×10^{-12}		1.6	.111	276	~.1		~.211
1.44	4.72	3.08	-0.9			69.5	13.87×10^{-12}		1.47	.187	365	.2		.387
1.74	5.7	3.36	-2.3			68.0	9.93×10^{-12}		1.35	.250	496	.2		.450
2.03	6.65	3.67	-3.4			71.3	21.0×10^{-12}		1.23	.302	662	~.2		~.502
2.04	6.7	3.70	-3.5	Large Snow Region	LS_I	70.0	15.74×10^{-12}	3227	1.22	.300	672	0		.300
2.35	7.7	3.98	-4.6			67.5	8.85×10^{-12}	1815	0.94	.241	840	.2		.441
2.65	8.7	4.30	-6.0			65.0	4.98×10^{-12}	1020	0.72	.193	975	<.1		<.293
3.05	10.0	4.68	-8.1			62.5	2.80×10^{-12}	574	0.56	.155	1115	<.1		<.255
3.44	11.3	5.05	-10.7			60.0	1.57×10^{-12}	323	0.43	.124	1227	-		>.124
3.58	11.75	5.20	-11.7			57.5	0.89×10^{-12}	181	0.33	.099	1259	-		>.099
3.72	12.2	5.30	-12.6			60.0	1.57×10^{-12}	323	0.43	.124	1290	0		.124
3.99	13.1	5.55	-14.3			62.5	2.80×10^{-12}	574	0.56	.155	1368	0		.155
4.15	13.6	5.72	-15.4	S.S. to L.S. Trans. Zone	SS_S and LS_C	59.8	1.51×10^{-12}		0.59	.163	1417	0		.163
4.24	13.9	5.80	-15.5			58.2	1.04×10^{-12}		0.61	.166	1444	0		.166
4.30	14.1	5.86	-16.0			57.1	0.82×10^{-12}		0.63	.169	1472	0		.169
4.40	14.4	5.95	-16.7			55.5	0.56×10^{-12}		0.65	.173	1501	0		.173
4.42	14.5	5.96	-17.0	Small Snow Region	SS_S	55.0	0.50×10^{-12}	102	0.66	.174	1511	0		.174
5.30	17.4	6.84	-23.5			23.1	0.0003×10^{-12}	.066	0.007	.0034	1671.5	0		.0034
5.33	17.5	6.87	-23.6	Ice Crystal to S.S. Trans. Zone	C_1 and SS_S	22.0	0.0002×10^{-12}		0.006	.0032	1672	0		.0032
5.43	17.8	6.96	-24.3			18.7	0.0001×10^{-12}		0.005	.003	1672	0		.003
5.55	18.2	7.08	-25.3			14.3	0.00004×10^{-12}		0.003	.0027	1673	0		.0027
5.64	18.5	7.17	-25.9			11.0	0.00002×10^{-12}		0.002	.0022	1673.4	0		.0022
5.67	18.6	7.21	-26.1	Ice	C_1	9.9	0.00002×10^{-12}	.003	0.0016	.0018	1674	0		.0018
5.94	19.5	7.48	-28.2			0	0	0	0	0	1674	0		0

Table C10. Tabulation of the Numerical Values of the Radar and Hydrometeor Parameters for Missile Flight No. Q2-5892 (Unit No. R431405) of 22 March 1972, Launched at 1548:00 GMT

Missile Altitude		Horizontal Range from JAFNA	Radiosonde Temperature	Hydrometeor Region or Zone	Precipitation Type	Radar-Measured Parameters						Acft. Msd Params		Total
						Integrator Signal Values	Volume Reflectivity	Reflectivity Factor	Precipitation Rate	Liquid-Water-Content M	Integral of M Along Missile Path	Liquid-Water-Content		
										of Precipitation / of Ice Cloud		Water Cloud	Ice Cloud	
Km	K Ft	N.M.	°C			I_S dB	η cm^{-1}	Z $mm^6 m^{-3}$	P $mm hr^{-1}$	$gm\ m^{-3}$	$\int_0^z M dR_S$ $gm\ m^{-2}$	$gm\ m^{-3}$	$gm\ m^{-3}$	
0	0	1.80	10.7	Rain Region	R_D	56.8	1.24×10^{-12}	57	0.30	.020	0	0	CB	.020
.81	2.65	2.60	9.0			57.5	1.41×10^{-12}	65	0.33	.022	34	0		.022
1.62	5.3	3.23	3.9			60.0	2.51×10^{-12}	116	0.50	.032	79	-		>.032
1.72	5.65	3.42	3.2			62.5	4.47×10^{-12}	206	0.77	.047	87	-		>.047
1.83	6.0	3.55	2.3			65.0	7.94×10^{-12}	366	1.17	.069	100	-		>.069
1.86	6.1	3.59	2.2	Melting Zone		66.0	10.0×10^{-12}		1.16	.068	104	-		>.068
2.13	7.0	3.83	0.8			72.2	41.9×10^{-12}		1.09	.134	161	-		>.134
2.41	7.9	4.08	-0.5			68.7	18.55×10^{-12}		1.01	.191	252	.2E		.391
2.68	8.8	4.33	-1.9			66.3	10.75×10^{-12}		0.94	.240	372	.2E		.440
2.83	9.3	4.47	-2.6	Large Snow Region	LS_C	65.0	7.94×10^{-12}	1628	0.89	.234	445	.2E		.434
2.99	9.8	4.65	-3.5			62.5	4.47×10^{-12}	916	0.69	.185	510	.2E		.385
3.14	10.3	4.82	-4.2			60.0	2.51×10^{-12}	515	0.53	.148	562	.2E		.348
4.20	13.75	5.83	-10.1			57.5	1.41×10^{-12}	290	0.41	.119	848	.2		.319
5.24	17.2	6.88	-16.5			55.0	0.79×10^{-12}	163	0.31	.095	1078	-		>.095
5.33	17.5	6.96	-17.1	S.S. to L.S. Transition Zone	SS_S and LS_C	54.6	0.73×10^{-12}		0.31	.095	1096	-		>.095
5.74	18.83	7.35	-19.6			52.9	0.49×10^{-12}		0.31	.093	1174	-		>.093
6.15	20.16	7.77	-22.4			51.2	0.33×10^{-12}		0.31	.091	1250	-		>.091
6.55	21.5	8.17	-25.3			49.4	0.22×10^{-12}		0.30	.090	1325	-		>.090
7.01	23.0	8.63	-28.8	Small Snow Region	SS_S	47.5	0.14×10^{-12}	29	0.30	.089	1408	0		.089
7.93	26.0	9.58	-36.1			45.0	0.08×10^{-12}	16	0.21	.065	1551	-		>.065
8.23	27.0	9.86	-38.8			0	0	0	0	0	1571	-		> 0

Appendix D

Surface Measurements of Precipitation Rate and Liquid-Water-Content

The precipitation rate (rain rate) at the launch site of the missiles and in the nearby vicinity was measured by tipping-bucket and weighing gauges and was also determined indirectly from disdrometer instruments, as explained in R No. 1 and R No. 2. The sites of the measurements are indicated in Figure D1.

The rain rates measured by these gauges and by the two disdrometer instruments (A and B) are shown by the time plots of Figures D2 through D9. Plots are presented for each of the launch days for 3-hr periods centered approximately about the firing times of the missiles. The firing times are indicated.

Rain rates were also measured by tipping-bucket and or weighing gauges located at the RARF-JAFNA radar site. [See the map of Figure D1 and, at another site, the so-called "Coast Guard Site" located about 3.2 mi NE of the launch pad. Time plots of the rain rates for these gauges (for all days that the gauges were operating) are shown in the second diagrams of Figures D3, D5, D7, and D9.]

The diagrams of these figures, the sets for the individual days, show the comparability of the rain rates determined by different instruments at the same site, and between sites. The temporal variability of the rainfall in the Wallops storms is directly illustrated by the diagrams. The spatial variability of the rainfall between sites can be ascertained by diagram comparisons.

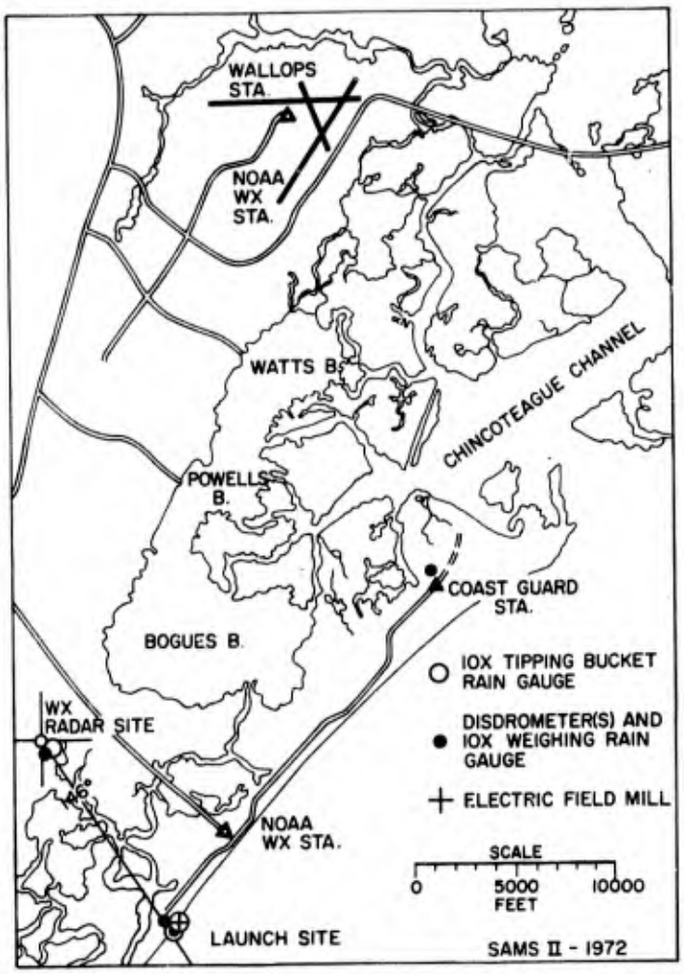

Figure D1. Map Showing Siting Locations of Rain Gauges and Disdrometers Relative to the Missile Launch Pad

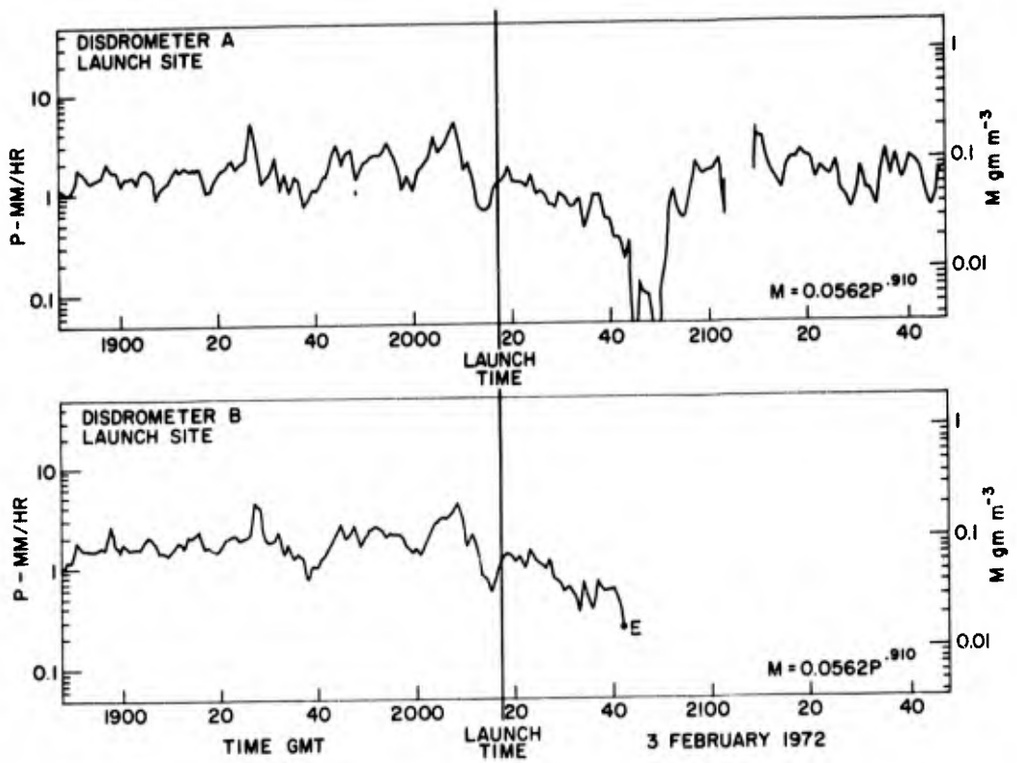

Figure D2. Time Plots of Precipitation Rate and Liquid-water-content at the Surface Level for the 3-Hr Period Centered About the Launch Time of the Missile, From Disdrometer Data Acquired at the Launch Site on 3 February 1972

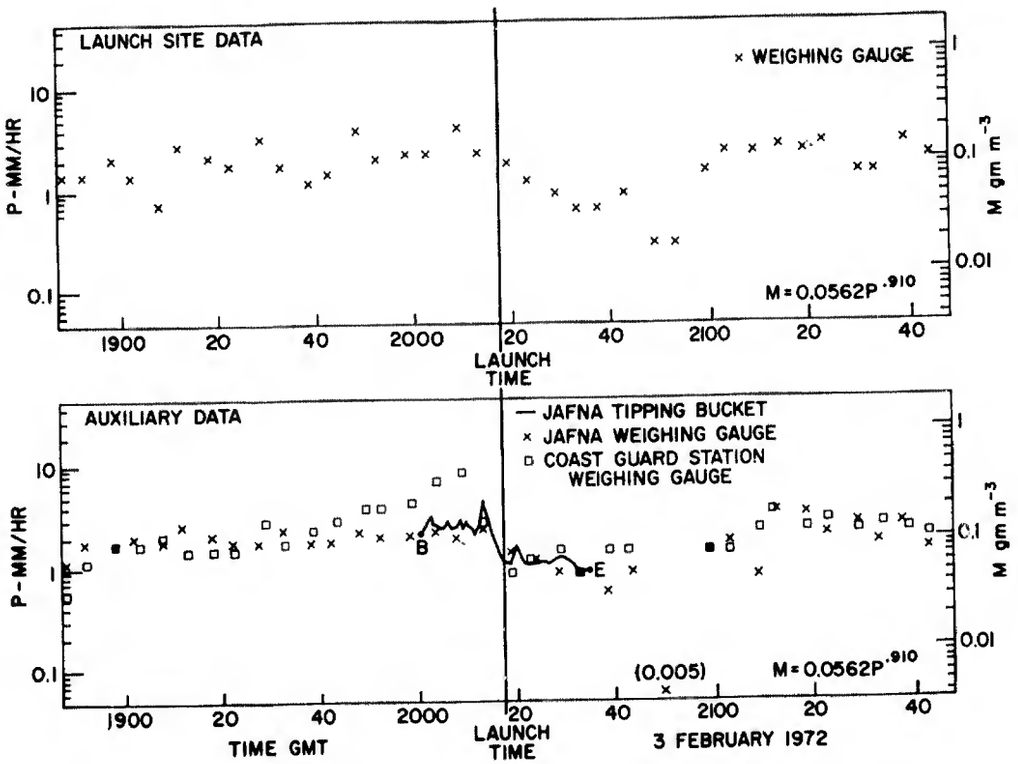

Figure D3. Time Plots of Precipitation Rate and Liquid-water-content at the Surface Level for the 3-Hr Period Centered About the Launch Time of the Missile, From Weighing Gauge and Tipping-bucket Data Acquired at the Launch Site and Other Sites on 3 February 1972

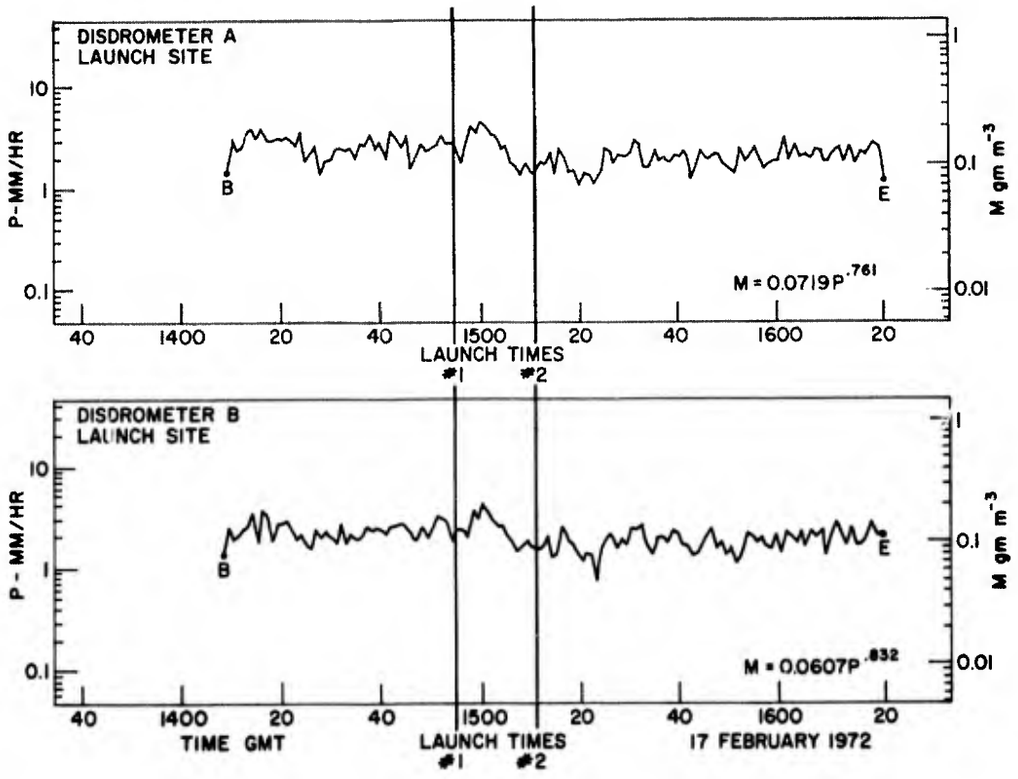

Figure D4. Time Plots of Precipitation Rate and Liquid-water-content at the Surface Level for the 3-Hr Period Centered About the Launch Times of the Missiles, From Disdrometer Data Acquired at the Launch Site on 17 February 1972

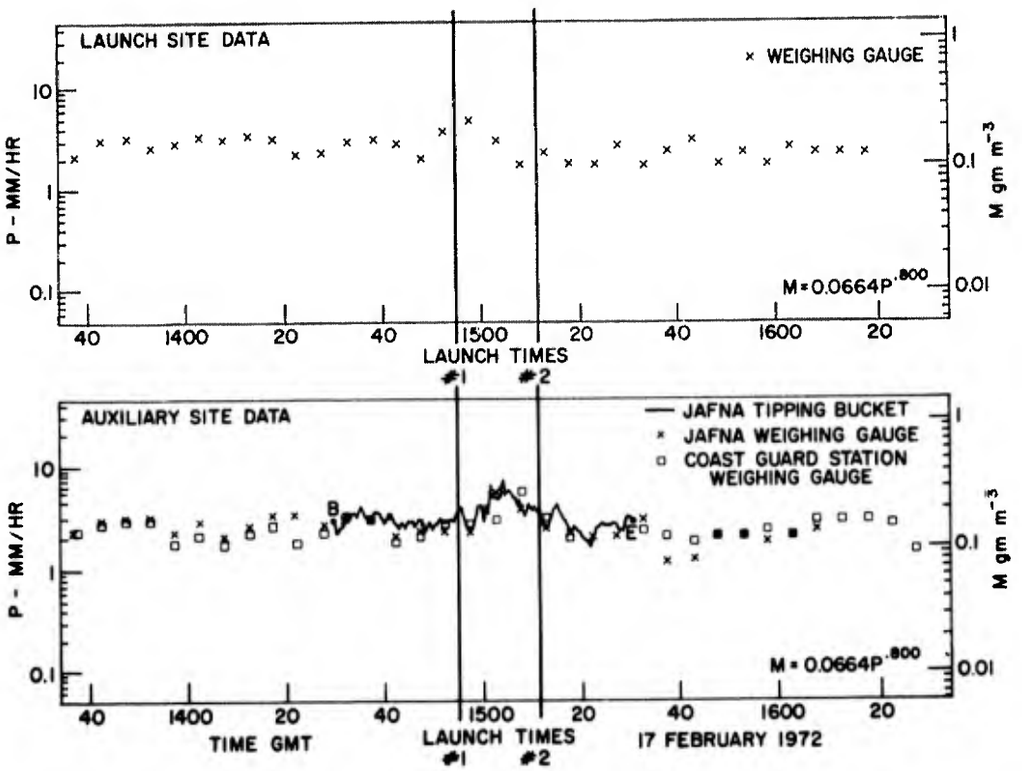

Figure D5. Time Plots of Precipitation Rate and Liquid-water-content at the Surface Level for the 3-Hr Period Centered About the Launch Times of the Missiles, From Disdrometer Data Acquired at the Launch Site on 17 February 1972

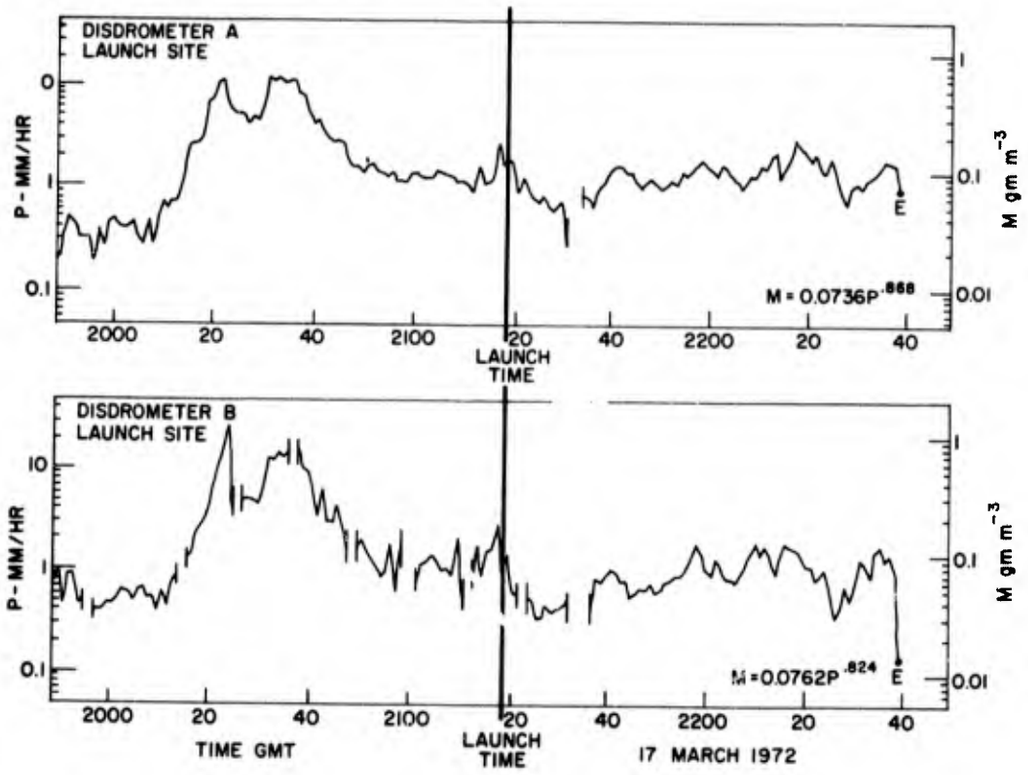

Figure D6. Time Plots of Precipitation Rate and Liquid-water-content at the Surface Level for the 3-Hr Period Centered About the Launch Times of the Missile, From Disdrometer Data Acquired at the Launch Site on 17 March 1972

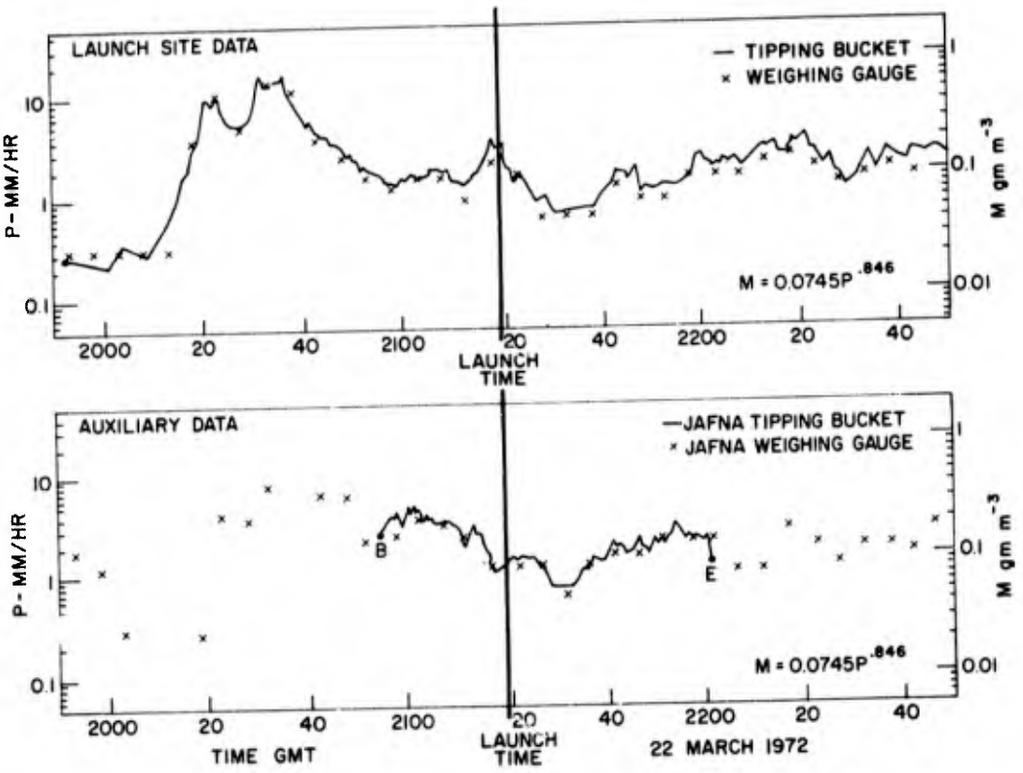

Figure D7. Time Plots of Precipitation Rate and Liquid-water-content at the Surface Level for the 3-Hr Period Centered About the Launch Time of the Missile, From Weighing Gauge and Tipping-bucket Data Acquired at the Launch Site and Other Sites on 17 March 1972

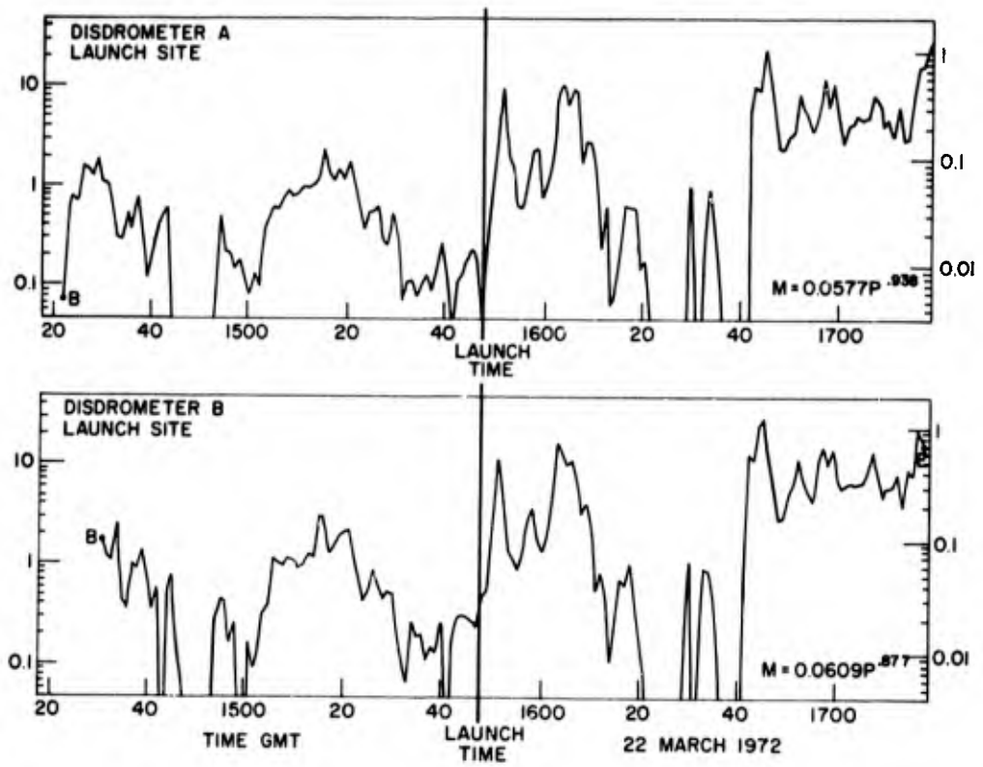

Figure D8. Time Plots of Precipitation Rate and Liquid-water-content at the Surface Level for the 3-Hr Period Centered About the Launch Time of the Missile, From Disdrometer Data Acquired at the Launch Site on 22 March 1972

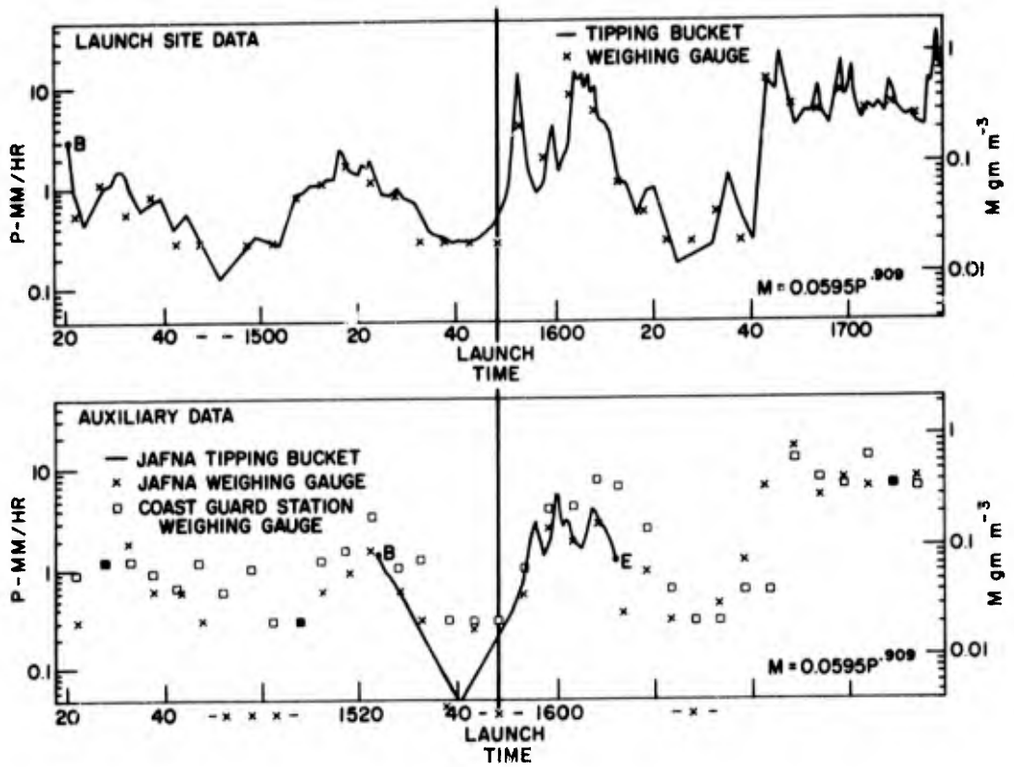

Figure D9. Time Plots of Precipitation Rate and Liquid-water-content at the Surface Level for the 3-Hr Period Centered About the Launch Time of the Missile, From Weighing Gauge and Tipping-bucket Data Acquired at the Launch Site and Other Sites on 22 March 1972

It is pertinent to mention that the time resolution of the rain-rate values determined from the disdrometer data is 1 min. The time resolution of the values from the tipping-bucket gauges is a variable function of the rain rate itself; it decreases (improves) as the rain rate increases. (For example, for the tipping-bucket gauge used at the launch site, the resolution times were, respectively, 72 sec and 7.2 sec for rain-rates of 1 mm/hr and 10 mm/hr.) With regard to the rain rates computed from the Belfort weighing gauges, the time resolution was approximately 5 min. The longer time resolution of these measurements relative to those of the tipping bucket and disdrometers is apparent in the comparison plots.

From knowledge of the size distribution of the raindrops in the Wallops storms acquired from disdrometer instruments as explained in R No. 1, the values of the liquid-water-content at the surface level could be computed from the rain rates. The techniques were described in R No. 1 in part, and supplementary information was provided in R No. 2. In the latter report, it was noted that the liquid-water-content, M, and the precipitation rate, P, are related (relatable) by an empirical equation of the form,

$$M = k P^{\epsilon} , \qquad (1)$$

where the constant k and exponent ϵ have particular values which, if size distribution data exist, are established by regression analyses (non-linear) or, if such data do not exist, are assumed to have values that are "characteristic" of the general type of rainfall of concern (for example, drizzle, widespread, showery).

Thus, when k and ϵ are established or specified for a given storm situation, any time-plot (or other plot) of the precipitation rate which is plotted on a logarithmic scale, as in the case of the diagrams of Figures D2 through D9 also becomes, with a simple change of scale, a plot of the liquid-water-content as well. These "scale conversions" were established for each of the rainfall situations illustrated in Figures D2 through D9, and the M scales pertaining to the plots have been drafted on the diagrams at the right. The particular equations relating M and P are also indicated. These, for the disdrometer plots, are the regression equations that were established from the data of the individual A or B disdrometers. For the tipping-bucket and weighing-gauge plots, they were assumed to be the equations listed in Table 2 of R No. 2, which are the "average equations" for both disdrometers.

The time trends and site differences of liquid-water-content at the surface levels, which are revealed by Figures D2 through D9, provided valuable, quantitative information for SAMS. They provide information concerning (1) the

correspondence between the radar-measured and rain-gauge values of M at the launch times of the missiles, and (2) the temporal-spatial variability of M at the launch times. The latter is indicative of the probable representativeness and uncertainties of the trajectory values of M within the rain region (of those shown plotted in Figures 1 through 5) and is also indicative of the probable representativeness of the aircraft measurements made in the particular storms (since these measurements were begun after the missiles were launched and were made through spatially different regions of the moving storms than those penetrated by the missiles).

A comparison of the Figures 1 through 5 profiles and the Figures D2 through D9 diagrams for the four individual storms of the 1971-72 season shows that the radar-measured values of M and those of the rain gauges at the launch site were in good correspondence during each of the storms. The comparisons also reveal that the storms of 3 February, 17 February, and 17 March were quite homogeneous in their precipitation structure at the surface level, while that of 22 March evidenced considerable variability of a convective type.

Appendix E

AFCRL, C-130 Flights in the 1971-72 Season

The AFCRL, C-130 aircraft was based at Hanscom Field, Bedford, Massachusetts during the 1971-72 season. When appropriate storm conditions were forecast for the Wallops area, the aircraft was flown from Hanscom Field to the Wallops area where it "stood by", in a holding pattern, awaiting the potential missile firing and the commencement of the supporting storm measurements.

The aircraft was flown from Hanscom Field to Wallops, and return, on five days during the month of January 1972, as identified in Table E1. However, no missiles were launched into these particular storms because of unsuitable conditions or for other reasons that will not be recounted.

Fuel leaks were discovered in one of the wing tanks of the C-130 on 25 January 1972. The aircraft had to be flown to Warner Robbins AFB for major repairs, which were not completed until 6 April 1972. Thus, although appreciable time and effort were expended in flying the aircraft in support of SAMS, no data were acquired in the storms of launch operations.

All aircraft data for the 1971-72 season were obtained with the MRI, Aztec aircraft, as discussed in the following appendix.

Table E1. Dates and Times of AFCRL, C-130 Flights in Support of SAMS-ABRES During the 1971-72 Season With Comments About Mission Results

Dates of Planned Missile Launches	AFCRL, C-130 FLIGHT INFORMATION		Comments
	Airfield of Departure and Take Off Time	Airfield of Landing and Landing Time	
11 January 1972	Bedford, Mass. 1310 EST	Wallops Station, Va. 1540 EST	Missile not fired.
11 January 1972	Wallops Station, Va. 1638 EST	Bedford, Mass. 1751 EST	Return flight from mission.
13 January 1972	Bedford, Mass. 1400 EST	Bedford, Mass. 1440 EST	Flight aborted due to oil leak in No. 1 engine.
14 January 1972	Bedford, Mass. 0557 EST	Bedford, Mass. 1013 EST	Aircraft flew from Bedford to Wallops Station thence back to Bedford. Missile not fired.
19 January 1972	Bedford, Mass. 0924 EST	Wallops Station, Va. 1130 EST	Missile not fired.
19 January 1972	Wallops Station, Va. 1224 EST	Bedford, Mass. 1347 EST	Return flight from mission.
22 January 1972	Bedford, Mass. 0927 EST	Wallops Station, Va. 1145 EST	Missile not fired.
22 January 1972	Wallops Station, Va. 1242 EST	Langley AFB, Va. 1506 EST	Missile not fired.
			NOTE: No C-130 sorties were flown after 22 January in this season because fuel leaks were discovered in one of the wing tanks. The aircraft was at Warner Robbins AFB, Ga., undergoing PDM*, from 25 January through 6 April 1972.

*Periodic Depot Maintenance

Appendix F

Liquid-Water-Content and Size Distribution Information Acquired from the MRI, Aztec Aircraft

A Piper-Aztec aircraft was flown contractually for SAMS purposes in the 1971-72 season by Meteorology Research, Inc. (MRI). The aircraft was based at Wallops Station Airfield. The pilot was Mr. Alfonso Ollivares.

When appropriate storm conditions for missile launch operations existed at Wallops, the Aztec aircraft was usually flown into the storm to near its ceiling altitude of approximately 23,000 ft. It remained there in a holding pattern until (a) the missile was fired, or (b) the launch operations were terminated, for one of a variety of reasons. If a missile was fired, the Aztec was flown from the holding pattern to the trajectory region of the storm, and the pilot began a measurement traverse along the line of the horizontal projection of the trajectory. The traverse was about 10 NM in length and the pilot was directed along the path by radar vectoring from one of the NASA tracking radars. When the first traverse was completed at the ceiling or near ceiling altitude of the aircraft, the pilot then descended to a lower flight altitude and began a second measurement traverse, followed by a third, a fourth, and so forth. The traverse altitudes were specified on the bases of the particular storm characteristics, together with the pilot's radio description of the hydrometeor conditions being encountered. About six to ten total traverses were usually made, separated in altitude by approximately 1 to 5000 ft. The time required to accomplish the traverses following missile firing was some 50 to 90 min.

The MRI, Aztec aircraft arrived at Wallops Station, Virginia on 1 February 1972. It was flown on all of the storm days of missile launch operations during the 1971-72 season. The dates and the takeoff and landing times of the aircraft are

listed in Table F1. Flight measurements, after the aircraft was airborn and at altitude, were made on 3 February 1972 between 1517 and 1610 EST, from a storm altitude of 15,000 ft descending to 1000 ft. The measurements on 17 February were made between 1027 and 1104 EST, from 20,000 to 1000 ft; on 17 March they were made between 1628 and 1730 EST, from 21,000 to 1500 ft; on 22 March they were made between 1058 and 1220 EST, from 23,000 to 1000 ft.

Table F1. Dates and Times of MRI, Aztec Flights in Support of SAMS-ABRES During the 1971-72 Season. The Aztec aircraft was based at Wallops Station, Virginia

AIRCRAFT TAKE OFF AND LANDING TIMES			
Date	Take Off EST	Landing EST	Comments
3 February 1972	1320	1345	Flight aborted due to windshield leak and water on radios.
3 February 1972	1450	1815	Missile launched at 1517 EST
17 February 1972	0910	1125	Missiles launched at 0956 and 1012 EST.
17 March 1972	1535	1740	Missile launched at 1619 EST.
22 March 1972	0945	1245	Missile launched at 1048 EST.

Transcripts of the pilot's comments about the general nature of the storm conditions that were encountered at the different flight levels in the four storms of the season are presented in Tables F2 through F5. These transcripts of the tape-recorded radio conversations between the flight controller at the RARF (JAFNA) radar site (see the map of Figure D1) and the aircraft pilot have been edited to delete all conversations excepting those directly concerned with reports of storm conditions and flight altitudes. Navagational and positioning instructions and comments were deleted because it was felt that the extra figures and text that would be required properly to describe the flight track of the aircraft in three dimensions and time were beyond the scope of the present appendix discussion.* (In lieu of this information, the reader should be informed that the cloud and hydrometeor conditions encountered along any given flight path level within the storms are

*It may be noted that "flight track diagrams" exist which have been related to the flight paths of the missiles and to the radar RHI photographs that were acquired during the aircraft sampling periods, but these will not be presented herein.

normally variable to an appreciable degree. Thus, the pilot's comments in Tables F2 through F5 should not necessarily be assumed to be indicative of the storm conditions in general or of the particular hydrometeor situations at the launch times of the missiles.)

Table F2. Edited Transcript of JAFNA Controller—Aircraft Pilot Radio Conversations During Measurement Portion of the Aztec Flight of 3 February 1972

Time (GMT)	Altitude K ft	Station*	Remark
2001:10	4.5	Y	31Y is in the cloud at 4.5K.
~2004:20	7.0	Y	Altitude is 7K and we're still in the cloud, in and out at times.
~2008:25	9.0	J	31Y, give us your condition and altitude again.
~2008:35	9.0	Y	Roger, we're still at 9K and in the cloud.
~2008:45	9.0	J	Roger, are you in snow?
~2008:50	9.0	Y	Negative, no precip. at all.
~2008:55	9.0	Y	Now it is just starting again.
~2012:30	10.7	Y	31Y is at 10,700 and we're in the cloud.
2013:00	11.0	J	31Y, this is J, be advised we are counting, we are at minus 3 and one-half minutes and counting.
2016:30	12.0	J	31Y, this is J, T minus 30.
2017:00	12.5	J	31Y, we have fired.
~2020:10	15.0	Y	We're at 15,000.
2021:00		J	31Y, what's your present altitude?
2021:10	15.0	Y	Roger, about 15,100.
2022.00	14.5	J	31Y, are you in the clear?
		Y	Negative, 31Y.
2022:30	14.5	J	When you get thru that cloud deck you can hold that altitude.
		Y	Roger, 31Y.
2030:00	15.0	Y	We're in the cloud, no precip. hitting the windshield now.
2030:30	15.0	J	31Y, J, is there any precip. visible from the side.
		Y	Negative, at the present time.

*J indicates JAFNA

Y indicates aircraft (31 Yankee)

Table F2. Edited Transcript of JAFNA Controller—Aircraft Pilot Radio Conversations During Measurement Portion of the Aztec Flight of 3 February 1972 (Cont)

Time (GMT)	Altitude K ft	Station*	Remark
2031:30	15.0	J	31, this is J, are you experiencing any icing?
		Y	31Y, we have some icing on the trailing edge of the pylon but none on the leading edge of the wing at the present time.
2034:45	15.0	Y	31Y is starting to get a very small trace of ice on the windshield.
~2036:50	15.0	Y	Present altitude 15,000.
2038:00	15.0	Y	31Y is picking up a little more ice on the windshield now.
~2039:40	15.0	J	Descend to 10,000 ft preferably to the left.
2040:00		Y	Descend 10,000 ft.
~2041:20		J	Are you at 10,000 ft now 31?
2041:30	14.0	Y	Negative, I'm at 14,000.
2044:30	11.9	Y	31Y is picking up ice on the nacelles and the leading edge of the wing.
2047:30	10.0	J	31, you're at 10,000 ft and the equipment is running?
~2047:40	10.0	Y	Roger, 31Y.
~2048:05	10.0	J	31, J, what is your condition now, are you in wet snow?
2048:15	10.0	Y	The ice is melting off the windshield but we can see white flakes going past the cabin.
~2050:20	10.0	Y	Descending from 10 to 5.
2052:00	9.0	J	31, what's your present condition?
2052:15	8.8	Y	Roger, in rain at the present time, very slow.
2053:00	8.0	J	31, what's your altitude now?
~2053:10	8.0	Y	8000 and descending.
2055:30	6.2	J	31, what is your altitude now?
		Y	6,200 descending.
2056:00	5.5	J	31, what's your condition now, is it all rain or some cloud and rain?
		Y	We're just about ready to enter into cloud.

Table F2. Edited Transcript of JAFNA Controller—Aircraft Pilot Radio Conversations During Measurement Portion of the Aztec Flight of 3 February 1972 (Cont)

Time (GMT)	Altitude K ft	Station*	Remark
2056:15	5.3	J	We'd like to have this run start now and hold 5,000 ft.
~2056:25	5.3	Y	Roger, I'll hold 5, I'm about 5,300 now.
2103:15	5.0	J	31, J, we'd like to have you descend to 1,000 ft.
		Y	Roger, descending to 1,000.

Table F3. Edited Transcript of JAFNA Controller—Aircraft Pilot Radio Conversations During Measurement Portion of the Aztec Flight of 17 February 1972

Time (GMT)	Altitude K ft	Station*	Remark**
1533	16.0	Y	Descending through 16,000, no precip.
1535	15.3	Y	31 Yankee starting to pick up some precip. at 15,300.
1553	1.5	J	31 Yankee, give me your position and altitude
		Y	We're at 1500 now.

*J indicates JAFNA

Y indicates Aircraft (31 Yankee)

**Sparseness of remarks for this date are mostly due to communication and aircraft-tracking problems. Missile recovery operations during this period was another contributing factor.

Table F4. Edited Transcript of JAFNA Controller—Aircraft Pilot Radio Conversations During Measurement Portion of the Aztec Flight of 17 March 1972

Time (GMT)	Altitude K ft	Station*	Remark
2123	21.0	J	31 Yankee, from JAFNA, are you still VFR, at what altitude?
		Y	Roger, we are VFR on top at 21,000.
		J	Roger, is that going to clear all the clouds?
		Y	Ah Roger, we will be clear of all clouds.
2127	21.0	J	31 Yankee, you're still a few thousand ft above the tops?
		Y	Roger. It looks like we're probably 3000 ft above the tops.
		J	OK. You only have about 2 more miles to go, why don't you descend down to the tops?
		Y	Roger.
2130	20.5	J	31 Yankee, the radar tops the highest outlooks about 18,500.
		Y	I'd say that'd probably check out about right.
		J	31 Yankee, what altitude are you at?
		Y	Roger, 20,000 descending.
2132	19.9	J	Are you in the cloud tops at all?
		Y	I will be entering the clouds in about 30 sec.
2133	19.5	Y	The wind up here is getting the best of me.
		J	Roger. It will. Have you hit the cloud top yet?
		Y	I'm at 19,500
2135	18.5	J	31 Yankee. How's those cloud tops?
		Y	Roger 31 Yankee. It's very thin up here. I can see a real lot below me. We haven't really got into the thick part of the clouds yet.
		J	Are you in clouds now?
		Y	Very thin. Very thin.

*J indicates JAFNA

Y indicates Aircraft (31 Yankee)

Table F4. Edited Transcript of JAFNA Controller–Aircraft Pilot Radio Conversations During Measurement Portion of the Aztec Flight of 17 March 1972 (Cont)

Time (GMT)	Altitude K ft	Station*	Remark
2137	17.0	J	Say again your altitude, please.
		Y	Roger, coming up on 17,000.
		J	Have you got the replicator going?
		Y	Roger, we've been sampling since 19,500.
		J	There was some snow drizzles in 19,5. Is that right?
		Y	Roger.
2138	16.3	J	Do you see anything at all on the windshield?
		Y	Negative on the windshield.
2139	15.0	J	31 Yankee. You're continuing to descend is that right?
		Y	Roger.
		J	OK, let's make a horizontal run at 15,000 ft.
		Y	Roger.
2142	15.0	Y	I think I can see a little cloud deck down there. We are in the clear between layers.
		J	You got a chance to put that snow stick on up?
		Y	Roger, we're picking up a very small trace of snow on it.
		J	On the snow stick, right?
		Y	Roger, very small though.
		J	Like a tenth of a millimeter or so?
		Y	Roger.

Table F4. Edited Transcript of JAFNA Controller–Aircraft Pilot Radio Conversations During Measurement Portion of the Aztec Flight of 17 March 1972 (Cont)

Time (GMT)	Altitude K ft	Station*	Remark
2143	15.0	Y	Now the clouds are starting to thicken up quite a bit.
		J	OK Roger. If you have a chance you can make a comment about what you see on the stick.
		Y	Very fine crystals are all I can see. They are just barely showing. Now we are starting to break out of the clouds.
		J	You're at 15 is that right?
		Y	Roger, 15000.
2147	15.0	J	31 Yankee from JAFNA. Could you descend to 10,000?
		Y	Roger, 31 Yankee starting descent from 15,000.
2151	13.0	J	Could you give us your altitude?
		Y	13,000.
		J	and what are the conditions?
		Y	Roger, we're in the clouds at present time and getting a slight trace on the snow stick.
		J	Is it a trace of small particles or what?
		Y	The particles are getting slightly larger now, I can see them a little better.
		J	The smallest division on that line is 1 mm. Are they that big yet?
		Y	Negative, sir, they are about a quarter of a division.
		J	Apparently you can't be getting much icing then, because that stick will ice up pretty easily.
		Y	Roger, we don't have a trace at all on the aircraft.
2154	11.3	J	And what altitude are you at now?
		Y	Roger, working up 11,000 now.
2156	10.0	J	Read again your altitude please.
		Y	Roger, 10,000, we're as little as 10,000.
		Y	The snow stick is starting to show . . . to about 1/2 a measure.
		J	Did you say 1/2 mm, is that right?
		Y	Ah, Roger.

Table F4. Edited Transcript of JAFNA Controller–Aircraft Pilot Radio Conversations During Measurement Portion of the Aztec Flight of 17 March 1972 (Cont)

Time (GMT)	Altitude K ft	Station*	Remark
2159	10.0	Y	We're starting to pick up a trace of ice on the windwhield.
2203	8.5	Y	My level is 8500 now.
2205	7.5	J	Does it appear that you're likely in snow and very little icy clouds?
		Y	- - - - a slight case on the windshield of ice.
		J	Roger, that's at about 8000?
		Y	About 8 to 7.
2206	7.0	J	?1 Yankee from JAFNA. These particles do they look like snow particles or do they look like graupel?
		Y	I'd say snow particles.
2209	7.0	J	31 Yankee, this 432, what is your altitude?
		Y	31 Yankee is at 7000, now.
2212	6.5	J	31 Yankee, the radar indicates that the melting level should be somewhere around 6000 ft.
		Y	At 7000 we had a temperature of -1°C.
		J	If you could watch that snow stick, we're going down to six to see if there are big flakes.
		Y	Roger, we're at 6500 and all we're getting rain drops now.
		J	Did you check that on the stick?
		Y	Roger, OK all rain at 6500.
		J	As far as you can tell, the foil sampler is working?
		Y	Roger.
2221	4.3	J	31 Yankee, your altitude?
		Y	4300 at the present time.
2222	~4.0	J	Any cloud decks there, at all?
		Y	We just broke out of the cloud at the turn and we're getting back into it now.

Table F4. Edited Transcript of JAFNA Controller–Aircraft Pilot Radio Conversations During Measurement Portion of the Aztec Flight of 17 March 1972 (Cont)

Time (GMT)	Altitude K ft	Station*	Remark
2226	~1.5	Y	JAFNA Radar this is 31 Yankee, could we descend below 1000 ft, we're still in clouds here.
2229	~1.2	J	You descend and see what you get for a ceiling there. Your far-seeing ceiling is 700 ft. Go ahead. Go ahead and descend.
		Y	Roger.

Table F5. Edited Transcript of JAFNA Controller–Aircraft Pilot Radio Conversations During Measurement Portion of the Aztec Flight of 22 March 1972

Time (GMT)	Altitude K ft	Station*	Remark
1556	23.0	J	What is your altitude?
		Y	23,000 now.
1602	23.0	Y	Starting descent to 15,000.
1604	22.0	J	What's the temperature up there?
		Y	We've go a minus 25 right now.
1606	20.2	Y	31 Yankee breaking out in an area of clear skies with ---- just below us.
		J	Roger. You are at what altitude?
		Y	Approaching 20,200 now.
1610	~18.0	Y	Roger, 31 Yankee still between layers. There's a thin layer above us and a pretty thick layer below and we are at 17,700.
1612	16.0	J	Are you still in the clear?
		Y	Roger.
1615	14.4	J	31 Yankee, does it look like the decks merge off to your right, there?
		Y	The clouds are a bit larger off to the right. Straight ahead It'd probably be 9 or 10,000, I'd say.

*J indicates JAFNA

Y indicates Aircraft (31 Yankee)

Table F5. Edited Transcript of JAFNA Controller–Aircraft Pilot Radio Conversations During Measurement Portion of the Aztec Flight of 22 March 1972. (Cont)

Time (GMT)	Altitude K ft	Station*	Remark
1617	14.0	J	Your altitude and weather please.
		Y	14,000 ft. I'm in the clear at present time. There seems to be a line of clouds at this altitude but it's off to my left maybe about a mile or so.
1619	14.0	J	Ok, take a 180 to the left
		Y	Roger. In cloud for a short period at this altitude.
1629	14.4	J	What's your present position and weather?
		Y	I'm in the clear but we'll be entering some clouds on this heading.
1630	14.0	Y	Level is 14.0 temp -8.
		Y	It looks like very fine raindrops or cloud droplets on snow stick.
		J	Do they have any whiteness at all to them.
		Y	Negative, water only.
1630	13.8	J	Any idea of the particle size?
		Y	Very fine, about 1/5 mm. No sign of icing. We have the sun shining down on top of us.
1632	13.0	Y	Starting descent to 10,000.
1634	12.0	Y	Passing 12,000.
1635	11.7	Y	We are in clouds.
		J	Is there any snow?
		Y	Negative, temp is -4 at 11,000, we're still getting water droplets on the snow stick.
1637	10.0	Y	At 10,000 now and holding this altitude.
1643	10.0	Y	We're starting to pick up a trace of ice on the windshield. We are getting quite a few small crystals on the snow stick about 1/10 mm.
1647	10.0	J	Could you give me some weather information?
		Y	Roger, we are getting very large droplets hitting the windshield very hard, we're picking up a pretty good layer of ice.
1648	10.0	Y	Descending to 8000.

Table F5. Edited Transcript of JAFNA Controller–Aircraft Pilot Radio Conversations During Measurement Portion of the Aztec Flight of 22 March 1972 (Cont)

Time (GMT)	Altitude K ft	Station*	Remark
1649	9.5	Y	31 Yankee is getting quite a few large particles going by the windshield.
		J	Does it look like water & snow mixed?
		Y	Sure looks that way.
		J	Altitude please.
	9.2	Y	9200 ft, descending.
	8.5	J	Altitude please.
1650	8.5	Y	8500.
1651	8.0	Y	Nothing shows on the snow stick, we got a little clear spot between layers.
1657	5.0	Y	31 Yankee at 5000 ft.
1658	4.5	J	Are you still in the rain?
		Y	Roger.
1659	3.6	J	What altitude are you at?
		Y	3600 now, in and out of cloud and continuous light rain.
1704	4.0	J	Have you reached any heavier rain in the last few minutes?
		Y	Roger, we're just getting out of it now and its tapering off very rapidly.
1709	2.5	Y	We are entering into pretty heavy rain, here.
1711	1.0	Y	We're at 1000 ft and a mile from the coast line.

The Aztec was equipped with sensing and recording instruments that provided measurements of the heading, altitude, and airspeed of the aircraft, and that recorded the temperatures and humidities at the flight levels. The liquid-water-content of the water droplets in the cloud-size range (generally smaller than about 80 microns) was measured by a Johnson-Williams (JW) hot-wire, liquid-water-content meter. The instrument provided measurements for droplets that were either "warm" (>0°C temperature) or "supercooled" (<0°C). A formvar-replicator instrument gave records of the numbers, sizes and appearance of the ice crystals, snow-particles and water droplets that entered the collector of the instrument and were captured and replicated on moving, formvar-coated film. The liquid-water-content of these hydrometeors was determinable, to a first

approximation, from size distribution analyses and computations performed on certain selected portions of the instrument records.

The sizes and numbers of the hydrometeors in the precipitation-size range (generally > 80 microns) were measured by a foil-impactor device aboard the Aztec aircraft. Aluminum foil was transported past an orifice exposed to the airstream, and the impact impressions of the impinging water drops and ice particles were recorded on the foil. The liquid-water-content of the recorded hydrometeors was approximately determinable from size-distribution analyses, as in the case of the formvar-replicator.

It was standard practice at Wallops, on the day following a missile firing, to hold a conference at which all of the meteorological, aircraft and radar data pertaining to the launch were reviewed and decisions made about the analyses to be conducted on the particular types, and/or portions, of the total available information. The foil-sampler and formvar-replicator records from the Aztec aircraft were examined at these conferences and the general hydrometeor structure of the storm (particle type and size-range vs altitude) was established. The findings were tabulated, as shown in Tables F6 through F9, and MRI was requested to perform special "number count and size-distribution analyses" on selected samples (time-period portions) of the records. Selections were made on the bases of available data (one or the other of the instruments sometimes malfunctioned, in certain storms, in certain altitude ranges), on the quality of the data, and on the general uniformity of the record traces within the sample periods (uniformity within the sample was desired). The number of samples selected also had to be drastically limited by the practical consideration that considerable time and effort would be involved in the manual sizing and counting of the hundreds of drops and particles contained in each sample.

Table F6. Summary of Formvar Observations for Storm of 3 February 1972

1.	Altitude 15,000 Ft, Time 2033-2034 Z	
	a.	Few snowflakes, conc. ~ 0.15 lit^{-1}, sizes smaller than about 1 mm.
	b.	Drops (dia. $> \sim 50$ μm) present in concentration of about 0.7 lit^{-1}.
	c.	No crystals evident.
	d.	Cloud droplets (dia. < 50 μm) present, but relatively low in number conc. (see droplet size-distributions). Therefore LWC remains low (< 0.3 g/m^3).

Table F6. Summary of Formvar Observations for Storm of 3 February 1972 (Cont)

2. Altitude 14,500 - 14,000 Ft, on Start of Descent, Time 2041 Z
   a. Snowflake conc. increasing, conc. ~ 0.43 lit^{-1}, size about 1 mm dia.
   b. Drops present in concentrations of about 0.5 to 0.8 lit^{-1}.
   c. Ice crystals (columns) present in conc. of about 0.1 lit^{-1}, sizes < 200 μm.
   d. Cloud droplets present, relatively low in concentrations.

3. Altitude ~ 12,500 Ft, Time ~ 2042:40 Z
   a. Snowflake conc. increased to about 2.0 lit^{-1}. Flakes as large as 3 mm.
   b. Drop concentration of about 0.5 lit^{-1}.
   c. Column concentration of about 0.36 lit^{-1}, sizes of up to 300 μm × 75 μm.
   d. Droplets present, relatively low concentration.

4. Altitude 10,000 Ft, Time 2048:00 Z
   a. Snowflake concentration increased to about 2.7 lit^{-1}. Snowflakes appear partially melted; drop splashing occurs simultaneously with large broken flakes. Flakes appear partially rimed. Flakes as large as 3 mm.
   b. Determination of drop concentration difficult due to melting snow. Guess would be less in number than at 12,500 ft.
   c. No crystals noted.
   d. Droplets present, see size-distribution for information of sizes, concentration, and LWC.

5. Altitude 5000 Ft, Time ~2057 Z
   a. No snowflakes present.
   b. Drops or raindrops present, see raindrop size distribution for this level.
   c. No crystals present.
   d. Cloud droplet size-distribution difficult to obtain due to:
      (1) Intermittent operation of instrument,
      (2) Raindrops splashing throughout most of record.
      Seems as if cloud droplets (dia. <~ 50 μm) very scarce.

Table F7. Summary of Formvar and Foil Sampler Observations for Storm of 17 February 1972

1. Altitude 20,000 Ft, Temp: -19C, Location: Orbit, Time: ~0950 LST
   a. Snowflake Conc: 4.5 lit^{-1} Max Sizes (dia.) less than 3 mm, probably less than 1-2 mm.
   b. Crystal Conc: 0.6 lit^{-1} Plates, Max. sizes less than 200 μm.
   c. No cloud droplets.
   d. Remarks: Snowflakes probably include large spacial dendrites.

2. Altitude 20,000 Ft, Temp: -19C, Location: Radial 150° to Pt K start descent, Time: 1028 LST
   a. Snowflake Conc: 11.4 lit^{-1} Max sizes less than 3 mm.
   b. Crystal Conc: 0.8 lit^{-1} Plates, sizes less than 200 μm.
   c. No cloud droplets.
   d. Remarks: As in 1, above.

3. Altitude 15,000 Ft, Temp: -10C, Location: See map, Time: 1034 LST
   a. Snowflake Conc: 9.6 lit^{-1} Max sizes < 3 mm but larger than at 2.
   b. Crystal Conc: 0.9 lit^{-1} Plates, sizes less than 200 μm.
   c. Cloud droplets present. Estimate LWC < .01 gm/m^3.
   d. Remarks: As in 1, above.

4. Altitude 13,000 Ft, Temp: ~ -5C, Location: IV on map, Time: 1037 LST
   a. Snowflake Conc: 4.7 lit^{-1} Max sizes > 3 mm.
   b. Crystal Conc: ~0.2 lit^{-1}, Columns, less than 200 μ long.

5. Altitude 10,000 Ft, Temp: ~0C, Location: V on map Radial to Pt K Time: 1041 + 20 sec LST
   a. Snowflake Conc: 3.6 lit^{-1} Max sizes > 3 mm.
   b. Crystal Conc: 0.06 lit^{-1} Plate ~ 300 μ.
   c. Droplets present: JW reading ~ 0.1 to 0.15 gm/m^3.
   d. May show early signs of melting.

6. Altitude ~ 9500 Ft, Temp: ~0C, Location: Close to V on map, Time: 1040 + 50 sec LST
   a. Snowflake Conc: Not read. Max Sizes > 3 mm.
   b. Crystal Conc: None < .05 lit^{-1}.
   c. Droplets present: JW reading ~ .15 gm/m^3.
   d. Remarks: Melting becoming quite evident from drop splashing and wet snow splashes.

Table F7. Summary of Formvar and Foil Sampler Observations for Storm of 17 February 1972 (Cont)

7. Altitude 8000 Ft, Temp: ~0 to +1C, Location: On map, Time: 1043 + 15 sec LST

   a. Snowflake Conc: 2.0 lit^{-1} Sizes > 3 mm.

   b. No crystals evident.

   c. Droplets appear in highest concentration here. JW LWC ~ 0.15 to 0.2 gm/m^3.

   d. Remarks: Part of high droplet counts due to splashing of completely melted snow. Drop splashes pronounced. Partially melted snow pronounced.

8. Altitude 5000 Ft, Temp: ~+2 to +3C, Location: See map Time: 1047 LST

   a. Snowflake Conc: 1.7 lit^{-1} Max sizes > 3 mm.

   b. No crystals evident.

   c. Droplets prese[illegible]: JW LWC reading: ~.15 gm.

   d. Remarks: T[illegible]egion or altitude marks the cloud base of the storm system. No evidence of cloud droplets at lower elevations on both the JW meter and Formvar records.

9. Altitude 4000 Ft, Temp: +3 to +4C, Location: See map Time: 1049 LST

   a. Snowflake Conc: 0.5 lit^{-1} Sizes < 3 mm.

   b. No crystals evident.

   c. No droplets.

   d. Remarks: No partially melted or dry snowflakes found at elevations lower than this altitude. This altitude marks the end of the melting. The splash signatures indicate that these almost completely melted snowflakes were smaller than about 3 mm in diameter. No dry flakes were evident. All precipitation primarily liquid in composition.

10. General Remarks:

   a. The snowflakes at the higher elevations (> 15,000 ft) are probably spacial dendrites, all smaller than about 2 mm diameter.

   b. These falling snowflakes grow further in the region 15,000 to 10,000 ft and some attain diameters of at least 3 mm. I would guess that these snowflakes ≥ 3 mm would be found in concentrations of 5 to 10 percent of that reported for these levels.

   c. Melting starts from about 10,000 ft (~0C) and is nearly complete by 4000 ft (3 to 4C).

Table F7. Summary of Formvar and Foil Sampler Observations for Storm of 17 February 1972 (Cont)

10. General Remarks: (Cont)

d. From the observation of heaviest splashing frequency at the 8000 ft level it seems quite probable that most of the falling snowflakes melt at temperatures slightly warmer than freezing. Observations of decreases in snowflake concentrations of about 1.6 lit^{-1} from 10,000 to 8,000 ft and a slight decrease of only about 0.3 lit^{-1} from 8000 ft to 5000 ft (+2 to +3C) also strongly support this probability. As it is obvious to you, the smaller snowflakes melt earlier than the larger flakes.

e. From the observations of the sizes (< 3 mm) of the last remaining melting snowflakes (at 4000 ft), it may be possible that the largest of the snowflakes had masses of less than a 3 mm raindrop. (Stretching)

f. In viewing the oscillograph recording and Formvar records of the entire flight, it becomes evident that the storm was characterized by individual cells. Indications of LWC (although low) on both the oscillograph and Formvar records at two different elevations without any indication of LWC between these different elevations suggest that cells (although weak) were present.

g. With the storm's cellular structure in mind, a best guess of the LWC vertical profile of the cloud droplets would be: From cloud base (at about 5000 ft) to about 10,000 ft the LWC is in the order of about .1 to .2 gm/m^3. The LWC decreases to less than about .01 gm/m^3 at 15,000 ft. At higher elevations the droplets are no longer present.

Table F8. Summary of Foil Sampler Observations for Storm of 17 March 1972

1. Altitude: 23-21 K Temp: -27C Source: Foil only

   Remarks: Regions of particles and no particles. Solid particles all smaller than 250 μm. Particle concentrations range from 0.1 to 5 lit^{-1} in regions of ice. No cloud droplets.

2. Altitude: 17-18 K Temp: ~ -21C Source: Foil and Formvar

   Remarks: Solid particles on foil records all smaller than 250 μm. Foil particle concentration varies between 0.4 to 1.7 lit^{-1}.

   Formvar records indicate the presence of fragile, low density, spatial type crystals. These crystals are characterized by multi-plate type growth from a nucleus. Estimated sizes smaller than about 200 μm. Estimated concentrations of 0.6 lit^{-1}. No cloud droplets.

3. Altitude: 15-17 K Temp: -16.5 to -19.5C Source: Foil only

   Remarks: Solid particles on foil records all smaller than 250 μm. Particle concentrations vary between 0.5 to 2.4 lit^{-1}.

4. Altitude: 15 K Temp: -16.5C Source: Foil and Formvar

   Remarks: Data from horizontal flight sampling. Foil records indicate regions containing particles and no particles. First evidence of particles to 500 μm. Total ice concentrations of between 0.4 to 3.4 lit^{-1}. 500 μm particles found in concentrations of up to 0.1 lit^{-1}.

   Formvar records disclose ice concentrations of the order of 10 lit^{-1}. Again majority of crystals are fragile and of low density. Spatial outgrowths of plate-like crystals are dominant.

   No indications of cloud droplets.

5. Altitude: 15-13 K Temp: -16.5 to -12C Source: Foil only

   Remarks: Particles smaller than about 500 μm. Concentrations vary between 1.2 to 3.2 lit^{-1}. Concentrations of 500 μm particles between 0.05 to 0.1 lit^{-1}.

   No indications of cloud droplets.

6. Altitude: 13-12 K Temp: -12 to -10C Source: Foil only

   Remarks: First indications of snowflakes. Average snowflake concentrations of 0.005 lit^{-1}. Average sizes of 1.5 mm with a maximum observed size of 4 mm. Total ice concentration of the order of about 2 to 3 lit^{-1}.

   No indications of cloud droplets.

7. Altitude: 12-7 K Temp: -10 to -2C Source: Foil only

   Remarks: Increase in snowflake concentration with decrease in altitude. Noted the aggregation of snowflakes starting at about 10 K (-7C). Foil impressions of these aggregates of up to 9 mm.

   Presence of droplets not indicated.

Table F8. Summary of Foil Sampler Observations for Storm of 17 March 1972 (Cont)

8. Altitude: 7 K Temp: -2C Source: Foil

Remarks: Measured size distribution of well developed snowfall.

Dia. Range (mm)	Conc. (m^{-3})
0.2-1	442
-2	90.1
-3	65.4
-4	54.8
-5	15.9
-6	15.9
-7	3.53
-8	5.3
-9	1.77
Total	694.7

9. Altitude: 7-5 K Temp: -2 to 0C Source: Foil only

Remarks: Larger Aggregates noted. Frequent 1-cm particles noted. Maximum size of 1.4 cm noted.

10. Altitude: 5-4 K Temp: 0 to +1C Source: Foil only

Remarks: Melting begins at this 0C and is complete by 1C.

11. Altitude: 4-.7 K Temp: 1 to ~7C Source: Foil only

Remarks: Raindrops found in varying concentrations and sizes. Results of raindrop size distribution at .7 K ft above ground station.

Dia. Range (mm)	Conc. (m^{-3})
0.2-1	266
-2	11
-3	0

Table F9. Summary of Formvar and Foil Sampler Observations for Storm of 22 March 1972

1. Altitude: 22-23 K (orbit) Temp: -25 to -27C Source: Foil and Formvar

   Remarks: Occasional small particles of foil. All smaller than 250 μm. Concentration of the order of about 0.2 lit^{-1}.

   Formvar records disclose the presence of spatial crystals. Crystals appear rather dense due to outgrowths of column crystals from main nucleus. Estimated concentration of 6 lit^{-1}, all smaller than 1 mm.

2. Altitude: 22-14 K (descent) Temp: -25 to -8C Source: Foil only

   Remarks: No evidence of particles on foil records. No evidence of cloud droplets from J.W. device

3. Altitude: 14 K (horiz. sampling) Temp: -8C Source: Foil and Formvar

   Remarks: Regions of precipitation and no precipitation on foil records. Ice particles all smaller than 250 μm. Regions of precipitation have concentrations of order of about 0.25 lit^{-1}.

   Formvar records indicate the presence of cloud droplets in certain regions of horizontal traverse. Occasional spatial type crystals evidenced. Estimated crystal concentration in a region of 0.3 lit^{-1}. Large liquid drops (probably drizzle size) evidenced and found in concentration of 0.1 lit^{-1}.

   J.W. recordings of LWC on order of 0.1 to 0.3 g/m^3 in regions of about 1 to 2 km.

4. Altitude: 14-10 K (descent) Temp: -8 to -2C Source: Foil and Formvar

   Remarks: Foil records show regions containing occasional snowflakes starting at about 11 K (-4C). Concentrations appear to be low and of the order of 0.1 lit^{-1}.

   Formvar records disclose regions of relatively high (0.1 to 3 g/m^3) cloud droplet water concentrations. Regions of low ($<<$ 0.1 g/m^3) cloud droplet concentrations are associated with the presence of higher concentrations of snowflakes (and vice versa). Drizzle drops are evident.

   J.W. recordings show LWC of about 0.1 to 0.2 g/m^3 in certain regions.

5. Altitude: 10 K (horiz. sampling) Temp: -2C Source: Foil and Formvar

   Remarks: First indications of heavy snowfall. Size-distributions are being determined. Impressions look firm on records suggesting possible denser particles. Presence of raindrops having diameters of 1 mm quite evident.

   Formvar records show presence of appreciable numbers of cloud droplets in certain regions. Melting of particles indicated in certain regions. Snow particles appear to be spatial particles with columnar outgrowths. Slight riming indicated on solid particles.

   J.W. recordings of up to 0.4 to 0.5 g/m^3 not uncommon with heaviest of 0.7 g/m^3 recorded. Cellular structure of liquid water regions of order of about 1.5 to 2.5 km.

Table F9. Summary of Formvar and Foil Sampler Observations for Storm of 22 March 1972 (Cont)

6.	Altitude: 8 K	Temp: 0C	Source: Foil only
	Remarks: Foil shows particles smaller than 500 μm in a cell of about 1.5 km wide. Concentration of solid particles about 0.4 lit. LWC averages about 0.4 g/m^3 across cloud.		
7.	Altitude: ~7.3-7 K	Temp: ~ 1C	Source: Foil only
	Remarks: Melting starts at 7.3 K and is complete by 7 K (1.5C). Size distribution being determined for this level.		
8.	As opposed to storm on 17 March, ice particles appear to be much denser in this storm. This result is probably due to the higher LWC found in a fairly deep layer (14-8 K) which favors the formation of rimed graupel particles. The cellular structure of the storm also suggests that this storm was more convective in nature which again favors the formation of graupel type particles.		

Summary information about the type, size-range and concentrations of the hydrometeors, of precipitation size, also of cloud size, that existed at the different flight altitudes in the storms of 3 February, 17 February, 17 March, and 22 March 1972 is presented in Tables F10 through F13. The altitudes and mid-times of the samples are shown in the first two columns and the liquid-water-content values (for the cloud-size particles) are indicated in the last columns. The hydrometeor types are identified by "letter code". This code is explained at the bottom of the first table, Table F10.

The cloud liquid-water-content values of these tables were used, in conjunction with information about the temporal-spatial structure of the storms, to estimate the probable cloud-liquid-water contents along the trajectory paths of the missiles at their launch times. These estimates are listed in Tables C6 through C10 of Appendix C, also in Tables G2 through G6 of Appendix G.

Table F10. Summary Information About the Type, Size Range and Concentrations of the Hydrometeors That Existed at the Various Flight Altitudes in the Storm of 3 February 1972

Alt. (K ft)	Time (Z)	Precipitation Size			Cloud Size			LWC (gm/m^3)
		Type	Size Range (mm)	Conc. (m^{-3})	Type	Size Range (μm)	Conc. (m^{-3})	
5	2102	R	.18 to 3.0	597				
5	2059	R	.18 to 4.0	1159				
5	2057	R	.18 to 3.0	495	L	5 - 200	$\sim 10^8$	.15
7	2054-1/2	R	.18 to 3.0	2261	L	5 - 200	$\sim 10^8$	<.1
8	2053	R			R	5 - 200	$\sim 10^8$	<.1
9.25	2051-1/2	WS			WS	>3000	160	<.1
10	2048	WS R			L WS	6.5 - 90 >3000	$\sim 10^8$ 2700	.3 Formvar <.1 JW
11	2045	DS & WS			L WS & DS	6.5 - 90 >3000	$\sim 10^8$ 5400	<.1
12	2044	DS & WS			L SC, DS WS Cols	6.5 - 90 >3000 - 200	$\sim 10^8$ 5100 500	<.1
12.5	2043	DS			L SC Cols	6.5 - 90 <3000 - 300	$\sim 10^8$ 2000 460	<.1
13	2042	SC			L SC	6.5 - 90 <3000	$\sim 10^8$ 2400	<.1
14.5-14	2038-2040	SC			L SC Cols	6.5 - 90 <1000 - 200	$\sim 10^8$ 430 100	<.1
15	2033-2034	SC			L SC	6.5 - 90 <1000	$\sim 10^8$ 150	.17 Formvar <.1 JW

No Data - Instrument Malfunction

No Data

DS = Dry Snow (aggregates)
WS = Wet Snow (aggregates)
R = Rain
SC = Snow Crystals or Spacial Crystal
L = Liquid
Cols = Columns
Plates = Plates

Table F11. Summary Information About the Type, Size Range and Concentrations of the Hydrometeors That Existed at the Various Flight Altitudes in the Storm of 17 February 1972

Alt. (K ft)	Time (Z)	Precipitation Size			Cloud Size			LWC (gm/m^3)
		Type	Size Range (mm)	Conc. (m^{-3})	Type	Size Range (μm)	Conc. (m^{-3})	
4	1549	R WS			WS	<3000	500	0
5	1547-1/2	R WS			L WS	0 - 200 >3000	$\sim 10^8$ 1700	0.1
6	1546-1/2	R WS			L WS	0 - 200 >3000	$\sim 10^8$ 1400	0.15 - 0.2
7	1545	WS			WS	>3000	1400	0
8	1543:40	WS 75% DS 25%			L WS & DS	0 - 100 >3000	$\sim 10^8$ 2000	0.2
9	1543	WS 50% DS 50%			L WS & DS	0 - 100 >3000	$\sim 10^8$ 1750	0.15
10	1541-1/2	WS 20% DS 80%			L SC, WS DS Plates	0 - 100 >3000 - 300	$\sim 10^8$ 3600 60	0.1 - 0.15
11	1540	DS			L SC Cols	0 - 90 >3000 - 200	$\sim 10^8$ 5050 <100	<<.1
12	1539				L SC Cols	0 - 90 <3000 - 200	$\sim 10^8$ 4000 <100	<<.1
13	1537	SC	No Data - Instrument Malfunctions	No Data - Instrument Malfunction	L SC	0 - 90 >3000	$\sim 10^8$ 4700	0.15
15	1534				L SC Plates	0 - 90 - 1000 - 200	$\sim 10^8$ 9600 900	<<.1
15-20			No Data Taken					

Table F11. Summary Information About the Type, Size Range and Concentrations of the Hydrometeors That Existed at the Various Flight Altitudes in the Storm of 17 February 1972 (Cont)

Alt. (K ft)	Time (Z)	Precipitation Size			Cloud Size			LWC (gm/m^3)
		Type	Size Range (mm)	Conc. (m^{-3})	Type	Size Range (μm)	Conc. (m^{-3})	
20	1528				L SC Plates	 <1000 - 200	0 11400 800	0

Table F12. Summary Information About the Type, Size Range and Concentrations of the Hydrometeors That Existed at the Various Flight Altitudes in the Storm of 17 March 1972

Alt. (K ft)	Time (Z)	Precipitation Size			Cloud Size			LWC (gm/m^3)
		Type	Size Range (mm)	Conc. (m^{-3})	Type	Size Range (μm)	Conc. (m^{-3})	
0.7	2228	R	.18 to 2.0	277	L			0
1	2227	R	.18 to 2.0	482	L			0
2	2222	R	.18 to 2.0	271	L			0
3	2218	R	.18 to 2.0	597	L			0
4	2216-1/2	R	.18 to 2.0	432	L	0 - 80	$\sim 10^8$	0.2
5	2214	WS	.18 to 6.0	679		Bad Data: No Data		0.2
		R	.18 to 1.0	92				
6	2212	S	.18 to 5.0	560		" "		0.2
7	2205-2209	S	.18 to 9.0	297		" "		0
8	2203	S	.18 to 7.0	1000		" "		0.2
9	2201	SC	.18 to 4.0	2825		" "		<.1
10	2158-2200	SC	.18 to 4.0	1970		" "		≪.1
11	2155			No Data Taken				
12	2153	SC	.18 to 4.0	3100	L SC	>3000	8200	0
13	2151:26	SC	.18 to 1.0	1400	L SC Plates	<1000 -200	12000 500	0
14	2150:10	SC	.18 to 0.5	1750	L SC Plates	<500 150μ	9000 900	0

Table F12. Summary Information About the Type, Size Range and Concentrations of the Hydrometeors That Existed at the Various Flight Altitudes in the Storm of 17 March 1972 (Cont)

Alt. (K ft)	Time (Z)	Precipitation Size			Cloud Size			LWC (gm/m^3)
		Type	Size Range (mm)	Conc. (m^{-3})	Type	Size Range (μm)	Conc. (m^{-3})	
15	2139-2148	SC	.18 to 0.5	400-3500	L			0
					SC	<500	10000	
15-17	2138	SC	.18 to <.25	500-7500		No Data Taken		
17-18	2136	SC	.18 to <.25	400-7900	L			0
					SC	-200	600	
21	2129	SC	.18 to <.25	100-5000		No Data Taken		

Table F13. Summary Information About the Type, Size Range and Concentrations of the Hydrometeors That Existed at the Various Flight Altitudes in the Storm of 22 March 1972

Alt. (K ft)	Time (Z)	Precipitation Size			Cloud Size			LWC (gm/m^3)
		Type	Size Range (mm)	Conc. (m^{-3})	Type	Size Range (μm)	Conc. (m^{-3})	
5	1657	R	.18 to 4.0	795	L			0
7	1654	R	.18 to 1.2	385	L	0 - 200	$\sim 10^8$	0.2
8	1651	WS	.18 to 6.0	800	L	0 - 200	$\sim 10^8$	0.1 - 0.4
					WS	>3000	750	
					L	0 - 200	$\sim 10^8$	<0.1
75	1649	WS & DS	Not Read		SC & WS	>.3000	11200	
	1640-1348	WS & DS	.18 to 9.0	600-1300	L	0 - 200	$\sim 10^8$	0.2 - 0.8
		R	.18 to 1.25	140	SC & WS	>3000	7100	
	1334:40	SC	.18 to 0.75	2000	SC	<1000	6900	<.1
	1335:50	SC	.18 to 0.75	2000	SC	<1000	12100	<.1
13	1330	SC	.18 to <.25	1800	SC	< 500	8000	<.1
14	1326	SC	.18 to <.25	1800	SC	< 500	9400	0
15		SC	.18 to <.25	250	SC	< 500	300	0.2
22-14	16	No Particles Samples		0	Bad Data: No Data			0
23	1651 1601-17	SC	.18 to <.25	0-200	SC	< 500	0-6000	0

More detailed information is presented in Tables F14 through F16 concerning the number-concentration and liquid-water-content values of particular hydrometeor samples (in the precipitation size range) acquired at certain levels within the storms of 3 February, 17 March, and 22 March. (Data were unavailable for the storm of 17 February because the foil-sampler instrument of the aircraft failed to operate properly.) The number concentrations are listed for the diameter ranges shown in the first columns. The total number of the raindrops or snow particles, normalized to 1 m^3 of volume, is shown at the bottom of the tables. The values of liquid-water-content are likewise shown. These were computed by AFCRL from the MRI data. In the computations for snow, the geometric mid-diameters of the classes were used, and it was assumed that the equivalent melted diameters of the particles (D_e) were related to the physical dimensions (to the approximate average dimensions of the tables) as

$$D_e = 0.40\, \ell^{0.875} \tag{F1}$$

where ℓ is the average dimension (see R No. 2, Eq. (86)).

Table F14. Size Distribution of Raindrops in the Storm of 3 February 1972

Nature Altitude Dia. Range mm)	Rain 7 K Conc. (m^{-3})	Rain 5 K Conc. (m^{-3})	Rain 5 K Conc. (m^{-3})	Rain 5 K Conc. (m^{-3})
0.18-1	1917	511	396	1000
1-2	324	74.1	71	102
2-3	17.6	12.5	28	49
3-4				8
Total	2261	597	495	1159
LWC gm/m^3	.691	.226	.336	.742

As seen in Tables F14 through F16, two or more samples were sometimes analyzed for a given flight altitude. The samples, in such cases, were obtained from different spatial locations along the traverse path of the aircraft.

Table F15. Size Distribution of Snow Particles and Raindrops in the Storm of 17 March 1972

Nature Alt. (K ft) Dia. Range (mm)	Snow 10 Conc. (m^{-3})	Snow 9 Conc. (m^{-3})	Snow 7 Conc. (m^{-3})	Snow 6 Conc. (m^{-3})	Snow 5 Conc. (m^{-3})	Rain 5 Conc. (m^{-3})	Rain 4 Conc. (m^{-3})	Rain 3 Conc. (m^{-3})	Rain 2 Conc. (m^{-3})	Rain 1 Conc. (m^{-3})	Rain 0.7 Conc. (m^{-3})
0.18-1	1831	2614	442	343	378	92	357	543	232	443	266
1-2	43	94	90.1	70	70		75	54	39	39	11
2-3	71	83	65.4	54	178						
3-4	27	34	54.0	50	32						
4-5			15.9	43	13						
5-6			15.9		6						
6-7			3.53								
7-8			5.3								
8-9			1.77								
9-10											
Total	1974	2825	297	560	679	92	432	597	271	482	277
LWC gm/m^3	.059	.076	.220	Melting Zone		.0037	.125	.102	.067	.075	.027

Table F16. Size Distribution of Snow Particles and Raindrops in the Storm of 22 March 1972

Nature Altitude (K ft) Dia. Range (mm)	Snow 10 Conc. (m^{-3})	Rain 10 Conc. (m^{-3})	Snow 10 Conc. (m^{-3})	Snow 10 Conc. (m^{-3})	Rain 7 Conc. (m^{-3})	Rain 5 Conc. (m^{-3})
0.18-1	308	138	426	902	381	686
1-2	213	3.55	306	272	4.26	71
2-3	60.3		226	80.9		33
3-4	35.5		119	4.26		5
4-5	24.8		59.6			
5-6	3.55		25.5			
6-7	10.6		8.51			
7-8			12.8			
8-9			4.26			
9-10						
Total	656	142	1190	1260	385	795
LWC gm/m^3	.172	.011	.549	.058	.022	.495

Formvar-replicator data were analyzed for two samples on 3 February and four samples on 17 February to provide information about the size distribution and liquid-water-content (contribution) of hydrometeors in the cloud size-range. The results of the analyses are presented in Tables F17 through F22. Tables F17 and F18 show the number concentration and percent liquid-water-content contribution for samples of water droplets obtained on 3 February at storm altitudes of 15,000 ft (at 1533:30 EST) and 10,000 ft (1548:00 EST). Tables F19 through F22 show the same for four samples of water droplets obtained on 17 February at storm altitudes of 13,000 ft (1037 EST), 10,000 ft (1041:20 EST), 9500 ft (1042 EST) and 5000 ft (1047 EST). These were the only analyzed data for clouds that were obtained during the season.

The data of Tables F14 through F22 do not really provide adequate information about the probable size-distribution of the hydrometeors that were present along the missile trajectories. The data were acquired at various places in the storm that were spatially removed from the trajectory locale of the missile and that were obtained an appreciable time after the missile firing. Also, the liquid-water-content values of the samples, at least in the precipitation size range, differ from those of the radar measurements for the missile trajectories.

For these reasons, the summary and "best estimate" information about the spectral distribution and total values of the number concentrations and liquid-water-content along the missile trajectories for the 1971-72 season were obtained from theoretical distribution functions, as is explained in the following Appendix.

Table F17. Size Distribution and Percent Liquid-Water-Content Contribution for a Formvar Replicator Sample of Cloud Droplets Obtained at 1533:30 (Mid-Sample Time) on 3 February 1972 at a Storm Altitude of 15,000 Ft

Sample Count 450 Avg Dia 7.7 μm Avg Dia (μm)	Sample Vol 2.57 cc Avg Sq Dia 10.1 μm		Total Con 174/cc Avg Vol Dia 12.3 μm		LWC 0.172 gm/m^3 VMD 22.3 μm Rep Dia (μm)
	Conc (/cc)	% LWC (c/o)	Ce	Dia (μm)	
0.5	10.494	0.0	1.00	1.0	1.0
1.5	17.102	0.0	1.00	2.0	2.0
2.5	11.272	0.0	1.00	3.0	3.0
3.5	13.604	0.1	1.00	4.0	4.0
4.5	19.823	0.5	1.00	5.0	5.0
5.5	20.212	1.0	1.00	6.0	6.0
6.5	13.993	1.1	1.00	7.0	7.0
7.5	10.883	1.3	1.00	8.0	8.0
8.5	5.441	1.0	1.00	9.0	9.0
9.5	8.162	2.1	1.00	10.0	10.0
10.5	7.385	2.5	1.00	11.0	11.1
11.5	4.664	2.1	1.00	12.0	12.2
12.5	2.720	1.6	1.00	13.0	13.4
13.5	0.777	0.5	1.00	14.0	14.6
14.5	4.664	4.3	1.00	15.0	15.8
15.5	1.943	2.2	1.00	16.0	17.1
16.5	1.554	2.1	1.00	17.0	18.4
17.5	1.166	1.9	1.00	18.0	19.7
18.5	2.332	4.4	1.00	19.0	21.1
19.5	2.332	5.2	1.00	20.0	22.5
20.5	1.554	4.0	1.00	21.0	23.9
21.5	3.109	9.3	1.00	22.0	25.3
22.5	1.554	5.3	1.00	23.0	26.8
23.5	1.554	6.1	1.00	24.0	28.4
24.5	2.720	12.1	1.00	25.0	29.9
25.5	0.388	1.9	1.00	26.0	31.6
26.5	1.166	6.5	1.00	27.0	33.2
27.5	0.388	2.4	1.00	28.0	35.0
28.5	0.777	5.4	1.00	29.0	36.7
29.5	0.388	3.0	1.00	30.0	38.5
30.5	0.000	0.0	1.00	31.0	40.4
31.5	0.388	3.6	1.00	32.0	42.3
32.5	0.000	0.0	1.00	33.0	44.3
33.5	0.000	0.0	1.00	34.0	46.3
34.5	0.388	4.8	1.00	35.0	48.4
35.5	0.000	0.0	1.00	36.0	50.6
36.5	0.000	0.0	1.00	37.0	52.8
37.5	0.000	0.0	1.00	38.0	55.1
38.5	0.000	0.0	1.00	39.0	57.5
39.5	0.000	0.0	1.00	40.0	60.0

Table F18. Size Distribution and Percent Liquid-Water-Content Contribution for a Formvar Replicator Sample of Cloud Droplets Obtained at 1548:00 EST on 3 February 1972 at a Storm Altitude of 10,000 Ft

Sample Count 347 Avg Dia 13.1 μm Avg Dia (μm)	Sample Vol 2.57 cc Avg Sq Dia 15.6 μm		Total Con 98/cc Avg Vol Dia 17.6 μm		LWC 0.285 gm/m^3 VMD 25.9 μm Rep Dia (μm)
	Conc (/cc)	% LWC (c/o)	Ce	Dia (μm)	
0.5	0.000	0.0	1.00	1.0	1.0
1.5	0.285	0.0	1.00	2.0	2.0
2.5	0.710	0.0	1.00	3.0	3.0
3.5	2.850	0.0	1.00	4.0	4.0
4.5	5.415	0.0	1.00	5.0	5.0
5.5	7.981	0.2	1.00	6.0	6.0
6.5	10.831	0.5	1.00	7.0	7.0
7.5	9.976	0.7	1.00	8.0	8.0
8.5	7.126	0.8	1.00	9.0	9.0
9.5	7.126	1.1	1.00	10.0	10.0
10.5	5.415	1.1	1.00	11.0	11.1
11.5	2.565	0.7	1.00	12.0	12.2
12.5	3.135	1.1	1.00	13.0	13.4
13.5	2.280	1.0	1.00	14.0	14.6
14.5	1.140	0.6	1.00	15.0	15.8
15.5	0.570	0.3	1.00	16.0	17.1
16.5	1.140	0.9	1.00	17.0	18.4
17.5	0.285	0.2	1.00	18.0	19.7
18.5	1.140	1.3	1.00	19.0	21.1
19.5	0.855	1.1	1.00	20.0	22.5
20.5	0.570	0.9	1.00	21.0	23.9
21.5	1.140	2.0	1.00	22.0	25.3
22.5	1.710	3.5	1.00	23.0	26.8
23.5	3.420	8.1	1.00	24.0	28.4
24.5	3.135	8.4	1.00	25.0	29.9
25.5	4.845	14.7	1.00	26.0	31.6
26.5	3.990	13.6	1.00	27.0	33.2
27.5	4.275	16.3	1.00	28.0	35.0
28.5	0.855	3.6	1.00	29.0	36.7
29.5	1.710	8.0	1.00	30.0	38.5
30.5	0.855	4.4	1.00	31.0	40.4
31.5	0.295	1.6	1.00	32.0	42.3
32.5	0.000	0.0	1.00	33.0	44.3
33.5	0.285	1.9	1.00	34.0	46.3
34.5	0.000	0.0	1.00	35.0	48.4
35.5	0.000	0.0	1.00	36.0	50.6
36.5	0.000	0.0	1.00	37.0	52.8
37.5	0.000	0.0	1.00	38.0	55.1
38.5	0.000	0.0	1.00	39.0	57.5
39.5	0.000	0.0	1.00	40.0	60.0

Table F19. Size Distribution and Percent Liquid-Water-Content Contribution for a Formvar Replicator Sample of Cloud Droplets Obtained at 1037 EST on 17 February at a Storm Altitude of 13,000 Ft

Sample Count 88 Avg Dia 8.6 μm Avg Dia (μm)	Sample Vol 1.57 cc Avg Sq Dia 10.3 μm		Total Con 55/cc Avg Vol Dia 11.5 μm		LWC 0.045 gm/m^3 VMD 16.4 μm Rep Dia (μm)
	Conc (/cc)	% LWC (c/o)	Ce	Dia (μm)	
0.5	1.266	0.0	1.00	1.0	1.0
1.5	0.633	0.0	1.00	2.0	2.0
2.5	2.533	0.0	1.00	3.0	3.0
3.5	3.234	0.4	1.00	4.0	4.0
4.5	8.234	0.8	1.00	5.0	5.0
5.5	6.967	1.3	1.00	6.0	6.0
6.5	1.266	0.4	1.00	7.0	7.0
7.5	1.900	0.9	1.00	8.0	8.0
8.5	3.167	2.2	1.00	9.0	9.0
9.5	1.900	1.8	1.00	10.0	10.0
10.5	1.900	2.5	1.00	11.0	11.1
11.5	0.633	1.1	1.00	12.0	12.2
12.5	0.633	1.4	1.00	13.0	13.4
13.5	1.266	3.6	1.00	14.0	14.6
14.5	2.533	8.9	1.00	15.0	15.8
15.5	3.167	13.6	1.00	16.0	17.1
16.5	4.433	23.1	1.00	17.0	18.4
17.5	1.266	7.8	1.00	18.0	19.7
18.5	2.533	18.6	1.00	19.0	21.1
19.5	1.266	10.8	1.00	20.0	22.5
20.5	0.000	0.0	1.00	21.0	23.9
21.5	0.000	0.0	1.00	22.0	25.3
22.5	0.000	0.0	1.00	23.0	26.8
23.5	0.000	0.0	1.00	24.0	28.4
24.5	0.000	0.0	1.00	25.0	29.9
25.5	0.000	0.0	1.00	26.0	31.6
26.5	0.000	0.0	1.00	27.0	33.2
27.5	0.000	0.0	1.00	28.0	35.0
28.5	0.000	0.0	1.00	29.0	36.7
29.5	0.000	0.0	1.00	30.0	38.5
30.5	0.000	0.0	1.00	31.0	40.4
31.5	0.000	0.0	1.00	32.0	42.3
32.5	0.000	0.0	1.00	33.0	44.3
33.5	0.000	0.0	1.00	34.0	46.3
34.5	0.000	0.0	1.00	35.0	48.4
35.5	0.000	0.0	1.00	36.0	50.6
36.5	0.000	0.0	1.00	37.0	52.8
37.5	0.000	0.0	1.00	38.0	55.1
38.5	0.000	0.0	1.00	39.0	57.5
39.5	0.000	0.0	1.00	40.0	60.0
40.5	0.000	0.0	1.00	41.0	62.5
41.5	0.000	0.0	1.00	42.0	65.1
42.5	0.000	0.0	1.00	43.0	67.8
43.5	0.000	0.0	1.00	44.0	70.7
44.5	0.000	0.0	1.00	45.0	73.6
45.5	0.000	0.0	1.00	46.0	76.6
46.5	0.000	0.0	1.00	47.0	79.8
47.5	0.000	0.0	1.00	48.0	83.0
48.5	0.000	0.0	1.00	49.0	86.4
49.5	0.000	0.0	1.00	50.0	90.0

Table F20. Size Distribution and Percent Liquid-Water-Content Contribution for a Formvar Replicator Sample of Cloud Droplets Obtained at 1541 EST on 17 February 1972 at a Storm Altitude of 10,000 Ft

Sample Count 106 Avg Dia 8.3 μm	Sample Vol 1.84 cc Avg Sq Dia 9.4 μm		Total Con 57/cc Avg Vol Dia 10.3 μm		LWC 0.033 gm/m^3 VMD 13.6 μm
Avg Dia (μm)	Conc (/cc)	% LWC (c/o)	Ce	Dia (μm)	Rep Dia (μm)
0.5	0.000	0.0	1.00	1.0	1.0
1.5	0.000	0.0	1.00	2.0	2.0
2.5	4.343	0.1	1.00	3.0	3.0
3.5	8.687	0.5	1.00	4.0	4.0
4.5	9.229	1.3	1.00	5.0	5.0
5.5	2.171	0.5	1.00	6.0	6.0
6.5	2.171	0.9	1.00	7.0	7.0
7.5	1.628	1.0	1.00	8.0	8.0
8.5	1.628	1.5	1.00	9.0	9.0
9.5	3.800	5.1	1.00	10.0	10.0
10.5	4.886	8.9	1.00	11.0	11.1
11.5	2.171	5.2	1.00	12.0	12.2
12.5	3.257	10.0	1.00	13.0	13.4
13.5	5.429	21.0	1.00	14.0	14.6
14.5	5.972	28.6	1.00	15.0	15.8
15.5	1.085	6.3	1.00	16.0	17.1
16.5	0.542	3.8	1.00	17.0	18.4
17.5	0.542	4.5	1.00	18.0	19.7
18.5	0.000	0.0	1.00	19.0	21.1
19.5	0.000	0.0	1.00	20.0	22.5
20.5	0.000	0.0	1.00	21.0	23.9
21.5	0.000	0.0	1.00	22.0	25.3
22.5	0.000	0.0	1.00	23.0	26.8
23.5	0.000	0.0	1.00	24.0	28.4
24.5	0.000	0.0	1.00	25.0	29.9
25.5	0.000	0.0	1.00	26.0	31.6
26.5	0.000	0.0	1.00	27.0	33.2
27.5	0.000	0.0	1.00	28.0	35.0
28.5	0.000	0.0	1.00	29.0	36.7
29.5	0.000	0.0	1.00	30.0	38.5
30.5	0.000	0.0	1.00	31.0	40.4
31.5	0.000	0.0	1.00	32.0	42.3
32.5	0.000	0.0	1.00	33.0	44.3
33.5	0.000	0.0	1.00	34.0	46.3
34.5	0.000	0.0	1.00	35.0	48.4
35.5	0.000	0.0	1.00	36.0	50.6
36.5	0.000	0.0	1.00	37.0	52.8
37.5	0.000	0.0	1.00	38.0	55.1
38.5	0.000	0.0	1.00	39.0	57.5
39.5	0.000	0.0	1.00	40.0	60.0
40.5	0.000	0.0	1.00	41.0	62.5
41.5	0.000	0.0	1.00	42.0	65.1
42.5	0.000	0.0	1.00	43.0	67.8
43.5	0.000	0.0	1.00	44.0	70.7
44.5	0.000	0.0	1.00	45.0	73.6
45.5	0.000	0.0	1.00	46.0	76.6
46.5	0.000	0.0	1.00	47.0	79.8
47.5	0.000	0.0	1.00	48.0	83.0
48.5	0.000	0.0	1.00	49.0	86.4
49.5	0.000	0.0	1.00	50.0	90.0

Table F21. Size Distribution and Percent Liquid-Water Content Contribution for a Formvar Replicator Sample of Cloud Droplets Obtained at 1542 EST on 17 February 1972 at a Storm Altitude of 9,500 Ft

Sample Count 177 Avg Dia 7.5 μm Avg Dia (μm)	Sample Vol 1.31 cc Avg Sq Dia 10.1 μm		Total Con 134/cc Avg Vol Dia 11.3 μm		LWC 0.102 gm/m^3 VMD 20.2 μm Rep Dia (μm)
	Conc (/cc)	% LWC (c/)	Ce	Dia (μm)	
0.5	0.760	0.0	1.00	1.0	1.0
1.5	2.280	0.0	1.00	2.0	2.0
2.5	13.682	0.1	1.00	3.0	3.0
3.5	23.563	0.5	1.00	4.0	4.0
4.5	18.242	0.8	1.00	5.0	5.0
5.5	17.482	1.4	1.00	6.0	6.0
6.5	12.921	1.8	1.00	7.0	7.0
7.5	6.841	1.4	1.00	8.0	8.0
8.5	6.080	1.9	1.00	9.0	9.0
9.5	2.280	0.9	1.00	10.0	10.0
10.5	0.760	0.4	1.00	11.0	11.1
11.5	3.800	2.9	1.00	12.0	12.2
12.5	3.800	3.7	1.00	13.0	13.4
13.5	0.760	0.9	1.00	14.0	14.6
14.5	1.520	2.3	1.00	15.0	15.8
15.5	3.800	7.2	1.00	16.0	17.1
16.5	4.560	10.4	1.00	17.0	18.4
17.5	1.520	4.1	1.00	18.0	19.7
18.5	0.000	0.0	1.00	19.0	21.1
19.5	1.520	5.7	1.00	20.0	22.5
20.5	3.040	13.3	1.00	21.0	23.9
21.5	2.280	11.5	1.00	22.0	25.3
22.5	1.520	8.8	1.00	23.0	26.8
23.5	0.000	0.0	1.00	24.0	28.4
24.5	0.760	5.7	1.00	25.0	29.9
25.5	0.000	0.0	1.00	26.0	31.6
26.5	0.000	0.0	1.00	27.0	33.2
27.5	0.000	0.0	1.00	28.0	35.0
28.5	0.000	0.0	1.00	29.0	36.7
29.5	0.000	0.0	1.00	30.0	38.5
30.5	0.000	0.0	1.00	31.0	40.4
31.5	0.000	0.0	1.00	32.0	42.3
32.5	0.760	13.3	1.00	33.0	44.3
33.5	0.000	0.0	1.00	34.0	46.3
34.5	0.000	0.0	1.00	35.0	48.4
35.5	0.000	0.0	1.00	36.0	50.6
36.5	0.000	0.0	1.00	37.0	52.8
37.5	0.000	0.0	1.00	38.0	55.1
38.5	0.000	0.0	1.00	39.0	57.5
39.5	0.000	0.0	1.00	40.0	60.0
40.5	0.000	0.0	1.00	41.0	62.5
41.5	0.000	0.0	1.00	42.0	65.1
42.5	0.000	0.0	1.00	43.0	67.8
43.5	0.000	0.0	1.00	44.0	70.7
44.5	0.000	0.0	1.00	45.0	73.6
45.5	0.000	0.0	1.00	46.0	76.6
46.5	0.000	0.0	1.00	47.0	79.8
47.5	0.000	0.0	1.00	48.0	83.0
48.5	0.000	0.0	1.00	49.0	86.4
49.5	0.000	0.0	1.00	50.0	90.0

Table F22. Size Distribution and Percent Liquid-Water-Content Contribution for a Formvar Replicator Sample of Cloud Droplets Obtained at 1547 EST on 17 February 1972 at a Storm Altitude of 5000 Ft

Sample Count 135 Avg Dia 7.6 μm	Sample Vol 1.31 cc Avg Sq Dia 9.0 μm		Total Con 102/cc Avg Vol Dia 10.3 μm		LWC 0.060 gm/m^3 VMD 14.4 μm
Avg Dia (μm)	Conc (/cc)	% LWC (c/o)	Ce	Dia (μm)	Rep Dia (μm)
0.5	0.000	0.0	1.00	1.0	1.0
1.5	0.000	0.0	1.00	2.0	2.0
2.5	9.121	0.1	1.00	3.0	3.0
3.5	23.563	0.8	1.00	4.0	4.0
4.5	15.202	1.2	1.00	5.0	5.0
5.5	9.121	1.3	1.00	6.0	6.0
6.5	4.560	1.0	1.00	7.0	7.0
7.5	3.040	1.1	1.00	8.0	8.0
8.5	1.520	0.8	1.00	9.0	9.0
9.5	0.760	0.5	1.00	10.0	10.0
10.5	5.320	5.3	1.00	11.0	11.1
11.5	5.320	7.0	1.00	12.0	12.2
12.5	5.320	9.0	1.00	13.0	13.4
13.5	7.601	16.2	1.00	14.0	14.6
14.5	4.560	12.0	1.00	15.0	15.8
15.5	3.040	9.8	1.00	16.0	17.1
16.5	3.800	14.7	1.00	17.0	18.4
17.5	0.000	0.0	1.00	18.0	19.7
18.5	0.000	0.0	1.00	19.0	21.1
19.5	0.000	0.0	1.00	20.0	22.5
20.5	0.000	0.0	1.00	21.0	23.9
21.5	0.000	0.0	1.00	22.0	25.3
22.5	0.000	0.0	1.00	23.0	26.8
23.5	0.000	0.0	1.00	24.0	28.4
24.5	0.000	0.0	1.00	25.0	29.9
25.5	0.000	0.0	1.00	26.0	31.6
26.5	0.000	0.0	1.00	27.0	33.2
27.5	0.000	0.0	1.00	28.0	35.0
28.5	0.000	0.0	1.00	29.0	36.7
29.5	0.000	0.0	1.00	30.0	38.5
30.5	0.760	18.6	1.00	31.0	40.4
31.5	0.000	0.0	1.00	32.0	42.3
32.5	0.000	0.0	1.00	33.0	44.3
33.5	0.000	0.0	1.00	34.0	46.3
34.5	0.000	0.0	1.00	35.0	48.4
35.5	0.000	0.0	1.00	36.0	50.6
36.5	0.000	0.0	1.00	37.0	52.8
37.5	0.000	0.0	1.00	38.0	55.1
38.5	0.000	0.0	1.00	39.0	57.5
39.5	0.000	0.0	1.00	40.0	60.0
40.5	0.000	0.0	1.00	41.0	62.5
41.5	0.000	0.0	1.00	42.0	65.1
42.5	0.000	0.0	1.00	43.0	67.8
43.5	0.000	0.0	1.00	44.0	70.7
44.5	0.000	0.0	1.00	45.0	73.6
45.5	0.000	0.0	1.00	46.0	76.6
46.5	0.000	0.0	1.00	47.0	79.8
47.5	0.000	0.0	1.00	48.0	83.0
48.5	0.000	0.0	1.00	49.0	86.4
49.5	0.000	0.0	1.00	50.0	90.0

G1. THE SELECTION OF THE SAMS DIAMETER CLASSES

The diameter classes indicated in Table G1, and used in Tables G2 through G6, were selected to span the total size range of the hydrometeors, encompassing both the cloud size-range and the precipitation size range. The cloud size-range of the hydrometeors is presumed to extend from 0.794 microns (.000794 mm) at the lower diameter boundary to 79.4 microns (0.0794 mm) at the upper boundary. The precipitation size-range of the hydrometeors is presumed to begin at 79.4 microns and to extend upward in diameter (or equivalent-melted-diameter, in the case of ice-hydrometeors) to the largest diameter size that is reasonably to be anticipated with the hydrometeors of the different categories (rain, snow, ice-crystals) that were described in R No. 2.

The diameter width of the selected SAMS classes increases in geometric progression from the smallest diameter class to the largest, and there are five classes per order of magnitude increase in diameter. In other words, the classes have a constant logarithmic width specified by

$$\log D_U - \log D_L = .20 \ , \tag{G1}$$

where D_U is the diameter at the upper boundary of any given class and D_L is the diameter at the lower boundary. The geometric mean diameter of the classes (the diameter values of the column headings of Tables G2 through G6) is specified by

$$D_c = 10^{(\log D_L + .1)} \ , \tag{G2}$$

or, alternately, by

$$D_c = 10^{(\log D_U - .1)} \ . \tag{G3}$$

It is also pertinent to note that, if n is the identity number of a given class, which has a diameter width ΔD_n, then the diameter width of the next larger class (of identity number n+1) is given by

$$\Delta D_{n+1} = 10^{.2} \, \Delta D_n \ , \tag{G4}$$

or

$$\Delta D_{n+1} = 1.58489 \, \Delta D_n \ . \tag{G5}$$

Table G1. Diameter Classes Specified for SAMS

Class Number	Class Boundaries (microns)	Class Boundaries (mm)	Geometric Mean-Diameter (See Eqs. G3 & G4) (microns)	Geometric Mean-Diameter (See Eqs. G3 & G4) (mm)	
	0.7943	0.0007943			
First			1.0	0.001	Cloud Size-Range
	1.259	0.001259			
Second			1.585	0.001585	
	1.995	0.001995			
Third			2.512	0.002512	
	3.162	0.003162			
Fourth			3.981	0.003981	
	5.012	0.005012			
Fifth			6.309	0.006309	
	7.943	0.007943			
Sixth			10.0	0.01	
	12.59	0.01259			
Seventh			15.85	0.01585	
	19.95	0.01995			
Eighth			25.12	0.02512	
	31.62	0.03162			
Ninth			39.81	0.03981	
	50.12	0.05012			
Tenth			63.09	0.06309	
	79.43	0.07943			
Eleventh			100.0	0.1	Precipitation Size-Range
	125.9	0.1259			
Twelfth			158.5	0.1585	
	199.5	0.1995			
Thirteenth			251.2	0.2512	
	316.2	0.3162			
Fourteenth			398.1	0.3981	
	501.2	0.5012			
Fifteenth			630.9	0.6309	
	794.3	0.7943			
Sixteenth			1000	1.0	
	1259	1.259			
Seventeenth			1585	1.585	
	1995	1.995			
Eighteenth			2512	2.512	
	3162	3.162			
Nineteenth			3981	3.981	
	5012	5.012			
Twentieth			6309	6.309	
	7943	7.943			
Twenty-first			10,000	10.0	
	12,590	12.59			

Appendix G

Summary and "Best Estimate" Information About the Spectral Distribution and Total Values of the Number Concentration and Liquid-Water-Content of the Hydrometeors Along the Missile Trajectories

Approximate information about the spectral distribution and total values of the number concentration and liquid-water-content of the hydrometeors along the missile trajectories for the storms of the 1971-72 SAMS season is presented in Tables G2 through G6. The information is supplied for the particular diameter classes (equivalent-melted diameter, in the case of ice hydrometeors) which are specified in Table G1.

The information in Tables G2 through G6 is based on theoretical models that are discussed later in this appendix. Three models were used which were descriptive (1) of the cloud size range of the hydrometeors, (2) of the precipitation size range of the hydrometeors, and (3) of the two types of hydrometeors, fully melted liquid drops and water-coated snow particles, that occur within the melting zones of the storms. Since independent models were used for the cloud-size portion of the spectrum and for the precipitation-size portion, there are spectral discontinuities that occur across the separation boundary (at 79.4 microns, or .0794 mm) between the two size ranges.

The diameter classes for SAMS were also selected such that the geometric mean diameters of the first, sixth, eleventh, sixteenth, and twenty-first classes would be 1, 10, 100, 1000, and 10,000 microns, respectively; that is, they would be unit order-of-magnitude values. Another consideration in the original selection of the classes involved the maximum diameter of raindrops. Raindrops larger than about 5000 microns (5 mm) tend to become aerodynamically unstable during their fall and to "break up" into smaller drops. Thus, it was desirable that the upper-diameter-boundary of one of the "to be chosen" classes have a value close to 5000 microns. It can be seen that the nineteenth class listed in Table G1 has an upper boundary at 5012 microns. (This is the basic reason for the specification of "five classes per cycle".)

It should be mentioned that the geometric mean diameters listed in the column headings of Tables G2 through G6 are specified in microns for the cloud-size portion of the spectrum, and in mm for the precipitation-size portion of the portion of the spectrum. These are the units conventionally employed.

G2. DESCRIPTION OF TABLES G2 THROUGH G6

The missile altitude is indicated in the first column of each of the Tables G2 through G6. The altitudes are listed for each 250 meters from the ground surface to the top altitude of the storm of the particular days. Size-distribution and liquid-water-content information is presented in the next sections of the table(s), first, for the cloud-size range of the spectrum and, second, for the precipitation-size range of the spectrum. Summary information about the cloud populations and about the precipitation populations is provided in the following two sections of the table. The total liquid-water-content of the liquid-drops and water-coated-ice of precipitation size within the melting zone is indicated in the next to the last column of the table(s). The grand total of the liquid-water-content for all types of hydrometeors, of both the cloud size and precipitation size, is listed in the last column of the table(s).

The numbers above the diagonal lines, in the table sections concerned with the spectral distribution of the hydrometeors, give the number concentration of the drops or ice particles within the particular diameter classes. For the cloud-size portion of the spectrum, the number concentrations (N_c) are listed in units of No. cm^{-3}; for the precipitation-size portion, they are listed in units of No. m^{-3}. The different units are used (1) because they are conventional and (2) to avoid tabulation difficulties that would otherwise arise because the number concentration of the cloud-size droplets is normally some 10^4 to 10^7 times larger than that of the precipitation-size drops or particles.

The numbers below the diagonal lines, in the first two sections, indicate the class contributions of the contained hydrometeors to the total liquid-water-content of the cloud population (first section tabulations) or to the total liquid-water-content of the precipitation (size) population (second section tabulations). The class contributions are listed in units of $gm\,m^{-3}$. Any contribution smaller than $0.001\,gm\,m^{-3}$ is listed as zero, in accord with the agreement of the SAMS-ABRES Conference at AFCRL on 7-8 March 1974.

Two types of precipitation-size hydrometeors exist within the melting zones of the Wallops storms. These are identified in Tables G2 through G6 as fully-melted-liquid (symbolized by "W") and water-coated-ice (symbolized by "I"). Number-concentration and class liquid-water-content information is supplied for both of these hydrometeor types. The information for the fully-melted-liquid, or raindrops, is listed in the first lines; information concerning the water-coated-ice is listed in the second lines.

Summary information is presented in the tables for the "cloud population" and for the "precipitation population". The type of population is identified first. The total number of drops or particles of all sizes within the population is listed second. The total liquid-water-content is listed third. It should be noted that this total, in the case of clouds, corresponds to the aircraft-measured value for the particular altitude and, in the case of precipitation, the total corresponds to the radar-measured value for the particular altitude point along the SAMS missile trajectory (that is, it corresponds to the profile value of liquid-water-content shown drafted in Figures 1 through 7, for the given missile trajectory and altitude).

Two additional parameters are also listed in the summary sections of Tables G2 through G6. These are the median volume diameter (D_o) and the maximum diameter (D_m). The maximum diameter, in the case of clouds, is always 79.4 microns, which is the assumed upper truncation boundary of the cloud-size portion (or "cloud population portion") of the spectrum. The maximum diameter, in the case of precipitation, is based on several assumptions (partially data supported) that were made for the different categories of precipitation (rain, snow, ice-crystals).

The following comments are pertinent concerning the N_c and M_c values of the last (largest) SAMS class in the precipitation size range. When the D_m values of the population (listed in the summary column) exceeded the geometric mean (mid) diameter of the given class, the N_c and M_c values were included and listed in the given class. When the D_m value was less than the geometric mean diameter of the given class, the N_c and M_c contribution within the class were included and listed in the prior (next smaller) SAMS class. It was computationally convenient

to do this and there are no important consequences except in the case of appreciable upper diameter truncation of the population, as in the case of a population of raindrops having very large liquid-water-content.

Several other comments are pertinent concerning the information presented in Tables G2 through G6. First, the cloud measurements of the MRI, Aztec aircraft were rather sparce and qualitative during the 1971-72 season, as noted earlier. Hence, in many instances in the tables, the liquid-water-content values are unknown, are estimated, or are stated as being smaller than some particular value. Although not noted in the tables, other than in the summary column listing the total liquid-water-content values, these stipulations of unknown, estimated or "less than" also pertain to the number concentration and class liquid-water-content values that are presented in the first section of the tables.

Only one cloud type is identified in the tables. This is nimbostratus (Ns). It was assumed that the storm clouds of the 1971-72 season were mostly of this type.

The precipitation types are identified by symbols in the tables. These symbols conform to the category-type specifications of Table 2 of R No. 2. Rain is "R"; large-snow is "LS"; small-snow is "SS"; ice-crystals are "C". The subscripts on these symbols identify the hydrometeor type.

The "totals information" presented in the last two columns of Tables G2 through G6 should be more-or-less "self explanatory". The total values of liquid-water-content in the precipitation-size range, in the melting zone, are listed in the first of these columns. The values are the sum of the liquid-water content (contribution) of the "fully-melted drops" (W) plus that of the "water-coated ice" (I). The grand-total values of the last columns of the tables are the sum of the liquid-water-content (contribution) of the cloud-size hydrometeors plus that of the precipitation-size hydrometeors. The stipulations on these grand-total values (as being "approximate", or "less than", the listed values) result, of course, from the corresponding stipulations concerning the cloud liquid-water-content values measured by the MRI, Aztec aircraft.

G3. RELATIONS BETWEEN EQUIVALENT MELTED DIAMETER AND APPROXIMATE PHYSICAL SIZE

The diameter classes of Tables G2 through G6 are specified in terms of equivalent-melted diameter. For erosion assessment purposes, it is important, in the case of ice-hydrometeors, to know the relationships between the equivalent-melted diameter, D_e, and the approximate physical dimension (average dimension) of the particles. These relationships (which were also stated in R No. 2, except in inverse form) are

$$\ell = 2.66\ D_e^{1.19}\ , \tag{G6}$$

for ice crystals (specifically of Type C_1),

$$\ell = 4.05\ D_e^{1.24}\ , \tag{G7}$$

for small snow (specifically of Type SS_s), and

$$\ell = 2.84\ D_e^{1.14}\ , \tag{G8}$$

for large-snow (specifically of Type LS_5), where ℓ is the approximate, average dimension of the particles. These relationships are rather qualitative and tentative, at present. It is anticipated that more accurate, improved relationships will be obtained from the SAMS-4 data that can be reported later.

G4. COMMENTS ABOUT THE CLOUD AND PRECIPITATION MODELS

It is beyond the scope of the present report to describe the details of the models that provided the computational bases for the information presented in Tables G2 through G6. These details will have to be reported later. However, we can comment briefly about the general nature of the models.

Three models were used, which we will call the "precipitation model", the "model for the melting zone", and the "cloud model". Each of these models were based on theoretical distribution functions (double truncated) which are descriptive of the observed (or physically logical) characteristics of the particular hydrometeors, as reported in the literature or determined from AFCRL/SAMS measurement data.

G4.1 The "Precipitation Model"

The "precipitation model" was referenced in R No. 2. Basically, this is a double-truncated model based on the exponential distribution function,

$$N = N_o\ e^{-\Lambda D}\ , \tag{G9}$$

where N is the number concentration of the drops or particles (number per unit volume per unit diameter bandwidth) and D, the independent variable, is the drop or particle diameter (equivalent melted diameter, in the case of ice hydrometeors). The coefficient, N_o, and the exponent, Λ, have particular values for each category

and type of precipitation of concern. The distribution function for liquid-water-content is dependent on the third moment of the above equation; the distribution function for the radar-reflectivity-factor is dependent on the sixth moment of the equation. The integrals of these latter distribution functions, when integrated between the lower truncation diameter, D = d, and the upper truncation diameter, D = D_m, give the total liquid-water-content (M) and the total radar-reflectivity-factor (Z). The equations of the precipitation model were written such that the M vs Z relationship of these integrals was consistent (identical) with the empirical, power-function relationships that were listed in Table 2 of R No. 2 (for the particular precipitation categories and types). It may be noted that the lower truncation diameter used in the computations of Tables G2 through G6 was D = d = 0.0794 mm. The upper truncation diameter was D = D_m. The D_m values are listed in the tables. The assumptions regarding D_m will not be discussed.

G4.2 The "Model for the Melting Zone"

This model is basically an interpolative model which, at the upper boundary of the zone, provides results that are consistent with those of the "precipitation model" for the large-snow region immediately above the boundary, and which, at the lower boundary of the zone, provides results that are consistent with those of the "precipitation model" for the rain region immediately below the boundary. It is assumed in the model that the smallest snowflakes will be the first to melt, while falling gravitationally through the zone, and that the largest snowflakes will melt last, and fall farthest before melting completely. The model provides for the continuity of liquid-water-content in transfers from the one category of hydrometeors, the melting snowflakes, or "water-coated ice", to the second category of hydrometeors, the "fully-melted liquid", or raindrops. The size distribution properties of each of the hydrometeor categories were assumed to be describable by separate (but interrelated) distribution functions of exponential type (double truncated). The number concentration of the "fully-melted drops" in the first size class in the precipitation portion of the spectrum (the eleventh class specified in Table G1, which extends from 0.0794 mm to 0.1259 mm) was presumed to increase exponentially with depth through the zone, from zero concentration, at the upper boundary, to a concentration value, at the lower boundary, which conformed to that in the rain region immediately below. The largest hydrometeors, at any given level within the zone, were assumed always to be those of the first category, and it was further assumed that the maximum equivalent-melted-diameter of these "water-coated-ice" particles would vary linearly with fall distance within the zone and would also conform with the boundary condition values of D_m at the top and bottom of the zone. The general characteristics of this model can be seen from an

inspection of Tables G2 through G6. It would seem that the model provides a "reasonable first estimate" of the general hydrometeor conditions within the melting zone, involving the two categories of water substance. It might also be mentioned that the equations of the model can be readily modified to change such things as the "spectral transfer rates", or the implicitly-assumed conditions of melting, should data results suggest the benefit of changes along these lines.

G4.3 The "Cloud Model"

The "cloud model" used to obtain the Table G2 through G6 results is based on the distribution equations of Khrgian and Mazin,[1] also Khrgian et al,[2] as modified for particular conformance with the visibility equation of Trabert.[3]

The basic distribution equation of Khrgian and Mazin may be written as

$$N = Q D^2 e^{-\Omega D}, \qquad \text{(G10)}$$

where N is the number concentration of the cloud droplets (per unit volume per unit diameter bandwidth) and D, the independent variable, is the diameter of the droplets. The values of the coefficient, Q, and the exponent, Ω, differ with the different cloud types. This equation of Khrgian and Mazin is based on and supported by considerable Russian data, some 660,000 droplets (see Khrgian et al).[2]

Khrgian et al have presented integrated forms of Eq. (G10) which give the liquid-water-content of the cloud populations and the "average" diameter (actually radius) of the droplets within the populations. These equations provide a "cloud model".

In the author's opinion, this "Russian Model" is unrealistic in the sense that the "average diameter" of the cloud droplets in cloud populations of any given type (stratus, stratocumulus, nimbostratus, and altocumulus) is assumed to be constant for all liquid-water-content values of the population(s). Such assumption implies that the cloud droplets of a population, during the formation of the population, as the liquid-water-content increases from zero, somehow attain a definite average diameter without ever having had a smaller average diameter. Alternately, in the

---

1. Khrgian, A. Kh., and Mazin, I. P. (1953) The size distribution of droplets in clouds, Trudy TsAO, No. 7, 1952.
2. Khrgian, A. Kh. et al (1961) Cloud Physics (translated from Russian), 392 pages (available from Offices of Technical Service, U. S. Dept. of Commerce, Washington, D. C.).
3. Trabert, W. (1961) Die extinktion des lichtes in einem trüben medium (Sichtweite in Wolken), MZ 18:518-524.

case of a dissipating cloud, the assumption implies that a step discontinuity is required to go from a definite average diameter, just before dissipation, to zero average diameter at dissipation (which must be the terminal situation).

The equations of Khrgian et al were modified for SAMS purposes for the reason cited above. They were modified to more accurately reflect the fact that the average diameter of the cloud droplets in the populations must decrease to zero, as the population liquid-water-content decreases to zero. This modification was accomplished by introducing the visibility equation of Trabert[3] into the equation set of the model. Trabert's equation specifies the visibility in terms of the "threshold of contrast" and the liquid-water-content (raised to a particular power), also see Houghton,[4] and Middleton.[5] Certain assumptions, regarded as reasonable, that will be discussed in a future report, were made concerning the values of the threshold of contrast and of the exponent applied to the liquid-water-content. With these assumptions, the model results were in close correspondence with those reported by Khrgian et al for their different cloud types, and for the range of average-diameter values that their book indicates were most frequently observed. Thus modified, the model also prescribes a progressive decrease in the average diameter of the droplets of the population as the population liquid-water-content decreased to zero.

The nature of the cloud model may be clarified somewhat by pointing out that visibility is functionally related to the integral of the second moment of the Khrgian-Mazin distribution equation, Eq. (G10); that is, optical extinction is dependent on the summed, cross-sectional areas of the cloud droplets. The liquid-water-content of the cloud population(s) is functionally related to the integral of the third moment of Eq. (G10). Visibility and liquid-water-content are therefore related through these moment equations and they are additionally related through the equation of Trabert.

The computational results listed in Tables G2 through G6 were obtained by use of the "cloud model" briefly described above. In this application, the equations were truncated at the diameter D = d = 0.794 microns, at the lower boundary, and at the diameter D = 79.4 microns, at the upper boundary. These values conform to the diameter extremes of the SAMS classes within the cloud-size portion of the spectrum, as stated earlier and shown in Table G1.

---

4. Houghton, H.G. (1939) On the relation between visibility and the constitution of clouds and fog, J. Aer. Sci. 6:408-411.

5. Middleton, W.E.K. (1952) Vision Through the Atmosphere, University of Toronto Press, 250 pages.

Table G2. Summary and "Best Estimate" Information About the Spectral Distribution and Total Values of Hydrometeor Number Concentration and Liquid-Water-Content Along the Missile Trajectory of Flight No. Q2-5297 (Unit No. R341403) of 3 February 1972, Launched at 2017:00 GMT. Reference text for description of table

Missile Altitude Km	Cloud Size-Range D_e - Equivalent Melted Diameter - microns										Precipitation Size-Range D_e - Equivalent Melted Diameter - mm									
	1.0	1.6	2.5	4.0	6.3	10	16	25	40	63	.10	.16	.25	.40	.63	1.0	1.6	2.5	4.0	6.3	10
	N_c Values are in No./cm^3										N_c Values are in No./m^3										
Sfc											54 / 0	72 / 0	88 / .001	88 / .003	70 / .009	38 / .019	11 / .021	1 / .007			
.25											55 / 0	73 / 0	88 / .001	90 / .003	72 / .010	39 / .020	12 / .022	1 / .007			
.50											56 / 0	74 / 0	89 / .001	92 / .003	74 / .010	41 / .021	13 / .023	1 / .008			
.75	Cloud Base Altitude										56 / 0	75 / 0	91 / .001	93 / .003	75 / .010	42 / .022	13 / .024	2 / .008			
1.00	.245 / 0	.824 / 0	2.51 / 0	6.59 / 0	13.6 / .002	19.3 / .011	15.6 / .033	5.40 / .040	.534 / .013	.008 / .001	60 / 0	80 / 0	98 / .001	102 / .004	85 / .012	48 / .025	15 / .031	2 / .013			
1.25	.245 / 0	.824 / 0	2.51 / 0	6.59 / 0	13.6 / .002	19.3 / .011	15.6 / .033	5.40 / .040	.534 / .013	.008 / .001	67 / 0	91 / 0	110 / .001	123 / .004	107 / .015	66 / .034	24 / .047	4 / .026			
1.50	.245 / 0	.824 / 0	2.51 / 0	6.59 / 0	13.6 / .002	19.3 / .011	15.6 / .033	5.40 / .040	.534 / .013	.008 / .001	84 / 0	117 / 0	150 / .001	171 / .006	162 / .023	114 / .061	51 / .102	12 / .090			
1.75	.245 / 0	.824 / 0	2.51 / 0	6.59 / 0	13.6 / .002	19.3 / .011	15.6 / .033	5.40 / .040	.534 / .013	.008 / .001	61 / 0	82 / 0	100 / .001	106 / .004	88 / .012	52 / .027	17 / .033	2 / .014			
2.00	.245 / 0	.824 / 0	2.51 / 0	6.59 / 0	13.6 / .002	19.3 / .011	15.6 / .033	5.40 / .040	.534 / .013	.008 / .001	48 / 0	63 / 0	74 / .001	73 / .003	55 / .007	28 / .014	8 / .016				
2.25	.245 / 0	.824 / 0	2.51 / 0	6.59 / 0	13.6 / .002	19.3 / .011	15.6 / .033	5.40 / .040	.534 / .013	.008 / .001	37 / 0	47 / 0	53 / 0	47 / .002	31 / .004	13 / .006	3 / .004				
Melting Zone W 2.50	.245 / 0	.824 / 0	2.51 / 0	6.59 / 0	13.6 / .002	19.3 / .011	15.6 / .033	5.40 / .040	.534 / .013	.008 / .001	35 / 0	33 / 0	21 / 0	10 / 0	2 / 0	.1 / 0					
I 2.50											78 / 0	94 / 0	98 / 0	80 / .003	45 / .006	15 / .007	2 / .003				
W 2.75	.245 / 0	.824 / 0	2.51 / 0	6.59 / 0	13.6 / .002	19.3 / .011	15.6 / .033	5.40 / .040	.534 / .013	.008 / .001	23 / 0	7 / 0	1 / 0								
I 2.75											353 / 0	403 / .001	381 / .003	270 / .009	123 / .015	28 / .012	2 / .004				
3.00	.245 / 0	.824 / 0	2.51 / 0	6.59 / 0	13.6 / .002	19.3 / .011	15.6 / .033	5.40 / .040	.534 / .013	.008 / .001	797 / 0	858 / .002	763 / .007	481 / .016	182 / .022	32 / .014	2 / .003				
3.25	.245 / 0	.824 / 0	2.51 / 0	6.59 / 0	13.6 / .002	19.3 / .011	15.6 / .033	5.40 / .040	.534 / .013	.008 / .001	462 / 0	561 / .001	584 / .005	478 / .018	270 / .035	87 / .041	12 / .020	.5 / .003			
3.50	.245 / 0	.824 / 0	2.51 / 0	6.59 / 0	13.6 / .002	19.3 / .011	15.6 / .033	5.40 / .040	.534 / .013	.008 / .001	325 / 0	414 / .001	466 / .004	431 / .015	293 / .039	125 / .062	26 / .046	3 / .012	.03 / .001		
3.75	.245 / 0	.824 / 0	2.51 / 0	6.59 / 0	13.6 / .002	19.3 / .011	15.6 / .033	5.40 / .040	.534 / .013	.088 / .001	271 / 0	353 / .001	410 / .004	399 / .014	294 / .040	141 / .071	36 / .065	3 / .021	.1 / .002		
4.00	.245 / 0	.824 / 0	2.51 / 0	6.59 / 0	13.6 / .002	19.3 / .011	15.6 / .033	5.40 / .040	.534 / .013	.088 / .001	242 / 0	318 / .001	378 / .003	378 / .013	291 / .039	150 / .076	42 / .077	5 / .030	.1 / .003		
4.25	.245 / 0	.824 / 0	2.51 / 0	6.59 / 0	13.6 / .002	19.3 / .011	15.6 / .033	5.40 / .040	.534 / .013	.088 / .001	288 / 0	372 / .001	428 / .004	410 / .014	294 / .039	138 / .068	32 / .058	3 / .018	.1 / .001		
4.50	.245 / 0	.824 / 0	2.51 / 0	6.59 / 0	13.6 / .002	19.3 / .011	15.6 / .033	5.40 / .040	.534 / .013	.088 / .001	345 / 0	439 / .001	488 / .004	441 / .015	291 / .038	118 / .058	23 / .040	1 / .009			
4.75											404 / 0	500 / .001	537 / .005	463 / .016	283 / .037	102 / .049	17 / .029	1 / .005			
5.00											1064 / .001	1154 / .003	1106 / .001	754 / .025	321 / .040	87 / .030	8 / .008	.1 / 0			
5.25											2692 / .002	2618 / .006	1934 / .016	933 / .030	334 / .027	72 / .009	5 / .001				
5.50											3203 / .002	2860 / .006	1850 / .015	728 / .022	135 / .015	8 / .003					
5.75											2993 / .002	2451 / .005	1388 / .011	446 / .013	61 / .006	2 / .001					
6.00											3897 / .002	2385 / .005	1230 / .010	359 / .011	43 / .005	1 / 0					
6.25											2783 / .002	2114 / .005	1057 / .008	383 / .008	38 / .003	.7 / 0					
6.50											2655 / .001	1898 / .004	869 / .007	303 / .006	17 / .002	.3 / 0					
6.75											2457 / .001	1810 / .003	648 / .005	134 / .003	5 / .001						
7.00											2133 / .001	1187 / .002	381 / .003	51 / .001	2 / 0						
7.25											1353 / .001	441 / .001	63 / 0	3 / 0							
7.32	Storm Top Altitude																				

No Reported Water Clouds

Preceding page blank

Summary Information for												
Cloud Population					Precipitation Population					Total Precipitation LWC for Melting Zone W + I	Grand Total LWC Cloud Plus Precipitation
Cloud Type	Total Number Cloud Particles	Cloud LWC	Median Volume Dia. D_{o_c}	Maximum Dia. D_{m_c}	Precip. Type	Total Number Precip. Particles	Precip. LWC	Median Volume Dia. D_o	Maximum Dia. D_m		
	No. cm^{-3}	gm m^{-3}	microns	microns		No. m^{-3}	gm m^{-3}	mm	mm	gm/m^3	gm/m^3
					R_D	421	.0608	1.195	2.534		.061
					R_D	430	.0635	1.205	2.555		.064
					R_D	439	.0664	1.215	2.577		.066
					R_D	447	.0690	1.225	2.595		069
N_S	<64.6	<.1	<20.8	79.4	R_D	493	.0851	1.275	2.703		<.185
N_S	<64.6	<.1	<20.8	79.4	R_D	595	.1271	1.375	2.918		<.227
N_S	<64.6	<.1	<20.8	79.4	R_D	861	.2831	1.605	3.401		<.383
N_S	<64.6	<.1	<20.8	79.4	R_D	508	.0909	1.290	2.737		<.191
N_S	<64.6	<.1	<20.8	79.4	R_D	349	.0408	1.110	2.347		<.141
N_S	<64.6	<.1	<20.8	79.4	R_D	229	.0170	.935	1.984		<.117
N_S	<64.6	<.1	<20.8	79.4	M.Z. Transition	103	.0009	.400	.843	.021	<.121
						412	.0201	.810	2.101		
N_S	<64.6	<.1	<20.8	79.4		31	.00003	.140	.257	.045	<.145
						1558	.0450	.865	2.269		
N_S	<64.6	<.1	<20.8	79.4	LS_C	3125	.0637	.555	2.368		<.184
N_S	<64.6	<.1	<20.8	79.4	LS_C	2456	.1217	.820	3.341		<.222
N_S	<64.6	<.1	<20.8	79.4	LS_C	2082	.1795	1.005	4.104		<.279
N_S	<64.6	<.1	<20.8	79.4	LS_C	1908	.2178	1.115	4.545		<.318
N_S	<64.6	<.1	<20.8	79.4	LS_C	1805	.2450	1.185	4.839		<.345
N_S	<64.6	<.1	<20.8	79.4	LS_C	1963	.2046	1.080	4.399		<.305
N_S	<64.6	<.1	<20.8	79.4	LS_C	2148	.1663	.970	3.947		<.267
					LS_C	2306	.1418	.890	3.623		.142
					Transition	4514	.1158	.640	2.593		.116
						8433	.0899	.450	1.813		.090
					SS_S	8783	.0639	.380	1.537		.064
					SS_S	7342	.0389	.330	1.332		.039
					SS_S	6406	.0320	.315	1.257		.032
					SS_S	6274	.0259	.295	1.183		.026
					SS_S	5638	.0200	.275	1.095		.020
					SS_S	4847	.0140	.250	.986		.014
					SS_S	3764	.0798	.215	.834		.008
					SS_S	1857	.0020	.150	.535		.002

Table G3. Summary and "Best Estimate" Information About the Spectral Distribution and Total Values of Hydrometeor Number Concentration and Liquid-Water-Content Along the Missile Trajectory of Flight No. Q2-5298 (Unit No. R341412) of 17 February 1972, Launched at 1456:00 GMT. Reference text for description of table

Missile Altitude Km	Cloud Size-Range: D_e – Equivalent Melted Diameter – microns										Precipitation Size-Range: D_e – Equivalent Melted Diameter – mm										
	1.0	1.6	2.5	4.0	6.3	10	16	25	40	63	.10	.16	.25	.40	.63	1.0	1.6	2.5	4.0	6.3	10
	N_c Values are in No. /cm^3										N_c Values are in No. /m^3										
Sfc											73 / 0	99 / 0	125 / .001	131 / .005	112 / .015	67 / .035	24 / .048	4 / .022			
.25						Cloud Base Altitude					70 / 0	96 / 0	120 / .001	131 / .005	115 / .016	73 / .038	21 / .053	5 / .031			
W .50											69 / 0	89 / 0	102 / .001	98 / .003	68 / .009	30 / .015	7 / .013				
I .50											19 / 0	27 / 0	37 / 0	45 / .002	47 / .007	30 / .021	22 / .048	8 / .057			
W .75											65 / 0	76 / 0	71 / .001	48 / .002	21 / .003	4 / .002					
I .75											49 / 0	68 / 0	89 / .001	104 / .004	102 / .014	76 / .041	37 / .074	10 / .079			
W 1.00											65 / 0	52 / 0	38 / 0	16 / .001	3 / 0						
I 1.00											78 / 0	107 / 0	138 / .001	156 / .006	148 / .020	101 / .054	44 / .088	10 / .082			
W 1.25						Unknown					59 / 0	38 / 0	15 / 0	3 / 0							
I 1.25											107 / 0	147 / 0	186 / .002	206 / .007	185 / .026	122 / .064	49 / .095	9 / .066	.6 / .013		
W 1.50											45 / 0	15 / 0	3 / 0								
I 1.50											141 / 0	191 / 0	238 / .002	257 / .009	223 / .031	138 / .072	51 / .098	9 / .058	.4 / .010		
W 1.75											27 / 0	4 / 0									
I 1.75											183 / 0	245 / .001	299 / .003	314 / .011	260 / .036	150 / .077	49 / .093	7 / .047	.3 / .007		
2.0											217 / 0	288 / .001	342 / .003	357 / .013	287 / .039	158 / .081	45 / .091	6 / .041	.2 / .005		
2.25											226 / 0	309 / .001	359 / .003	365 / .013	289 / .039	155 / .079	45 / .085	5 / .037	.2 / .004		
2.50	.202 / 0	.695 / 0	2.21 / 0	6.11 / 0	13.9 / .002	22.7 / .013	22.8 / .049	10.9 / .084	1.74 / .046	.054 / .005	241 / 0	318 / .001	377 / .003	378 / .013	292 / .039	151 / .077	42 / .078	5 / .031	.1 / .003		
2.75	.219 / 0	.748 / 0	2.34 / 0	6.34 / 0	13.8 / .002	21.4 / .012	19.7 / .042	8.27 / .063	1.09 / .028	.025 / .002	256 / 0	336 / .001	394 / .004	389 / .014	294 / .040	146 / .074	39 / .071	4 / .026	.1 / .002		
3.0	.245 / 0	.824 / 0	2.51 / 0	6.59 / 0	13.6 / .002	19.3 / .011	15.6 / .033	5.40 / .040	.534 / .013	.008 / .001	270 / 0	351 / .001	408 / .004	398 / .014	294 / .039	142 / .071	36 / .065	3 / .022	.1 / .002		
3.25	.245 / 0	.824 / 0	2.51 / 0	6.59 / 0	13.6 / .002	19.3 / .011	15.6 / .033	5.40 / .040	.534 / .013	.008 / .001	348 / 0	439 / .001	488 / .004	441 / .015	291 / .038	118 / .058	23 / .040	1 / .009			
3.50	.245 / 0	.824 / 0	2.51 / 0	6.59 / 0	13.6 / .002	19.3 / .011	15.6 / .033	5.40 / .040	.534 / .013	.008 / .001	358 / 0	450 / .001	497 / .004	446 / .015	290 / .038	115 / .056	22 / .038	1 / .008			
3.75	.245 / 0	.824 / 0	2.51 / 0	6.59 / 0	13.6 / .002	19.3 / .011	15.6 / .033	5.40 / .040	.534 / .013	.008 / .001	308 / 0	404 / .001	533 / .005	461 / .016	284 / .037	103 / .050	17 / .029	.9 / .005			
4.0	.219 / 0	.748 / 0	2.34 / 0	6.34 / 0	13.8 / .002	21.4 / .012	19.7 / .042	8.27 / .063	1.09 / .028	.025 / .002	393 / 0	489 / .001	529 / .005	453 / .016	284 / .037	105 / .051	18 / .030	.9 / .006			
4.25						Unknown					375 / 0	469 / .001	513 / .005	453 / .016	287 / .038	110 / .053	20 / .034	1 / .007			
4.50	.245 / 0	.824 / 0	2.51 / 0	6.59 / 0	13.6 / .002	19.3 / .011	15.6 / .033	5.40 / .040	.534 / .013	.008 / .001	456 / 0	554 / .001	579 / .005	477 / .016	272 / .035	89 / .042	12 / .021	.5 / .003			
4.75											544 / 0	642 / .001	654 / .006	511 / .017	269 / .034	77 / .036	9 / .015	.3 / .002			
5.0											1035 / 0	1183 / .001	1121 / .010	793 / .027	358 / .045	82 / .037	7 / .011	.1 / 0			
5.25											1860 / .001	2032 / .005	1797 / .016	1143 / .038	438 / .053	78 / .034	4 / .007				
5.50											3187 / .002	3316 / .007	2719 / .023	1538 / .050	494 / .059	68 / .028	3 / .004				
5.75											3563 / .002	3602 / .009	3241 / .028	1947 / .064	685 / .083	108 / .046	5 / .008				
6.0											3509 / .002	3617 / .008	2924 / .025	1618 / .052	503 / .059	65 / .027	2 / .003				
6.25											3497 / .002	3583 / .008	2867 / .025	1563 / .050	474 / .058	60 / .025	2 / .003				
6.50						No Reported Water Clouds					3484 / .002	3544 / .008	2806 / .024	1504 / .048	445 / .052	54 / .022	2 / .002				
6.75											3471 / .002	3505 / .008	2744 / .023	1446 / .046	417 / .049	48 / .020	1 / .002				
7.0											3456 / .002	3463 / .008	2678 / .023	1385 / .044	388 / .045	43 / .018	1 / .002				
7.25											3440 / .002	3418 / .008	2610 / .022	1323 / .042	360 / .042	38 / .016	1 / .001				
7.50											7306 / .004	6481 / .014	4150 / .034	1606 / .049	291 / .032	17 / .007					
7.75											17025 / .010	14504 / .032	8726 / .072	3075 / .093	483 / .052	23 / .009					
8.0											22248 / .012	18113 / .039	10161 / .083	3219 / .096	431 / .046	16 / .006					
8.25											22077 / .012	17765 / .038	9789 / .079	3018 / .090	388 / .041	13 / .005					
8.50											19620 / .011	13388 / .028	5730 / .045	1205 / .034	87 / .009	1 / 0					
8.53						Storm Top Altitude															

Melting Zone

Summary Information for												
Cloud Population					Precipitation Population					Total Precipitation LWC for Melting Zone W + I	Grand Total LWC Cloud Plus Precipitation
Cloud Type	Total Number Cloud Particles No. cm^{-3}	Cloud LWC $gm\ m^{-3}$	Median Volume Dia. D_{o_c} microns	Maximum Dia. D_{m_c} microns	Precip. Type	Total Number Precip. Particles No. m^{-3}	Precip. LWC $gm\ m^{-3}$	Median Volume Dia. D_o mm	Maximum Dia. D_m mm	gm/m^3	gm/m^3
--	--	--	--	--	R_D	833	.1241	1.335	2.830		.134
--	--	--	--	--	R_D	636	.1437	1.405	2.976		.144
--	--	--	--	--	M.Z. Transition	462	.0419	1.010	2.141	.175	.175
--	--	--	--	--		243	.1330	1.650	3.306		
--	--	--	--	--		269	.0070	.615	1.300	.220	.220
--	--	--	--	--		535	.2126	1.710	3.648		
--	--	--	--	--		182	.0013	.375	.789	.252	.252
--	--	--	--	--		781	.2510	1.610	3.660		
--	--	--	--	--		115	.0003	.235	.479	.273	.273
--	--	--	--	--		1011	.2733	1.515	4.233		
--	--	--	--	--		89	.0001	.155	.291	.281	.281
--	--	--	--	--		1247	.2810	1.425	4.575		
--	--	--	--	--		30	.0000	.115	.177	.275	.275
--	--	--	--	--		1507	.2747	1.325	4.917		
--	--	--	--	--	LS_C	1710	.2732	1.260	5.146		.273
--	--	--	--	--	LS_C	1746	.2613	1.235	5.025		.261
N_S	81.4	.2	24.3	79.4	LS_C	1804	.2454	1.19	4.854		.445
N_S	73.9	.15	20.1	79.4	LS_C	1858	.2306	1.15	4.695		.381
N_S	64.6	.1	20.8	79.4	LS_C	1902	.2178	1.12	4.559		.318
N_S	<64.6	<.1	<20.8	79.4	LS_C	2148	.1663	.97	3.947		<.266
N_S	<64.6	<.1	<20.8	79.4	LS_C	2179	.1616	.955	3.886		<.262
N_S	<64.6	<.1	<20.8	79.4	LS_C	2292	.1437	.895	3.650		<.244
N_S	73.9	.15	20.1	79.4	LS_C	2278	.1456	.905	3.676		.286
--	--	--	--	--	LS_C	2227	.1537	.930	3.783		.154
N_S	<64.6	<.1	<20.8	79.4	LS_C	2440	.1238	.83	3.371		<.224
					Transition	2711	.1114	.765	3.112		.111
						4581	.1328	.67	2.720		.133
						7354	.1536	.59	2.390		.154
						11326	.1736	.52	2.110		.174
					SS_S	13351	.2386	.555	2.246		.239
					SS_S	12239	.1777	.510	2.063		.178
					SS_S	12046	.1686	.500	2.033		.169
					SS_S	11839	.1584	.495	2.00		.159
					SS_S	11633	.1505	.485	1.967		.151
					SS_S	11416	.1416	.475	1.933		.142
					SS_S	11190	.1328	.470	1.898		.133
					Transition	10853	.1407	.375	1.519		.141
						43835	.367	.350	1.418		.367
					C_1	54189	.2815	.330	1.319		.282
					C_1	53049	.3653	.325	1.295		.365
					C_1	40033	.1267	.26	1.035		.127

Table G4. Summary and "Best Estimate" Information About the Spectral Distribution and Total Values of Hydrometeor Number Concentration and Liquid-Water-Content Along the Missile Trajectory of Flight No. Q2-5299 (Unit No. R341404) of 17 February 1972, Launched at 1512:00 GMT. Reference text for description of table

Missile Altitude	Melting Zone	Cloud Size-Range: D_e – Equivalent Melted Diameter – microns										Precipitation Size-Range: D_e – Equivalent Melted Diameter – mm										
Km		1.0	1.6	2.5	4.0	6.3	10	16	25	40	63	.10	.16	.25	.40	.63	1.0	1.6	2.5	4.0	6.3	10
		N_c Values are in No./cm^3										N_c Values are in No./m^3										
Sfc												77 / 0	103 / 0	126 / .001	131 / .005	108 / .015	62 / .032	20 / .038	2.5 / .015			
.25		Cloud Base Altitude										73 / 0	98 / 0	122 / .001	131 / .005	112 / .015	68 / .035	24 / .046	4 / .023			
.50	W											92 / 0	82 / 0	104 / .001	96 / .003	66 / .009	28 / .014	6 / .011				
.50	I											19 / 0	27 / 0	37 / 0	44 / .002	46 / .006	37 / .020	20 / .042	6 / .046			
.75	W											71 / 0	79 / 0	72 / .001	48 / .002	20 / .002	4 / .002					
.75	I											49 / 0	69 / 0	89 / .001	103 / .004	99 / .014	72 / .038	34 / .067	8 / .065			
1.00	W											68 / 0	61 / 0	39 / 0	15 / .001	3 / 0						
1.00	I											78 / 0	108 / 0	137 / .001	154 / .006	142 / .020	97 / .051	41 / .081	9 / .071			
1.25	W											62 / 0	39 / 0	15 / 0	3 / 0							
1.25	I											107 / 0	146 / 0	184 / .002	203 / .007	181 / .025	118 / .062	45 / .090	9 / .060	.5 / .011		
1.50	W											51 / 0	18 / 0	3 / 0								
1.50	I											138 / 0	188 / 0	233 / .002	252 / .009	219 / .030	136 / .071	50 / .097	8 / .058	.4 / .010		
1.75	W											28 / 0	4 / 0									
1.75	I											175 / 0	237 / .001	290 / .003	308 / .011	250 / .035	153 / .079	52 / .099	8 / .053	.3 / .008		
2.0		Unknown										209 / 0	279 / .001	338 / .003	351 / .012	286 / .039	169 / .082	51 / .095	7 / .045	.25 / .006		
2.25												231 / 0	306 / .001	365 / .003	370 / .013	299 / .039	154 / .078	45 / .083	5 / .034	.16 / .004		
2.50		.202 / 0	.696 / 0	2.21 / 0	6.13 / 0	13.8 / .002	22.7 / .011	22.6 / .049	10.9 / .084	1.74 / .046	.054 / .005	250 / 0	328 / .001	387 / .004	384 / .014	292 / .039	148 / .075	40 / .074	4 / .027	.11 / .002		
2.75		.219 / 0	.748 / 0	2.34 / 0	6.33 / 0	13.8 / .002	21.4 / .012	19.7 / .042	8.27 / .063	1.09 / .021	.025 / .002	310 / 0	397 / .001	451 / .004	423 / .015	294 / .039	130 / .064	28 / .051	2 / .014	.03 / .001		
3.0		.245 / 0	.824 / 0	2.51 / 0	6.59 / 0	13.6 / .002	19.3 / .011	15.6 / .033	5.40 / .040	.534 / .013	.008 / .001	396 / 0	492 / .001	531 / .005	460 / .016	284 / .037	104 / .050	17 / .030	.9 / .005			
3.25		.245 / 0	.824 / 0	2.51 / 0	6.59 / 0	13.6 / .002	19.3 / .011	15.6 / .033	5.40 / .040	.534 / .013	.008 / .001	449 / 0	547 / .001	574 / .005	475 / .016	273 / .035	90 / .043	13 / .021	.5 / .003			
3.50		Unknown										473 / 0	571 / .001	592 / .005	481 / .016	268 / .035	84 / .040	11 / .019	.4 / .002			
3.75		.245 / 0	.824 / 0	2.51 / 0	6.59 / 0	13.6 / .002	19.3 / .011	15.6 / .033	5.40 / .040	.534 / .013	.008 / .001	473 / 0	571 / .001	592 / .005	481 / .016	268 / .035	84 / .040	11 / .019	.4 / .002			
4.0		Unknown										499 / 0	597 / .001	610 / .005	485 / .017	262 / .034	78 / .037	10 / .016	.31 / .002			
4.25		.219 / 0	.748 / 0	2.34 / 0	6.33 / 0	13.8 / .002	21.4 / .012	19.7 / .042	8.27 / .063	1.09 / .021	.025 / .002	528 / 0	626 / .001	630 / .006	489 / .017	255 / .032	72 / .034	8 / .013	.23 / .001			
4.50												473 / 0	571 / .001	592 / .005	481 / .016	268 / .035	84 / .040	11 / .018	.41 / .002			
4.75												466 / 0	569 / .001	599 / .005	499 / .017	282 / .037	96 / .046	14 / .024	.58 / .003			
5.0												979 / .001	1135 / .003	1102 / .010	810 / .027	387 / .049	96 / .044	9 / .014	.19 / .001			
5.25												1835 / .001	2022 / .005	1811 / .016	1175 / .039	464 / .057	87 / .038	5 / .008				
5.50												3187 / .002	3326 / .007	2738 / .024	1552 / .051	506 / .060	70 / .030	3 / .004				
5.75												3563 / .002	3802 / .009	3241 / .028	1948 / .064	685 / .083	108 / .046	5 / .008				
6.0												3528 / .002	3684 / .008	3036 / .026	1731 / .056	563 / .067	78 / .033	3 / .005				
6.25		No Reported Water Clouds										3473 / .002	3510 / .008	2752 / .024	1453 / .047	420 / .049	48 / .020	1.5 / .002				
6.50												3492 / .002	3567 / .008	2842 / .024	1539 / .050	463 / .054	57 / .024	2 / .003				
6.75												3558 / .002	3786 / .008	3213 / .028	1917 / .063	667 / .080	103 / .044	5 / .007				
7.0												3542 / .002	3728 / .008	3112 / .027	1810 / .059	606 / .072	88 / .037	4 / .005				
7.25												3517 / .002	3843 / .008	2965 / .025	1680 / .054	524 / .052	70 / .029	3 / .004				
7.5												7765 / .004	7618 / .017	5702 / .048	2804 / .086	728 / .084	72 / .029	2 / .002				
7.75												17375 / .010	15298 / .033	9884 / .080	3685 / .113	650 / .071	37 / .014					
8.0												22630 / .013	18930 / .041	11073 / .091	3738 / .112	550 / .089	23 / .009					
8.25												22297 / .013	18215 / .039	10273 / .084	3281 / .098	445 / .047	17 / .006					
8.50												19621 / .011	13388 / .028	5730 / .045	1203 / .034	87 / .009	1 / 0					
8.53		Storm Top Altitude																				

Summary Information for											
Cloud Population					Precipitation Population					Total Precipitation LWC for Melting Zone W + I	Grand Total LWC Cloud Plus Precipitation
Cloud Type	Total Number Cloud Particles No. cm^{-3}	Cloud LWC $gm\ m^{-3}$	Median Volume Dia. D_{oc} microns	Maximum Dia. D_{mc} microns	Precip. Type	Total Number Precip. Particles No. m^{-3}	Precip. LWC $gm\ m^{-3}$	Median Volume Dia. D_o mm	Maximum Dia. D_m mm	gm/m^3	gm/m^3
–	–	–	–	–	R_D	629	.1054	1.26	2.674		.105
–	–	–	–	–	R_D	633	.1262	1.345	2.846		.126
–	–	–	–	–	M,Z, Transition	464	.0378	.870	2.057	.153	.153
–	–	–	–	–		236	.1155	1.760	3.095		
–	–	–	–	–		293	.0065	.595	1.258	.196	.196
–	–	–	–	–		525	.1893	1.655	3.473		
–	–	–	–	–		186	.0013	.365	.769	.231	.231
–	–	–	–	–		767	.2296	1.570	3.850		
–	–	–	–	–		118	.0003	.230	.470	.258	.258
–	–	–	–	–		994	.2573	1.495	4.228		
–	–	–	–	–		72	.0001	.150	.288	.278	.278
–	–	–	–	–		1226	.2780	1.430	4.606		
–	–	–	–	–		32	.0000	.115	.176	.289	.289
–	–	–	–	–		1482	.2886	1.355	4.983		
–	–	–	–	–	LS_C	1680	.283	1.285	5.245		.283
–	–	–	–	–	LS_C	1767	.256	1.22	4.967		.256
N_S	81.4	.2	24.3	79.4	LS_C	1833	.236	1.165	4.754		.436
N_S	73.8	.15	20.1	79.4	LS_C	2036	.1887	1.035	4.219		.339
N_S	64.6	.1	20.8	79.4	LS_C	2285	.1446	0.90	3.663		.245
N_S	<64.6	<.1	<20.8	79.4	LS_C	2422	.125	.835	3.398		<.225
–	–	–	–	–	LS_C	2481	.119	.81	3.297		.119
N_S	<64.6	<.1	<20.8	79.4	LS_C	2481	.119	.81	3.297		<.219
–	–	–	–	–	LS_C	2542	.112	.785	3.191		.112
N_S	73.9	.15	20.1	79.4	LS_C	2607	.105	.76	3.083		.255
					LS_C	2481	.1187	.81	3.297		.119
					Transition	2532	.1344	.84	3.429		.134
						4518	.1483	.70	2.854		.148
						7399	.1636	.60	2.445		.164
						11389	.1773	.525	2.123		.177
					SS_S	13351	.2386	.555	2.246		.239
					SS_S	12624	.1972	.525	2.126		.197
					SS_S	11658	.1515	.485	1.971		.152
					SS_S	11961	.1647	.50	2.019		.165
					SS_S	13250	.2325	.55	2.229		.233
					SS_S	12889	.2115	.535	2.169		.212
					SS_S	12381	.1847	.515	2.086		.185
					Transition	24693	.2745	.455	1.846		.274
						46731	.3216	.37	1.499		.322
					C_1	56944	.3244	.34	1.376		.324
					C_1	54527	.2865	.33	1.326		.286
					C_1	40033	.1267	.26	1.034		.127

Table G5. Summary and "Best Estimate" Information About the Spectral Distribution and Total Values of Hydrometeor Number Concentration and Liquid-Water-Content Along the Missile Trajectory of Flight No. Q2-5891 (Unit No. R341413) of 17 March 1972, Launched at 2119:00 GMT'. Reference text for description of table

Missile Altitude Km	Cloud Size-Range: D_e – Equivalent Melted Diameter – microns										Precipitation Size-Range: D_e – Equivalent Melted Diameter – mm										
	1.0	1.6	2.5	4.0	6.3	10	16	25	40	63	.10	.16	.25	.40	.63	1.0	1.6	2.5	4.0	6.3	10
	N_c Values are in No. /cm^3										N_c Values are in No. /m^3										
Sfc											194 / 0	251 / .001	287 / .003	272 / .010	193 / .026	88 / .044	21 / .040				
.25											194 / 0	250 / .001	286 / .003	271 / .009	192 / .026	87 / .043	20 / .039				
.50	Cloud Base Altitude Unknown										194 / 0	250 / .001	285 / .003	270 / .009	190 / .025	86 / .043	20 / .038				
.75	Unknown										194 / 0	248 / .001	284 / .003	268 / .009	189 / .025	85 / .042	20 / .037				
1.0	.245 / 0	.824 / 0	2.51 / 0	6.59 / 0	13.6 / .002	19.3 / .011	15.6 / .033	5.40 / .040	.534 / .013	.008 / .001	193 / 0	248 / .001	282 / .003	265 / .009	186 / .025	83 / .041	19 / .035				
W 1.25	.245 / 0	.824 / 0	2.51 / 0	6.59 / 0	13.6 / .002	19.3 / .011	15.6 / .033	5.40 / .040	.534 / .013	.008 / .001	192 / 0	227 / .001	226 / .002	173 / .006	88 / .011	26 / .014					
I 1.25											38 / 0	54 / 0	70 / .001	78 / .003	74 / .010	52 / .027	26 / .064				
W 1.50	.202 / 0	.696 / 0	2.21 / 0	6.13 / 0	13.8 / .002	22.7 / .013	22.8 / .049	10.9 / .084	1.74 / .046	.054 / .005	186 / 0	154 / 0	88 / .001	30 / .001	4 / 0	.44 / 0					
I 1.50											115 / 0	156 / 0	192 / .002	205 / .007	174 / .024	104 / .054	36 / .070	6 / .040			
W 1.75	.202 / 0	.696 / 0	2.21 / 0	6.13 / 0	13.8 / .002	22.7 / .013	22.8 / .049	10.9 / .084	1.74 / .046	.054 / .005	157 / 0	62 / 0	11 / 0								
I 1.75											163 / 0	220 / .001	268 / .002	282 / .010	235 / .032	136 / .070	45 / .086	7 / .044	.25 / .005		
W 2.0	.202 / 0	.696 / 0	2.21 / 0	6.13 / 0	13.8 / .002	22.7 / .013	22.8 / .049	10.9 / .084	1.74 / .046	.054 / .005	32 / 0	1 / 0									
I 2.0											210 / 0	281 / .001	341 / .003	356 / .013	291 / .040	165 / .085	53 / .100	7 / .048	.28 / .006		
2.25	Unknown										229 / 0	303 / .001	362 / .003	368 / .013	290 / .039	155 / .079	45 / .085	5 / .036	.17 / .004		
2.50	.202 / 0	.696 / 0	2.21 / 0	6.13 / 0	13.8 / .002	22.7 / .013	22.8 / .049	10.9 / .084	1.74 / .046	.054 / .005	272 / 0	354 / .001	411 / .004	400 / .014	294 / .039	141 / .071	35 / .064	3 / .021	.07 / .002		
2.75	.245 / 0	.824 / 0	2.51 / 0	6.59 / 0	13.6 / .002	19.3 / .011	15.6 / .033	5.40 / .040	.534 / .013	.008 / .001	318 / 0	406 / .001	459 / .004	426 / .015	293 / .039	127 / .063	27 / .048	2 / .012	.03 / .001		
3.0	.245 / 0	.824 / 0	2.51 / 0	6.59 / 0	13.6 / .002	19.3 / .011	15.6 / .033	5.40 / .040	.534 / .013	.008 / .001	362 / 0	455 / .001	501 / .004	448 / .016	289 / .038	114 / .056	21 / .037	1 / .008			
3.25	Unknown										411 / 0	508 / .001	544 / .005	465 / .016	281 / .037	100 / .048	16 / .027	.75 / .005			
3.50	Unknown										495 / 0	593 / .001	607 / .005	484 / .017	262 / .034	78 / .037	10 / .016	.32 / .002			
3.75											446 / 0	544 / .001	572 / .005	475 / .016	274 / .036	91 / .043	13 / .022	.53 / .003			
4.0											482 / 0	581 / .001	599 / .005	482 / .016	268 / .034	82 / .039	11 / .018	.37 / .002			
4.25											1176 / .001	1355 / .003	1302 / .011	941 / .032	439 / .055	106 / .048	9 / .015	.18 / .001			
4.50											3482 / .002	3537 / .008	2794 / .024	1493 / .048	439 / .052	53 / .022	2 / .002				
4.75	No Reported Water Cloud										3382 / .002	3280 / .007	2406 / .020	1147 / .036	284 / .033	26 / .011	.55 / .001				
5.0											3190 / .002	2834 / .006	1819 / .015	707 / .022	129 / .014	8 / .003					
5.25											2415 / .001	1553 / .003	807 / .005	111 / .003	7 / .001						
5.50											3515 / .002	556 / .001	27 / 0								
5.75											Non-Computable										
5.94	Storm Top Altitude																				

Melting Zone

Summary Information for											
Cloud Population					Precipitation Population					Total Precipitation LWC for Melting Zone W + I	Grand Total LWC Cloud Plus Precipitation
Cloud Type	Total Number Cloud Particles No. cm^{-3}	Cloud LWC $gm\ m^{-3}$	Median Volume Dia. D_{o_c} microns	Maximum Dia. D_{m_c} microns	Precip. Type	Total Number Precip. Particles No. m^{-3}	Precip. LWC $gm\ m^{-3}$	Median Volume Dia. D_o mm	Maximum Dia. D_m mm	gm/m^3	gm/m^3
					R_D	1307	.1223	1.02	2.165		.122
					R_D	1299	.120	1.02	2.155		.120
					R_D	1295	.119	1.015	2.149		.119
					R_D	1286	.117	1.01	2.140		.117
N_S	~64.6	~.1	~20.8	79.4	R_D	1276	.114	1.005	2.125		~.214
N_S	~64.6	~.1	~20.8	79.4	↑	932	.033	.715	1.511	.139	~.239
						395	.106	1.435	2.467		
N_S	81.4	.2	24.3	79.4	M.Z.	463	.002	.325	.681	.200	.400
					Tran-	989	.198	1.355	3.279		
N_S	81.4	.2	24.3	79.4	sition	231	.0003	.160	.307	.252	.452
						1358	.252	1.33	4.091		
N_S	~81.4	~.2	~24.3	79.4		34	.0000	.100	.139	.297	~.497
					↓	1705	.297	1.30	4.903		
–	–	–	–	–	LS_C	1758	.260	1.225	5.00		.260
N_S	81.4	.2	24.3	79.4	LS_C	1911	.216	1.115	4.539		.416
N_S	<64.6	<.1	<20.8	79.4	LS_C	2058	.183	1.02	4.115		<.283
N_S	<64.6	<.1	<20.8	79.4	LS_C	2191	.160	0.95	3.861		<.260
–	–	–	–	–	LS_C	2325	.138	0.88	3.580		.138
–	–	–	–	–	LS_C	2531	.112	.785	3.205		.112
					LS_C	2415	.127	0.84	3.413		.127
					LS_C	2503	.116	0.80	3.257		.116
					Tran.	5328	.166	.685	2.796		.166
					SS_S	11799	.158	0.49	1.993		.158
					SS_S	10532	.110	.445	1.796		.110
					SS_S	8686	.062	.375	1.523		.062
					SS_S	4692	.013	.245	.964		.013
					Tran.	4097	.003	.12	.357		.003
					C_1	<4097	<.003	<.12	<.357		<.003

Table G6. Summary and "Best Estimate" Information About the Spectral Distribution and Total Values of Hydrometeor Number Concentration and Liquid-Water-Content Along the Missile Trajectory of Flight No. Q2-5892 (Unit No. R341405) of 22 March 1972, Launched at 1548:00 GMT. Reference text for description of table

Missile Altitude Km	Melting Zone	Cloud Size-Range D_e – Equivalent Melted Diameter – microns; N_c Values are in No./cm^3										Precipitation Size-Range D_e – Equivalent Melted Diameter – mm; N_c Values are in No./m^3										
		1.0	1.6	2.5	4.0	6.3	10	16	25	40	63	.10	.16	.25	.40	.63	1.0	1.6	2.5	4.0	6.3	10
Sfc												42/0	54/0	60/.001	54/.002	36/.005	15/.007	3/.005				
.25												43/0	54/0	61/.001	56/.002	38/.005	16/.008	3/.006				
.50												43/0	54/0	61/.001	56/.002	38/.005	16/.008	3/.006				
.75												44/0	56/0	63/.001	58/.002	39/.005	16/.008	3/.006				
1.0												45/0	58/0	65/.001	60/.002	41/.005	18/.009	4/.007				
1.25		Cloud Base Altitude										48/0	61/0	69/.001	65/.002	45/.006	20/.010	4/.008				
1.50												50/0	65/0	74/.001	70/.002	49/.007	22/.011	5/.010				
1.75												52/0	81/0	93/.001	84/.003	71/.010	36/.013	10/.021				
	W 2.0						Unknown					61/0	71/0	69/.001	50/.002	24/.003	6/.003					
	I 2.0											28/0	38/0	50/0	51/.002	55/.008	40/.021	19/.037	4/.025			
	W 2.25											56/0	42/0	21/0	6/0							
	I 2.25											86/0	117/0	145/.001	155/.008	133/.018	81/.042	29/.05[illegible]	5/.034			
	W 2.50	.202/0	.696/0	2.21/0	6.13/0	13.9/.002	22.7/.013	22.8/.049	10.9/.084	1.74/.046	.054/.005	38/0	11/0									
	I 2.50											184/0	218/.001	263/.002	270/.010	217/.030	119/.061	32/.069	5/.031	.15/.003		
2.75		.202/0	.696/0	2.21/0	6.13/0	13.9/.002	22.7/.013	22.8/.049	10.9/.084	1.74/.046	.054/.005	250/0	328/.001	387/.004	384/.014	292/.039	148/.075	40/.074	4/.027	0.1/.002		
3.0		.202/0	.696/0	2.21/0	6.13/0	13.9/.002	22.7/.013	22.8/.049	10.9/.084	1.74/.046	.054/.005	319/0	408/.001	480/.004	427/.015	293/.039	126/.062	27/.048	2/.012	.03/.001		
3.25		.202/0	.696/0	2.21/0	6.13/0	13.9/.002	22.7/.013	22.8/.049	10.9/.084	1.74/.046	.054/.005	396/0	492/.001	531/.005	400/.016	284/.037	104/.050	17/.030	.8/.005			
3.50		Unknown										414/0	511/.001	545/.005	466/.016	281/.037	99/.048	18/.027	.7/.004			
3.75		Unknown										434/0	531/.001	562/.005	471/.016	276/.036	94/.045	14/.024	.6/.004			
4.0		Unknown										456/0	554/.001	579/.005	477/.016	272/.035	89/.042	12/.021	.48/.003			
4.25		.202/0	.696/0	2.21/0	6.13/0	13.9/.002	22.7/.013	22.8/.049	10.9/.084	1.74/.046	.054/.005	476/0	575/.001	594/.005	481/.016	267/.034	84/.039	11/.018	.39/.002			
4.50												499/0	597/.001	610/.005	485/.017	262/.034	78/.037	10/.016	.31/.002			
4.75												523/0	622/.001	627/.006	489/.017	256/.033	73/.034	8/.014	.24/.001			
5.0												545/0	644/.001	642/.006	491/.017	250/.032	69/.032	7/.012	.19/.001			
5.25												575/0	672/.002	660/.006	493/.017	242/.031	63/.029	6/.010	.15/.001			
5.50												809/0	916/.002	853/.007	591/.020	258/.032	56/.025	4/.007	.05/0			
5.75												1238/.001	1338/.003	1164/.010	721/.024	266/.032	45/.019	2/.004				
6.0							Unknown					1787/.001	1845/.004	1498/.013	831/.027	260/.031	34/.014	1/.002				
6.25												2417/.001	2393/.005	1816/.015	912/.029	245/.028	25/.010	.6/.001				
6.50												3172/.002	3008/.007	2135/.018	968/.030	223/.025	18/.007	.32/0				
6.75												3325/.002	3129/.007	2196/.018	979/.031	219/.025	17/.007	.28/0				
7.0												3321/.002	3120/.007	2184/.018	969/.030	215/.024	17/.007	.27/0				
7.25												3287/.002	3086/.007	2112/.018	914/.029	198/.022	15/.006	.21/0				
7.50												3266/.002	2996/.007	2021/.017	847/.026	173/.019	12/.005	.18/0				
7.75												3231/.002	2932/.006	1938/.016	788/.024	154/.017	10/.004					
8.0												3102/.002	2857/.006	1812/.013	575/.017	92/.010	4/.002					
8.23		Storm Top Altitude																				

Summary Information for											
Cloud Population					Precipitation Population					Total Precipitation LWC for Melting Zone W + I	Grand Total LWC Cloud Plus Precipitation
Cloud Type	Total Number Cloud Particles No. cm^{-3}	Cloud LWC $gm\ m^{-3}$	Median Volume Dia. D_{0c} microns	Maximum Dia. D_{m_c} microns	Precip. Type	Total Number Precip. Particles No. m^{-3}	Precip. LWC $gm\ m^{-3}$	Median Volume Dia. D_0 mm	Maximum Dia. D_m mm	gm/m^3	gm/m^3
					R_D	264	.020	.945	2.0		.020
					R_D	271	.021	.95	2.016		.021
					R_D	271	.021	.95	2.016		.021
					R_D	278	.022	.96	2.033		.022
					R_D	292	.024	.975	2.06		.024
–	–	–	–	–	R_D	311	.027	.99	2.1		.027
–	–	–	–	–	R_D	336	.031	1.015	2.152		.031
–	–	–	–	–	R_D	449	.053	1.11	2.351		.053
–	–	–	–	–	↑ M.Z. Tran- sition	281	.009	.675	1.424	.102	.102
–	–	–	–	–		291	.093	1.545	2.762		
–	–	–	–	–		124	.0005	.28	.585	.158	.158
–	–	–	–	–		752	.157	1.38	3.492		
N_S	~81.4	~.2	~24.3	79.4		49	.0000	.135	.341	.206	~.406
					↓	1293	.206	1.26	4.222		
N_S	~81.4	~.2	~24.3	79.4	LS_C	1833	.235	1.165	4.754		~.436
N_S	~81.4	~.2	~24.3	79.4	LS_C	2063	.182	1.015	4.144		~.382
N_S	~81.4	~.2	~24.3	79.4	LS_C	2285	.145	.90	3.663		~.345
–	–	–	–	–	LS_C	2333	.138	.875	3.567		.138
–	–	–	–	–	LS_C	2383	.130	.85	3.468		.130
–	–	–	–	–	LS_C	2440	.124	.83	3.371		.124
N_S	81.4	.2	24.3	79.4	LS_C	2490	.118	.805	3.282		.318
					LS_C	2542	.112	.785	3.191		.112
					LS_C	2598	.106	.76	3.099		.106
					LS_C	2649	.101	.74	3.021		.101
					LS_C	2712	.095	.72	2.924		.095
					↑ Tran- sition	3489	.094	.65	2.641		.094
						4775	.093	.57	2.322		.093
						6254	.092	.51	2.072		.092
						7809	.091	.465	1.882		.091
					↓	9524	.090	.425	1.721		.090
					SS_S	9866	.090	.42	1.696		.090
					SS_S	9626	.089	.42	1.690		.089
					SS_S	9600	.083	.41	1.657		.083
					SS_S	9315	.076	.4	1.615		.076
					SS_S	9061	.070	.39	1.577		.070
					SS_S	8042	.050	.355	1.431		.050

☆ U. S. GOVERNMENT PRINTING OFFICE: 1974--600-015--32